

# DEPHOSPHORIZATION OF HIGH CARBON FERROMANGANESE USING $\text{BaCO}_3$ BASED FLUXES

Thesis submitted  
in partial fulfillment of the requirements  
for the award of the degree of

**Doctor of Philosophy**

In  
ENGINEERING

By

**PANKAJ NARAYAN CHAUDHARY**



DEPARTMENT OF METALLURGICAL AND MATERIALS ENGINEERING  
INDIAN INSTITUTE OF TECHNOLOGY  
KHARAGPUR: 721 302  
1999

**Department Of Metallurgical and Materials Engineering**  
**INDIAN INSTITUTE OF TECHNOLOGY**  
**Kharagpur**

**CERTIFICATE**

This is to certify that the thesis entitled **DEPHOSPHORIZATION OF HIGH CARBON FERROMANGANESE USING BaCO<sub>3</sub> BASED FLUXES** being submitted by **Sri Pankaj Narayan Chaudhary** is a record of bonafide research work carried out by him at the National Metallurgical Laboratory, Jamshedpur, India and in the Department of Metallurgical and Materials Engineering, Indian Institute of Technology, Kharagpur, India, under our guidance and supervision. In our opinion the thesis has fulfilled the requirements according to the regulations of this Institute and has reached the standards necessary for submission.

To the best of our knowledge the results incorporated in this thesis are original and have not been submitted to any other university or institute for the award of degree or diploma.

R. P. GOEL

(G. G. ROY)

**Deputy Director**

Assistant Professor

**National Metallurgical**

Department of Metallurgical & Materials

**Laboratory**

Engg.

Indian Institute of Technology

**Jamshedpur 831007 India**

Kharagpur 721302 India

ACKNOWLEDGEMENT

The investigations reported in this thesis were mostly carried out at National Metallurgical Laboratory (NML), Jamshedpur under the guidance of Dr. R. P. Goel, Dy Director, NML Jamshedpur. I am grateful to him for his valuable suggestions and advice through out the work, especially in the formulation of the work plan, patent document and finally in the preparation of the thesis.

I am thankful to Dr. G. G. Roy, Assistant professor, Department of Metallurgical and Materials Engineering, Indian Institute of Technology (IIT), Kharagpur, for his advice in kinetic study, interpretation of experimental data and overall guidance in the preparation of the thesis. I am also thankful to Dr. S. B. Sarkar, ex- Associate Professor, IIT, Kharagpur. for guidance during the initial stages of this work. I wish to record my appreciation for the suggestions made by the members of Doctoral Scrutiny Committee during various stages of this work.

I am indebted to Prof. Ahindra Ghosh, IIT Kanpur for generating in me an abiding interest in scientific research during my association with him for my Masters Degree.

I am grateful to Prof. S. Banerjee, ex-Director, NML, Jamshedpur, for his kind approval to initiate this research work. I wish to express my deep sense of gratitude to Prof. P Ramchandra Rao, Director, NML, Jamshedpur for his continued encouragement to accomplish this work. I am grateful to Dr. K. K. Mishra, Head, Information and Research Management (IRM) Division, for his constant support.

I am thankful to the management of Ferro Alloy Corporation (FACOR), Visakhapatnam for providing a sample of ferromanganese for the kinetic study. My sincere thanks are also due to the management of Tata Steel, Ferroalloy Plant (FAP), Joda especially to Mr J.L. Tripathi, and Mr. N. K. Das, for their help in the collection of operating data.

I am thankful to my colleagues at NML particularly to Mr R.K. Minj, Dr. S. Srikanth, Dr. S. Ghosh, Dr. Ajay K Ray, Dr. K. Chandra Sekhar, Mr. K.G. Sengupta, Mr. M.C. Goswami, Dr. Rakesh Kumar, Dr. S. Bhattacharjee and Mr. Ravi Kumar for their support in experimental work and help in analysing the results. I am also thankful to Dr. D.K. Biswas for his help in designing the injection system used in the kinetic study.

I would be failing in my duty, if I do not thank my mother, my wife Anita, daughter Aditi and son Aaditya, without whose support it would not have been possible for me to complete this work.

Pankaj Narayan Chaudhary

## **BIO DATA**

**NAME** Pankaj Narayan Chaudhary  
**DATE OF BIRTH** January 15, 1956  
**ADDRESS** Scientist  
Information and Research Division  
National Metallurgical Laboratory  
Jamshedpur 831007, India

**ACADEMIC QUALIFICATION** B. Sc.Engg. (Met. Engg),  
BIT Sindri  
I Class with Distinction  
  
M.Tech (Met. Engg),  
IIT Kanpur,

**WORKING EXPERIENCE** 9 years with Tata- Yodogawa Ltd Jamshedpur,  
India.  
  
9 years with NML, Jamshedpur,  
India.

**FIELD OF SPECIALIZATION** Process Metallurgy (Ferrous)

### **MEMBERSHIP OF PROFESSIONAL BODIES**

1. The Indian Institute of Metals
2. The Indian Institute of Foundrymen
3. The Institutes of Engineers (India)
4. The Indian Society of Non Destructive Testing

## AWARDS

The publication Trans. IIM, 38 (1985) :31 based on M.Tech. thesis work was adjudged best paper of the year for the Kamani Gold Medal.

## PATENTS

1. Patent No 897/ DEL/92 on “ An improved process for continuous production of steel by the electroslag smelting of a rod or slab made up of direct reduced iron”  
S. Banerjee, Upkar Singh, S. K. Biswas, S. Chattopadhyay, R. G. Ganguli and P. N. Chaudhary.
2. Patent No 2459/DEL/95 dated 29/ 12 /95 “ A process for the preparation of a novel flux useful for the dephosphorization of high carbon ferromanganese and an improved process therefor using the said flux” - P. N. Chaudhary, R.P. Goel, and R.K. Minj

## PUBLICATIONS:

1. A. Ghosh and P. N. Chaudhary, “ An investigation of deoxidation of liquid steel by silicon and manganese” , Trans. IIM, 38 (1985) :31
2. P. N. Chaudhary and R. P. Goel, “ Dephosphorization of liquid ferromanganese” presented during 4<sup>th</sup> Refresher course on Ferro Alloys held at N.M.L Jamshedpur during 12-14 January, 1994.
3. P. N. Chaudhary, R.P. Goel, R.K. Minj, K. Chandrasekhar and K. G. Sengupta, “ Dephosphorization of high carbon liquid ferromanganese using basic fluxes” presented during 48<sup>th</sup> ATM held at Visakhapatnam, 14-17<sup>th</sup> November, 1994.
4. A. K. Ray, P. N. Chaudhary, A. Chakraborty, Amitav Ray and K.K. Mishra, “Optimising the life of a cold mill work roll” presented during poster session at 47<sup>th</sup> ATM 1993 held at Hyderabad.
5. P. N. Chaudhary, S. Prasad and Upkar Singh , “Effective Utilization of R&D results through Feasibility Report (FR) and Detailed Project Report (DPR)” in NML Technical Journal Vol . 36, No3, July- September 1994.
6. P. N. Chaudhary, R. P. Goel, R. K. Minj and S. B. Sarkar, “ A flux based dephosphorization process for high carbon liquid ferromanganese” presented during national seminar on ferroalloy held at TISCO , organized jointly with IIM, Jamshedpur Chapter during 5<sup>th</sup>-6<sup>th</sup> May, 1995
7. A. K. Ray, K.K.Mishra and P. N. Chaudhary, “Failure analysis of rolls of cold rolling mill in steel plant” presented during “Clinic on Failure Analysis (COFA-97)” held at NML, Jamshedpur during 18<sup>th</sup>-19<sup>th</sup> February 1997.
8. P. N. Chaudhary, A.N. Sinha & K.K.Mishra , “Factors affecting roll performance” during Forged Roll Users Meet on 10<sup>th</sup> May ,1997 at H.E.C. Ranchi

9. P. N. Chaudhary, A. K. Ray, A.N. Sinha & K.K.Mishra, “ Forge Roll Life-Operation Vs Manufacture” presented during 51<sup>st</sup> ATM held at Jamshedpur during 14-17 November, 1997.
10. R.P.Goel and P. N. Chaudhary, “Pretreatment of Hot Metal for the removal of Silicon, Phosphorus and Sulphur “ Communicated for publication in the year 1998 for the book “ Iron and Steel Making : Principles and Practices “ to be published by Allied Publishers , New Delhi.

## LIST OF FIGURES

Figure No	Caption	Page No
Fig 2.1	Ellingham diagram showing oxygen potential is lower for the Formation of impure oxide	32
Fig 2.2	Phosphate capacities of various flux systems	33
Fig 2.3	Phosphorus partition ratio as a function of Mn content of Fe-Mn-C <sub>satd.</sub> Alloy	34
Fig 2.4	Ternary showing solubility of MnO in the BaO-BaF <sub>2</sub> system at 1573 K	35
Fig 2.5	Iso-sulphur removal contours on a-E map at the end of powder- injection period [65]	36
Fig 3.1	XRD pattern for BaCO <sub>3</sub>	47
Fig 3.2	XRD pattern for calcined BaCO <sub>3</sub> flux pellet sample	48
Fig 3.3	XRD pattern for unreacted flux/ slag sample	49
Fig 3.4	DTA of slag samples	50
Fig.4.1	Phosphate capacities of various flux systems	70
Fig 4.2	Liquidus line of BaO-MnO obtained by the experiment of heating BaO-MnO <sub>2</sub> briquette[20]	71
Fig 4.3	Flow sheet of the dephosphorization process carried out in induction furnace	72
Fig 4.4	Schematic of injector	73
Fig 4.5	Experimental set up for powder injection	74

<b>Figure No</b>	<b>Caption</b>	<b>Page No</b>
Fig 5.1	Predominance area diagrams at 1673 K (a) Ba-P-O system and (b) Ca-P-O systems (at standard states)	88
Fig.5.2	Predominance area diagram for Ba-P-O and Mn-O systems 1573 K (at standard states)	89
Fig.5.3	Predominance area diagram for Ba-P-O and Mn-O systems at 1773 K (at standard states)	90
Fig.5.4	Predominance area diagram for Ba-P-O and Mn-O systems at 1873 K (at standard states)	91
Fig.5.5	Predominance area diagram for Ba-P-O and Mn-O systems at 1573 K for non standard states	92
Fig.5.6	Phosphate capacities of various flux systems[27]	93
Fig.5.7	Activities of carbon and manganese at 1300-1600 <sup>0</sup> C (Standard states are for carbon and pure liquid for manganese) [76].	94
Fig.5.8	Activity of phosphorus in molten ferromanganese at 1873 K[4]	95
Fig.5.9	Variation of degree of dephosphorization with initial silicon content in HC Fe Mn alloy[23]	96
Fig.5.10	Phosphorus partition ratio between the BaO-MnO, BaO-MnO-BaF <sub>2</sub> and BaO- CaO <sub>satd</sub> -MnO fluxes and Fe-Mn-C <sub>satd</sub> . Alloy at 1573 K, 1623, and 1673 K as a function of Mn content in Fe-Mn- C <sub>satd</sub> alloy [27].	97
Fig.5.11	Relationship between oxygen partial pressure and phosphorus at different phosphate capacities [41]	98
Fig.5.12	Flow Sheet of the dephosphorization process carried out in induction furnace	118
Fig.5.13	Liquidus line of BaO-MnO obtained by the experiment of heating BaO-MnO <sub>2</sub> briquette[20]	119
Fig.5.14		

<b>Figure No</b>	<b>Caption</b>	<b>Page No</b>
Fig.5.15	Variation of degree of dephosphorization with initial silicon content in Fe-Mn	120
Fig.5.16	Variation of phosphorus content in the metal [%P] with time after addition of flux	121
Fig.5.17	Variation of degree of dephosphorization with weight of flux for different types of flux	122
Fig.5.18	Solubility of MnO in the BaO-BaF <sub>2</sub> system at 1573 K[28]	123
Fig.5.19	Variation of degree of dephosphorization with time for BaCO <sub>3</sub> + BaCl <sub>2</sub> flux	124
Fig.5.20	Differential thermal analysis (DTA) of slag samples obtained after dephosphorization	125
Fig.5.21	Results of calcination of MnO <sub>2</sub> pellets in carbolyte furnace	140
Fig.5.22	XRD results of calcination of BaCO <sub>3</sub> based pellets	141
Fig.5.23	Variation of [P] in metal with change in flux metal ratio when calcined BaCO <sub>3</sub> -MnO <sub>2</sub> -BaF <sub>2</sub> reagent was used	142
Fig.5.24	Variation of P <sub>2</sub> O <sub>5</sub> in slag with change in flux metal ratio	143
Fig.5.25	Variation of [P] in metal with change in flux metal ratio when calcined BaCO <sub>3</sub> -MnO <sub>2</sub> -BaCl <sub>2</sub> reagent was used	144
Fig.5.26	Variation of phosphorus partition ratio with change in temperature at a given flux metal ratio	145
Fig.5.27	Variation of phosphorus partition ratio with change in MnO <sub>2</sub> content in the reagent	146
Fig.5.28	Variation of (P) in slag with change in MnO <sub>2</sub> content in the reagent when calcined BaCO <sub>3</sub> -MnO <sub>2</sub> -BaCl <sub>2</sub> reagent was used	147
	Variation of phosphorus partition ratio with % MnO <sub>2</sub> content in the reagent when calcined BaCO <sub>3</sub> -MnO <sub>2</sub> -BaF <sub>2</sub>	148

<b>Figure No</b>	<b>Caption</b>	<b>Page No</b>
Fig.5.29	reagent was used Variation of (P) in slag with change in MnO content in the reagent	
Fig.5.30	Variation of MnO content in the slag with change in % MnO <sub>2</sub> content in the reagent when calcined BaCO <sub>3</sub> -MnO <sub>2</sub> -BaF <sub>2</sub> reagent was used	149
Fig.5.31	Variation of MnO content in the slag % MnO <sub>2</sub> content in the reagent when calcined BaCO <sub>3</sub> -MnO <sub>2</sub> -BaCl <sub>2</sub> reagent was used	150
Fig.5.32	Variation of (P) content in the slag with change in MnO content in the slag when BaCO <sub>3</sub> -MnO <sub>2</sub> -BaF <sub>2</sub> flux was used	151
Fig.5.33	Variation of (P) content in the slag with change in MnO content in the slag when BaCO <sub>3</sub> -MnO <sub>2</sub> -BaCl <sub>2</sub> flux was used	152
Fig.5.34	XRD pattern for unreacted slag sample	153
Fig.5.35	Schematic of a typical injection process showing various reaction zones	154
Fig.5.36	Electrical analogy of reactions involved during injection process	163
Fig.5.37	Concentration profile in the metal bulk, metal side boundary layer and slag bulk	164
Fig.5.38	Comparison of experimental data with model prediction of injection process	165
Fig.5.39	Relation showing relative contribution of transitory and permanent contact reaction	166
		167

## INTRODUCTION

Ferromanganese used for de-oxidation and alloying of steel is one of the main sources of phosphorus contamination of steel. For typical additions of ferromanganese (Fe-Mn) at 16 kg per ton of liquid steel having phosphorus content 0.35-0.40 %, the phosphorus content increases by about 30-50 ppm which makes the steel unsuitable for various applications. The high phosphorus content (~0.4%) of ferromanganese originates from the manganese ores, majority of which contain significant amount (~0.2%) of phosphorus which is reduced almost completely during carbothermic reduction of manganese ores. Low phosphorus ores are depleting fast and the coke from the steel plants contains high phosphorus (0.25%). Hence the ferromanganese plants in India will continue to produce high carbon ferromanganese with phosphorus content (>0.4%).

Attempts have been made to remove phosphorus from manganese ores but the techno - economics is not considered favorable [1]. Dephosphorization of liquid ferromanganese appears to be a more viable alternative to the removal of phosphorus using mineral beneficiation techniques. Removal of phosphorus from hot metal under oxidizing conditions has limitation because the oxide of manganese is more stable than that of phosphorus [2] and, consequently, there will be a significant loss of manganese. The alternative way of removing phosphorus as phosphides under highly reducing conditions at high temperatures is considered environmentally unfriendly since the reaction product in slag is likely to release phosphene when it comes into contact with moisture [3]. The phosphorus removal in the gaseous form is also not possible because the partial pressure of manganese is more than that of phosphorus at smelting temperatures.

In view of the above, the selective removal of phosphorus (i.e. without loss of manganese) under oxidizing and highly controlled conditions is found to be appropriate. Systematic investigations [4 -7] have been made to develop a viable

process for selective removal of phosphorus from high carbon ferromanganese using different fluxes. The reaction kinetics has been also studied for effective utilization of flux [8].

## **1.1 ROLE OF MANGANESE IN STEEL**

Ferro alloys are essential inputs in quality steel making and are used as a deoxidizer and more importantly, as alloying addition in liquid steel to impart desired properties. Amongst the ferroalloys, ferromanganese is the most widely used ferro alloy in steel making. The present consumption of ferromanganese in India is reported to be 16 kg / tonne of steel produced [9]. It is well known that manganese improves hardenability, yield strength and ultimate tensile strength of steel. Steels containing about 1 percent carbon and 11-13 percent manganese are distinguished by a high abrasion resistance [10]. These steels are used in manufacturing balls for ball mills, by the dredge parts, tramway switches etc. Manganese is also added in steel to prevent hot shortness when sulfur exceeds 0.04-0.05 % [13]. In addition, the solute strengthening of manganese is appreciable. It lowers the critical temperature and promotes the formation of fine pearlite. Manganese dissolves in solid solution of ferrite, combines with carbon to form carbides. It improves weldability, wear resistance and strength without adversely affecting the ductility of steel. It also plays a role of nitrogen carrier which helps in improving the work hardening characteristics of steel. Extra soft steels containing around 0.35 % Mn are used for deep drawing. Manganese steels with higher carbon content (0.5-0.79%) are used in making coils and springs. The HSLA steels used for gas and crude oil transportation contain around 1.2 to 2 % Mn. Austenitic Mn steel of AISI 200 series containing 5 % Mn find use in cooking appliances. Manganese is also used for improving machinability. Thus ferromanganese has been used most widely in steel making and its consumption exceeds that of all other ferroalloys combined.

## 1.2 SPECIFICATION OF FERROMANGANESE AND ITS USES

The chemical composition of the ferromanganese (4 th revision) as per IS 1171 is given in Table 1.1 [11]. The phosphorus content varies between 0.3 and 0.5 % which is not suitable for various grades of steel such as ball bearing, 20 Mn Cr , SAE 52110 where phosphorus content is specified as less than 0.025 %. It has been observed that the phosphorus content in such steels increases by about 30-50 ppm with the use of high phosphorus (0.4-0.5 %) ferromanganese. Therefore, it is desirable to use ferromanganese having phosphorus content less than 0.2 % which can be obtained by external dephosphorization of ferromanganese.

**TABLE 1.1**  
**Specification of ferro-manganese as per IS 1171**

Grade Designation	% Mn	% C	%Si,Max	% S, Max	%P, Max
-------------------	------	-----	---------	----------	---------

### High Carbon Ferro Manganese

FeMn 80	78-82	6-8	1.50	0.050	0.50
FeMn76	74-78	6-8	1.50	0.050	0.50
FeMn72	70-74	6-8	1.50	0.050	0.50
FeMn68	65-70	6-8	1.50	0.050	0.50

### Medium Carbon Ferro Manganese

2FeMn80	78-82	1-3	1.50	0.030	0.35
2FeMn76	74-78	1-3	1.50	0.050	0.35

### Low Carbon Ferro Manganese

05FeMn80	85Min	0.50	2.0	0.030	0.30
01FeMn83	80-85	0.10	1.0	0.050	0.30
02FeMn83	80-85	0.20	1.0	0.050	0.30
07FeMn83	80-85	0.70	1.0	0.050	0.30

### **1.3 EFFECT OF HIGH PHOSPHORUS ON THE MECHANICAL PROPERTIES OF STEEL**

The solubility of phosphorus in liquid iron is practically unlimited which lowers down during solidification. This leads to grain boundary segregation and results in a deterioration of mechanical properties . The solubility of phosphorus in  $\gamma$  iron phase is about 0.5 %. The presence of phosphorus in steel compresses the  $\gamma$  phase region and increases the grain size which reduces the notch toughness of steel. The transition temperature is raised by the presence of phosphorus, thus decreasing the notch toughness of steel. The presence of phosphorus makes the steel brittle. .

Segregation of phosphorus takes place at low temperatures due to low solubility and low diffusivity. This also affects the weldability of steel. It is well known that phosphorus induces cold shortness in steel and makes it unfit for low temperature application. Therefore, phosphorus content in steel should not exceed 0.025 %. Since ferroalloys are late additives in the steel making process, it is necessary to restrict the phosphorus content in the ferroalloy itself so that its entry to liquid steel is minimized.

### **1.4 ORIGIN OF HIGH PHOSPHORUS IN FERROMANGANESE**

For the production of high carbon ferromanganese, the manganese content of the ore should be about 45.0 % with a minimum Mn/Fe ratio of 6.0 and phosphorus less than 0.16 %[12]. It is found that manganese ore and coke contribute the major amounts of phosphorus (nearly 65%, 35% respectively) in the ferromanganese [36].

Majority of the recoverable reserves of manganese ores in India have phosphorus content more than 0.15 % which results in high phosphorus in ferromanganese. Ores of Madhya Pradesh - Maharashtra region, India contain around 0.6 % P though they

are high grade in terms of Mn / Fe ratio. The ores of southern Orissa (Koraput) and Andhra Pradesh (Srikakulam) contain phosphorus in the range of 0.2 to 1.0 % [14].

Since enough quantity of high grade ores from a single source are not available, several ore types containing high Mn / Fe ratio with high and low P, low Mn / Fe ratios with low phosphorus, high silica and low silica ores are blended to obtain an average composition required for feeding high carbon ferromanganese smelting furnaces. Another problem in manufacturing ferromanganese is that coke from the steel plants contains high phosphorus (~ 0.25 %). The ferromanganese industry is not willing to use low phosphorus coals because of high volatiles and ash content[15]. This will lead to increase in energy consumption. Imported coal with low phosphorus is not a favorable option because of the cost factor [15].

The requirement of manganese ores in India having phosphorus less than 0.16 % would be more than 1.0 million tonnes per annum by the turn of this century. Our low phosphorus manganese ores are depleting fast and ferromanganese manufacturers will have no option but to use medium and low grade ores having high phosphorus content. Thus the ferromanganese manufactured using these ores will continue to have high phosphorus in the product making it unsuitable for quality steel making.

### **1.5 BENEFICIATION TECHNIQUES FOR THE REMOVAL OF PHOSPHORUS FROM FERROMANGANESE ORE**

It is necessary to understand the mode of occurrence of phosphorus in manganese ores to appreciate the difficulties associated with various beneficiation techniques. Phosphorus is usually present in manganese ores as apatite, carbonate-apatite, mangan-apatite, collophane, frankolite , gorceinite kurskite , vivianite , xenotime and is often adsorbed within iron and manganese minerals. Study of manganese ore

under 1) electron microprobe and 2) scanning electron microprobe with WDS analyser shows that phosphorus is contained in the manganese phases and in the iron phase (geothite) besides being present in apatite [16]. Amorphous calcium phosphate (collophane) occasionally fills the voids in garnet. Chemical analysis showed that manganese- rich fractions are richer in iron and contain higher amount of phosphorus than silica rich fractions. Geothite contains significant amounts of  $P_2O_5$  (0.64 to 1.62 %). The phosphorus contained in geothite may be due to adsorption or chemisorption in solid solution. Geothite has the ability to accept phosphorus as the occurrence is based on a close packed hydroxyl lattice, in which tetragonal interstices are of suitable size to accommodate the phosphorus ion.

A detailed study [17] was taken up for the processing of high phosphorus ores. The ore samples were found to contain microfine grains of apatite in various proportions having  $P_2O_5$  content more than 1 %. The  $P_2O_5$  content was brought down to 0.34 % by using magnetic separation followed by flotation. The treatment cost was estimated at Rs 1250 per ton excluding the depreciation cost of the equipment and was not considered economical.

An attempt was made at RRL ,Bhubaneswar, India to remove phosphorus from ferromanganese ores. The methods consist of converting insoluble phosphorus into soluble sodium phosphate either by roasting with sodium salt at about  $700^{\circ}C$  and subsequently leaching in water or leaching ground ore in an alkaline solution but the techno-economics was not considered favorable.

Since phosphorus is intimately associated with manganese, physical beneficiation is unsuitable and chemical beneficiation is necessary. Phosphorus removal through chemical beneficiation requires comminution, flotation and / or leaching to be followed by agglomeration. However, this route is highly energy intensive whose techno- economics is not considered favorable[5].

It was therefore concluded [12] that mineral beneficiation techniques are not suitable for economic removal of phosphorus from ferromanganese ores.

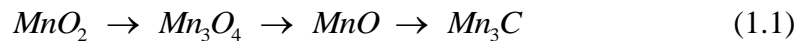
## 1.6 PRINCIPLES OF FERROMANGANESE PRODUCTION

Most of the bulk ferroalloys are produced commercially by reduction smelting of their oxide minerals with coke or charcoal in a submerged arc furnace. In general, the overall reduction reactions are highly endothermic, thus requiring large thermal energy inputs. The presence of iron oxides facilitates the reduction process due to dissolution of metal in iron and hence decreasing its activity. Further, the presence of a lower melting alloy results in better consolidation and slag-metal separation. The Ellingham Diagram shows that most of the oxide lines slope upward except the CO line[19]. That means stability of all oxides decreases with increasing temperature except for CO. Thus the smelting reduction should be conducted at temperatures higher than the temperature of intersection between MnO and CO lines in order to ensure thermodynamic feasibility of the reduction reaction at normal pressure[19]. A lower external pressure has a positive effect on the reduction reactions in which gaseous product is formed. The Ellingham diagram also suggests that all the oxides of iron and phosphorus would get reduced during the smelting of MnO. As a result the overall grade of the molten alloy is determined by the extent of oxide reduction and the burden of iron oxides and other easy-to-reduce oxides in the charge. The slag composition is determined by the total gangue from the ore, fuel, flux besides the unreacted metal oxides [19].

Manganese ores to be used for smelting ferromanganese should meet the following conditions :

- a) the content of manganese in ore should be at least 45 per cent ; a higher content of manganese ensures a higher productivity of furnace and a lower use of electric energy per ton of alloy.
- b) the content of silica in ore should be as low as possible

The reaction of manganese from pyrolusite occurs stepwise as follows:



The carbon monoxide (CO) produced can also reduce manganese oxide at lower temperatures. The energy efficiency of the process is enhanced by utilizing the CO formed by direct reduction for subsequent indirect reduction. Ferric oxide is reduced with carbon monoxide at low temperatures. Ferrous oxide is first reduced with CO at 500-600 ° C and after that with solid carbon in the deeper zones of the bath. With a reducing atmosphere in the furnace, the dissociation of manganese oxides take place at lower temperatures. Carbon monoxide can also reduce  $Mn_3O_4$  to MnO at low temperatures.

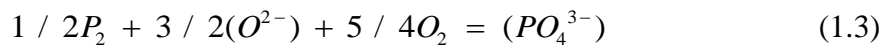
Energy requirement for the reaction (1.2) is 1.52 kwh /kg-metal. However, additional heat is required for melting the metal and slag and raising their temperature (for clean separation) as well as the gas temperature to the requisite values. It was estimated [19] that the heat requirement is about 2.45 kwh /kg for

smelting manganese ore. Because of such large thermal requirement, it is a standard practice to produce ferromanganese in a submerged arc furnace where the arc provides necessary heat thus maintaining the reaction zone at suitably high temperatures. The reducing conditions in the furnace ensure that phosphorus is reduced almost fully. The acid slags can not absorb phosphorus. Only about 20 pct phosphorus is removed with furnace gases and remaining 80 pct passes into the alloy. Phosphorus is a harmful impurity in ferromanganese. This must be removed before the ferromanganese is used in steel making for various applications.

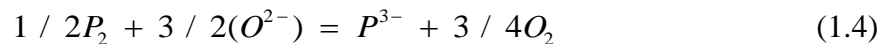
### 1.7 VARIOUS REACTION SCHEMES FOR DEPHOSPHORIZATION

Various reaction schemes considered for dephosphorization are as follows:

- I) Reaction between ferromanganese and a basic flux under oxidizing conditions, wherein the product is a phosphate as shown below :



- II) Reaction with basic fluxes under reducing conditions wherein phosphorus is removed as a phosphide as follows:



- III) Removal of phosphorus in vapor form as phosphene gas (through reaction between phosphorus and hydrogen dissolved in liquid metal ) as follows[20]:



Gaseous dephosphorization may also include the following reaction:



Gaseous dephosphorization may be useful only for metals with high phosphorus activity (for example Fe-Si and Fe-Cr-Si alloys). At 1300°C, the partial pressure of

manganese above high carbon ferromanganese is about  $6 \times 10^{-4}$  atm which is much higher than the partial pressure of phosphorus ( $3 \times 10^{-10}$  atm or lower). Application of this method for treating ferromanganese only results in enriching phosphorus instead of removing it.

The reaction product under reducing condition is phosphide. The presence of phosphide in the slag is likely to cause formation of toxic phosphene in contact with moisture, rendering this approach undesirable. Moreover this method is ineffective for high carbon ferromanganese. In case of using metallic Ca, Ba for dephosphorization under reducing conditions, the formation of  $\text{CaC}_2$  or  $\text{BaC}_2$  decreases the solubility of Ca / or Ba in the metal. When  $\text{CaC}_2$  or  $\text{BaC}_2$  are used, these carbides can not be dissociated into Ca or Ba and C for carbon saturated system.

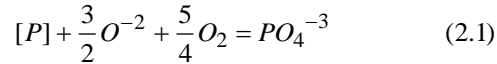
In view of these difficulties, the favorable choice is considered to be dephosphorization of ferromanganese under oxidizing conditions. However, the main problem in this route is the loss of manganese because the oxide of manganese is more stable than that of phosphorus at smelting temperatures[2]. Since ferromanganese is produced by carbothermic reduction process, it is also not possible to remove phosphorus during manufacturing. The treatment of liquid ferromanganese by means of a suitable flux for selective removal of phosphorus over manganese under oxidizing conditions is considered to be more viable alternative to any other processing techniques.

## 2.0 LITERATURE REVIEW

Ferromanganese is used as a deoxidizing and alloying agent in steel making. The high phosphorus levels in ferromanganese produced in India and most industrialized countries continue to be a problem in quality steel making. Majority of manganese ores contain significant amounts of phosphorus (>0.2%) most of which enters into the ferromanganese produced by carbothermic reduction of manganese ore. The dephosphorization of liquid ferromanganese has received considerable attention in the last decade[20-41]. Salient features of these work have been reviewed critically in this section, after defining some basic thermodynamic parameters which have been used frequently later on:

### 2.1 Definition of basic thermodynamic parameters:

Dephosphorization Equation: The oxidation of phosphorus dissolved in liquid ferromanganese by a basic slag can be written as:



for which the equilibrium constant ( $K_{2.1}$ ) can be expressed as:

$$K_{2.1} = \frac{(w_{PO_4^{3-}})f_{PO_4^{3-}}}{[a_P] \cdot (p_{O_2})^{5/4} \cdot (a_{O^{2-}})^{3/2}} \quad (2.2)$$

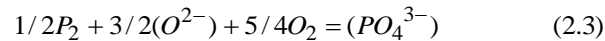
where  $w_{PO_4^{3-}}$  is the weight pct of phosphorus as phosphate in slag, ( $p_{O_2}$ ) is the partial pressure of oxygen.

From equation (2.2) it is obvious that to promote dephosphorization the favorable conditions are:

- i) a high activity coefficient of phosphorus( $f_{[P]}$ ) and a high oxygen partial pressure( $p_{O_2}$ ),
- ii) a high oxygen activity ( $a_{O^{2-}}$ ) in slag and a low activity

coefficient of the phosphate ion ( $f_{PO_4^{3-}}$ ) in the slag phase. A low temperature is also beneficial since the reaction involved is exothermic,

**Phosphate Capacity:** The phosphate capacity ( $C_{PO_4^{3-}}$ ), which is a measure of the ability of slag to absorb phosphorus in the form of phosphate, was first introduced by Wagner [31] who based his definition on the following reaction:



$$C_{PO_4^{3-}} = \frac{(w_{PO_4^{3-}})}{P_{P_2}^{1/2} \cdot P_{O_2}^{5/4}} = K_1 \frac{(a_{O^{2-}})^{3/2}}{f_{PO_4^{3-}}} \quad (2.4)$$

where  $w_{PO_4^{3-}}$  is the weight pct of phosphorus as phosphate in slag,  $P_{P_2}$  is the partial pressure of phosphorus.

From the above definition, the phosphate capacity is a function of the composition of slag, basicity and the temperature.

**Phosphorous Partition Coefficient:** This is an important parameter to measure the extent of dephosphorization and is defined as:

$$L_P = \frac{(\%P)}{[\%P]} \quad (2.5)$$

Where (%P) is the weight of phosphorus in slag and [%P] is the weight of phosphorus in metal.

Since, moles of phosphorus in slag = moles of phosphate in slag

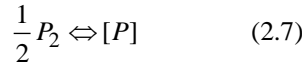
( one mole of phosphorus is oxidized to provide one mole of phosphate)

$$\frac{(\%P)}{M_P} = \frac{(w_{PO_4^{3-}})}{M_{PO_4^{3-}}}$$

Substituting the value of (%P) in equation (2.5)

$$L_P = \frac{M_P}{M_{PO_4^{3-}}} \cdot \frac{w_{PO_4^{3-}}}{[\%P]} \quad (2.6)$$

A relation between gaseous phosphorous and the dissolved phosphorous can be obtained by considering the following equation:



The equilibrium constant for this equation can be written as:

$$K_{2.7} = \frac{f_P [\%P]}{p_{P_2}^{1/2}} \quad (2.8)$$

An effective relation between phosphate capacity and partition ratio can be obtained by combining Eq. (2.4), Eq. (2.6) and Eq. (2.8) as:

$$\log L_P = \log C_{PO_4^{3-}} + 5/4 \log PO_2 + \log f_P - K_{2.7} - \log \left( \frac{M_P}{M_{PO_4^{3-}}} \right) \quad (2.9)$$

Equation (2.9) correlates partition ratio with phosphate capacity.

The partition ratio is the most reliable parameter to measure the extent of dephosphorization, since the ratio can be directly obtained from chemical analysis of flux and metal. However, the ratio depends on oxygen partial pressure (as per equation 2.9) which limits the comparison to systems that have the different partial pressure of oxygen. The ratio further indicates regarding the amount of flux required to carry out a certain percent of dephosphorization. A larger value of  $L_p$

means a certain amount of dephosphorization can be carried out with lower amount slag.

### Oxygen potential :

The Gibbs energy data indicate the relative stability of various oxides at a given temperature under the conditions of standard states. From the Gibbs energy data, the partial pressure of oxygen in equilibrium with a pure metal and its pure oxide is obtained as given below:

$$\Delta G^\circ = RT \ln p_{O_2(\text{equilibrium})} \quad (2.10)$$

The quantity  $RT \ln p_{O_2(\text{equilibrium})}$  is called the oxygen potential of the system. For the formation of impure oxide (activity less than unity) from pure metal the required oxygen potential is lower than that for the formation of pure oxide as shown in the Fig.2.1, whereas if the metal is impure then the required oxygen potential is raised i. e. it is difficult to oxidize. Since the activity of phosphorus penta-oxide ( $P_2O_5$ ) is reduced when present as phosphate in a slag solution, it should be possible to remove phosphorus from a liquid alloy even at relatively low oxygen potentials.

## **2.2 Dephosphorization under oxidizing conditions:**

As discussed in Section 1.7 dephosphorization of ferromanganese has been investigated under oxidizing as well as reducing conditions. However, much more attention has been devoted to dephosphorization under oxidizing conditions due to the following advantages: a) the activity coefficient of phosphate is much less (of the order of 0.5) compared to the activity coefficient of phosphide (of the order of

10) in molten basic fluxes. Thus the flux consumption is much less for the formation of phosphate than phosphide (see Appendix 1 for sample calculation). b) unlike oxidizing conditions, there is need to maintain extremely low  $PO_2$  ( $10^{-21}$  to  $10^{-25}$  atm) under reducing conditions c) phosphate formation being exothermic is favored at lower temperatures. d) The reaction product under reducing condition is phosphide which produces toxic phosphene in the presence of atmospheric moisture.

Several investigations have been carried out on dephosphorization of manganese-based alloys under oxidizing conditions as discussed below:

Fujita et. al. [20] used different fluxes such as  $BaCO_3$ ,  $BaCO_3 / BaCl_2$ ,  $Li_2CO_3$ ,  $Na_2CO_3 / NaF$ ,  $CaCO_3, CaCl_2$  for the removal of phosphorus from synthetically prepared liquid Fe-Mn-C-P alloys. They carried out experiments on a 70 kg scale using a flux to metal (weight) ratio of 0.04. For manganese content in the alloy ranging from 5 to 60 %, they achieved a maximum phosphorus partition coefficient in the range of 15-20. They observed that dephosphorization hardly proceeds with  $CaCO_3$  - based fluxes and amongst the various fluxes investigated the  $BaCO_3$  -based fluxes showed highest dephosphorization capability. They further observed that dephosphorization by  $BaCO_3$  based fluxes is i) favored at lower temperatures (1300-1500<sup>o</sup>C), ii) increases with carbon content and reaches a maximum near about its solubility in iron (6-7%), iii) favored at lower contamination of flux by  $SiO_2$ . However, their work was confined to manganese content in the range 5-60%, while in conventional high carbon ferromanganese, the manganese content is usually more than 70%.

Ma et. al. [21] derived the favorable thermodynamic conditions for removing phosphorus using BaO-based fluxes while avoiding oxidation of manganese in Mn-based alloys by constructing the predominance area diagrams for the Ba-P-O ternary superimposed with the Mn-MnO line. On the basis of theoretical analysis, they used  $BaCO_3$  flux for dephosphorization of synthetically prepared Mn-Fe-C-P alloys. They observed that dephosphorization in Mn-based alloy attains equilibrium within 7

minutes and for all subsequent experiments 7 minutes was chosen to represent the condition of near equilibrium for dephosphorization. They reported the optimum quantity of the  $\text{BaCO}_3$  flux to be 15 pct of the ferromanganese alloy because beyond that quantity there was no noticeable improvement in dephosphorization. They further quantified the percentage reduction of phosphorus with temperature varied in the range of 1573 to 1673 K, initial carbon varied in the range of 3.31 to 6.66%, and silicon content from 0.13 to 0.48% and observed that dephosphorization is favored at high carbon (6-7%), low silicon content (0.1 to 0.2%) and low temperature (1573-1623K). They also found that the dephosphorization reaction is of the first order. They reported a maximum of 60% removal of phosphorus under most favorable experimental conditions (C-6.66%, Si-0.13%, T-1573K) for an initial phosphorus content of 0.78%.

Lee et. al.[22] used  $\text{BaCO}_3$ ,  $\text{BaCO}_3/\text{BaCl}_2$  flux for the treatment of ferromanganese. The experiments were carried out in a 3.4 kg induction furnace using about 300 g barium carbonate as flux and they found that dephosphorization reached near equilibrium in 15 minutes. In comparison Ma et al.[21] had observed a similar equilibrium being attained in 7 minutes; however, with a smaller quantity of alloy (<100g). They also found that when barium carbonate is used as a flux rather than barium oxide, no auxiliary oxygen supplier (like, MnO, or bottom injection of  $\text{CO}_2$  or oxygen as carrier gas) is required since the decomposition of  $\text{BaCO}_3$  supplies the required  $\text{CO}_2$  gas in the melt. They further observed that the initial silicon content has a direct impact on the oxygen potential of the melt and demonstrated that phosphorus can be removed in the form of phosphate under moderately oxidizing conditions when the initial silicon content does not exceed 0.6%.

In a more recent study Lee [23] investigated dephosphorization of high carbon ferromanganese alloy (3.5 kg) in a graphite crucible by varying the  $\text{BaCO}_3$  addition from 1.4 % to 8.6 % of the weight of ferromanganese alloy. It was found that the

degree of dephosphorization increased with increasing addition of BaCO<sub>3</sub> up to 7%. The effect of substitution of BaCO<sub>3</sub> with Na<sub>2</sub>CO<sub>3</sub>, CaCO<sub>3</sub>, BaF<sub>2</sub>, BaCl<sub>2</sub>, CaF<sub>2</sub> and SiO<sub>2</sub> in different proportions was also examined. It was found that the degree of dephosphorization is enhanced by BaF<sub>2</sub> but deteriorated by BaCl<sub>2</sub>, CaF<sub>2</sub> and SiO<sub>2</sub>. The maximum extent of removal of phosphorus was about 50 % for silicon content less than 0.2 % in the alloy. The slag formed contained a large amount of MnO (>55%) indicating a significant loss (7%) of manganese into the slag phase. Higher manganese in the slag also adversely affects the phosphate capacity of the slag.

Sano [24,35] compared the phosphate capacity of various flux system as shown in Fig 2.2. It is seen that logarithm of  $C_{PO_4^{3-}}$  for BaO- BaF<sub>2</sub> flux ranges from 24 to 27 compared to 23-24 and 19-20 for the CaO- CaF<sub>2</sub> and CaO- SiO<sub>2</sub>-FeO slags respectively. Thus the phosphate capacity of the BaO-BaF<sub>2</sub> system is higher than that of the CaO-CaF<sub>2</sub> system by 3 orders of magnitude. Further the presence of silica in the flux deteriorates its phosphate capacity.

Nassaralla et. al. [33] investigated the dephosphorization of liquid steel using comparatively cheap CaO-Al<sub>2</sub>O<sub>3</sub> and CaO-Al<sub>2</sub>O<sub>3</sub>-CaF<sub>2</sub> fluxes in preference to the costly BaO-based fluxes. The eutectic composition of 38 pct CaO -22 pct Al<sub>2</sub>O<sub>3</sub>-40 pct CaF<sub>2</sub> was chosen as a master flux to study the effect of addition of BaO, Li<sub>2</sub>O and Na<sub>2</sub>O. Addition of BaO increased the phosphorus partition ratio by a factor of 4.6 ( $L_P=0.15$ ) for additions of BaO up to 30 pct ( $X_{BaO} = 0.15$ ) at 1400<sup>0</sup> C. Addition of Li<sub>2</sub>O increased the phosphorus partition ratio by a factor of 14 ( $L_P=13$ ) for Li<sub>2</sub>O additions up to 10 pct ( $X_{LiO_2} =0.23$  ). Addition of Na<sub>2</sub>O increased the  $L_P$  by a factor of 15 ( $L_P=15$ ) for Na<sub>2</sub>O content up to 3.5 pct or  $X_{Na_2O} = 0.04$ . It is interesting to note that the  $L_P$  can not exceed a value of 1 even by adding highly basic BaO in CaO-based slag. Addition of Li<sub>2</sub>O and Na<sub>2</sub>O appears to be effective (a  $L_P$  of the order of 10 could be realized). Thus the phosphate capacity of these eutectic lime based compositions increased in the following order Na<sub>2</sub>O > Li<sub>2</sub>O >.BaO. It is interesting to note that  $L_P$  can not exceed a value of 1 even by adding

BaO in CaO- based slag. Addition of  $\text{Li}_2\text{O}$  and  $\text{Na}_2\text{O}$  appears to be effective ( a  $L_p$  of the order of 10 can be realized. Further the phosphate capacity of these slags increased four orders of magnitude with the decrease in temperature from 1500 to  $1300^\circ\text{C}$ . However these fluxes may not be suitable for high carbon ferromanganese because the partition ratio of phosphorus decreases with increase in manganese content of the alloy necessitating the use of much stronger flux of higher basicity than lime based flux.

Wang et. al. [34] carried out dephosphorization of liquid ferromanganese using 50 CaO- 30  $\text{CaF}_2$ -20  $\text{Mn}_2\text{O}_3$ . Under the best possible experimental conditions they could achieve dephosphorization up to 40 % at  $1500^\circ\text{C}$ . The reason for low degree of dephosphorization may be the use of relatively higher temperature as well as the calcium oxide based reagents known for their low phosphate capacity[24].

Sano et al. [35] reported that BaO-MnO slags are suitable for the treatment of Fe-Mn alloys for the removal of phosphorus without a loss of manganese. Further the BaO-MnO system forms a liquid solution over a concentration range even at 1573 K. Also  $\text{BaF}_2$  addition was reported to decrease the  $L_p$  value but it widened the concentration range in which liquid solution forms.

In a yet another recent investigation [27] Watanabe et. al. carried out oxidative dephosphorization of synthetically prepared carbon saturated Fe-Mn alloy with BaO-MnO, BaO-MnO- $\text{BaF}_2$  and BaO- $\text{CaO}_{\text{satd}}$ -MnO fluxes at temperatures between 1573-1673 K and found that phosphorus partition ratio decreased with increase in temperature. They further noticed that at a fixed temperature, the partition ratio of phosphorus decreased with increase in the manganese content of the alloy (Fig. 2.3). The figure shows that at 75 % Mn the partition ratio of phosphorus increases from 4 to about 10 when temperature is decreased from 1673 to 1623 K and may possibly become 30 when temperature is further reduced to 1573 K. The above results indicates that BaO-MnO flux may be useful for the removal of phosphorus from high carbon ferromanganese if the flux could be melted at 1573 K. Interestingly they

further found that BaO-MnO flux could be melted at 1573 K in presence of carbon. The carbon in the form of BaC<sub>2</sub> in BaO-MnO flux helps in lowering the melting temperature of flux. They also reported that the manganese partition ratios between the BaO-MnO flux and Fe-Mn-C<sub>satd</sub> alloy were at 0.64, 0.33, and 0.23 at 1573, 1623, and 1673 K respectively indicating that the manganese content in the metal will be higher with increase in temperature at a fixed composition of flux.

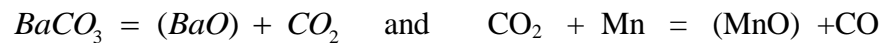
Shim et al [28] studied the thermodynamic properties of the ternary BaO-MnO-BaF<sub>2</sub> flux system by equilibrating the flux with an Ag-Mn alloy using a gas mixture of CO/CO<sub>2</sub> at 1573 and 1673 K. They observed that the solubility of MnO is higher at higher partial pressures of CO<sub>2</sub> and this fact was attributed to the presence of a carbonate phase. Further the MnO solubility decreases with increasing BaF<sub>2</sub> content of the flux (Fig.2.4).

In a recent work [38], Liu et al. studied the equilibrium distribution ratio of phosphorus between BaO-BaF<sub>2</sub>-MnO slags and Mn(62-73%) -Fe-C<sub>sat.</sub>-P alloys using different slag compositions at temperatures 1573-1673 K. The results indicated that the phosphate capacity of BaO-BaF<sub>2</sub>-MnO slags increases with increase in the BaO content and decreases with MnO content. Continuing with this study, Liu et al. reported in a subsequent paper [39] that the equilibrium distribution ratio of manganese increased with increase in oxygen partial pressure and BaO content in the slags. However, as mentioned above higher BaO is advantageous for dephosphorization. Therefore, for selective dephosphorization, the amount of BaO in the slag needs to be optimized. In a more recent study Liu et al.[41] investigated dephosphorization of ferromanganese alloys containing 70% Mn and 7% carbon using BaO-based flux containing 50% BaO, 30% BaF<sub>2</sub> and 20% MnO in a 1 kg scale in an induction furnace and reported a 70-80% phosphorus removal at 1300<sup>o</sup>C and a flux consumption of 10 weight percent. The manganese loss was restricted to 0.4%. However, the manganese loss was more (about 5%) when barium carbonate was used as a flux which indicated to higher oxygen

potential in the system due to release of CO<sub>2</sub> from the decomposition of BaCO<sub>3</sub>. High carbon content (6-7pct) in ferromanganese was found to be favorable for dephosphorization. The dephosphorization capacity of flux was found to decrease with increase in reaction temperature but it has favorable effect on reducing the manganese loss. They reported a decrease in the MnO content in slag from 24.3 % to 16.4 % when temperature was increased from 1573 K to 1673 K.

The above discussions focused mostly on laboratory scale tests which use synthetically prepared ferro-manganese alloys and various flux systems. There have been few studies on dephosphorization of ferromanganese at larger scale, except that by Liu et al.[41], who investigated the use of BaO-based fluxes for selective dephosphorization of ferromanganese in a 1 kg scale induction furnace. Similarly, the use of Barium Carbonate as a flux has remained largely un-investigated despite its commercial potential as a low cost flux and the additional advantages as discussed below. Besides, they did not pay much attention to enhance the reaction kinetics of the process to bring down the time of dephosphorization to a practical level. so as to render the process scheme economically viable.**Advantage of BaCO<sub>3</sub> over BaO**

1. The addition of *BaCO<sub>3</sub>* helps in the formation of low melting point slag of BaO+MnO as per the reaction given below:



2. The gases generated from the decomposition of BaCO<sub>3</sub> helps in stirring the bath for effective mass transfer as well as supplies oxygen for phosphorus oxidation
3. The presence of carbonate ions and the presence of carbon helps in lowering the melting temperature of flux[28].
4. For a given activity of MnO, the activity coefficient of MnO is higher due to weaker interaction between *BaCO<sub>3</sub>* and MnO than that between BaO and MnO and therefore, manganese loss will be more which is restricted by adding mixture of *BaCO<sub>3</sub>* and BaF<sub>2</sub> since there is a strong repulsive interaction between *BaCO<sub>3</sub>* and BaF<sub>2</sub> [28].
5. Lower cost of *BaCO<sub>3</sub>* compared to BaO.

Some industrial scale trials has been conducted in India using lime as well as

barium based fluxes which are briefly reviewed below:

Trial runs were conducted by Tata Steel at their ferromanganese plant, Joda, India [36]. The reagents used were mixtures of lime-mill scale and Soda-mill scale. It was found that the overall efficiency was poor and the degree of dephosphorization never exceeded 15%. The reason could be a lower phosphate capacity of the lime based slag [24]. Soda ( $\text{Na}_2\text{O}$  bearing agent) is usually considered to be highly basic than BaO but it is unstable at high temperatures which results in a high oxygen potential ( $\text{Na}_2\text{O} = 2 \text{Na} + \text{O}_2$ ) and is not suitable for dephosphorization of Fe-Mn owing to the loss of manganese [3].

Laboratory scale as well as plant scale trials were conducted by researchers at SAIL, India [37] using barium based fluxes. About 25-40 % phosphorus could be removed when the flux was added in a 30kg induction furnace. But only 15 % phosphorus could be removed in large scale trials. The reason for the poor efficiency of flux was attributed to an incomplete dissociation and dissolution of flux in the absence of adequate heating of ladle and insufficient superheat available with metal.

In view of the above discussion, the fluxes used so far for the oxidative dephosphorization of ferromanganese suffer from the following drawbacks:

- a) Lower phosphate capacity due to improper composition of flux used.
- b) Loss of manganese in the slag. Further, the presence of higher manganese oxide (MnO) content in the slag reduces its phosphate capacity.
- c) Difficulty in melting BaO- MnO flux at moderate temperatures ( $< 1673 \text{ K}$ ) due to high melting points of pure BaO and MnO namely  $2198 \text{ K}$  and  $2058 \text{ K}$  respectively
- d) Loss of effectiveness of flux at high level of silicon ( $> 0.2 \%$ )
- e) Lower partition ratio of phosphorus when BaO-MnO flux is used for dephosphorization of high carbon ferromanganese having Mn content ( $> 70 \%$ ). The partition ratio decreases with increase in melting temperature of flux and increase in manganese content of the alloy.

## 2.3 DEPHOSPHORIZATION KINETICS

The dephosphorization process is a heterogeneous one consisting of following stages: i) transfer of phosphorus from the bulk of metal to the interface of “metal bulk” - “metal side boundary layer” (mixing in the metal bulk), ii) transfer of phosphorus through “metal side boundary layer” (mass transfer on the “metal side boundary layer”), iii) chemical reaction at the interface, iv) transfer of reaction product (phosphate ion) through “slag-side boundary layer” (mass transfer in the “slag boundary layer”), v) transfer of phosphate ion from the interface of “slag side boundary layer” - “slag bulk” to the bulk of the slag (mixing in slag phase). The above mentioned steps may be viewed as several mass transfer resistances in series. Sometimes, step (i) and (ii) collectively represent the overall mass transfer resistance on the metal side and similarly step (iv) and (v) collectively represent that for slag side. At high temperature, as in the present case (1573-1773 K) the rate controlling steps are most frequently transport barriers whereas chemical reaction is not a problem. Therefore, it is required to have a brief discussion on mass transfer resistances for species transport through bulk as well as boundary layer.

### Mass Transfer in Boundary Layer:

The rate of transfer of a species i through a boundary layer can be represented as:

$$\eta_i = k_m A (C_i^{\text{int}} - C_i^b) \quad (2.11)$$

Where  $k_m$  is known as mass transfer coefficient and A is the surface area across which mass transfer is taking place,  $C_i^{\text{int}}, C_i^b$  refer to the interface and bulk

concentration of species 'i' respectively. Obviously, the reaction rate is possible to increase by increasing mass transfer coefficient, surface area and the concentration gradient. In general, the mass transfer coefficient ( $k_m$ ) depends on the geometry, location, fluid velocity, and other properties of the fluid. For unsteady state situation, it also depends on time. If mass transfer is the only rate controlling step, then interfacial equilibrium can be assumed. In literature [45], various interesting models for mass transfer coefficients are available.

### Mass Transfer Models

a) when mass transfer occurs as diffusion through a film, the mass transfer coefficient is defined as

$$K_m = \frac{D}{\delta} \quad (2.12)$$

$\delta$  is the thickness of the film also called diffusion layer and D is the diffusion coefficient

This model assumes a stagnant film which is an idealization of complex flow situation. The more practical is the surface renewal model.

b) The surface renewal models (or penetration theory) postulates that a fluid comes in contact with the surface for a certain time period, during which unsteady diffusion occurs between the fluid element and the surface. At the end of this time period, the fluid element is swept away from the surface and replaced by a new element from the bulk. The mass transfer coefficient for low concentration of the diffusing substance is given as[45]:

$$K_m = 2 \left( \frac{D}{\pi \cdot t_e} \right)^{1/2} \quad (2.13)$$

where  $t_e$  is the contact time

In the case of bubble rising in a liquid , the contact time between the bubble and a fluid element in its path may be approximated by:

$$t_e = \frac{d_b}{u_b} \quad (2.14)$$

where  $d_b$  and  $u_b$  are the bubble diameter and velocity respectively.

Since the rising velocity of bubble is well established, the surface renewal model provides a convenient way of calculating mass transfer coefficient. Danckwerts defined the mass transfer coefficient as below:

$$K_m = (D_i S)^{1/2} \quad (2.15)$$

where S is known as Danckwerts surface renewal factor which is to be determined experimentally. It varies from 10 per sec for mild turbulence to 300 per sec for violent turbulence [46,].  $D_i$  is the diffusion coefficient of the species being transferred through molten alloy .

In addition to these theoretical models, several empirical correlations are available in literature for determination of mass transfer coefficient for different situations in the following general form:

$$Sh = f(Re, Sc)$$

where, Sh is the sherwood number (non-dimensional mass transfer coefficient), Re and Sc are the Reynold and Smith number respectively.

Some investigator[48] has correlated the overall mass transfer resistance on metal side (mixing + mass transfer on the boundary layer) with stirring energy and dimension of the vessel as:

$$\log K_m = 1.98 + 0.5 \log(\xi \cdot H^2 / L / 100) - 125000 / RT/2.5 \quad (2.16)$$

$\xi$  stirring energy (W./ Kg)

- H bath depth (cm)
- L diameter of furnace (cm)

The phenomenon of mixing has frequently and successfully been correlated with the stirring energy input. In this context the empirical correlation proposed by Nakanishi et. al. [49] for recirculatory flow as encountered in ladle metallurgy, may be mentioned:

$$t_{mix} = 800. \xi^{-0.04} \quad (2.17)$$

#### Powder injection in the melt:

From the above discussion, it is clear that the resistance due to mass transfer and mixing can be reduced by introducing stirring in the system. Again the rate of phosphorus transport can be enhanced by increasing the slag-metal interfacial area. Powder injection provides both the advantages of stirring ( buoyant energy of bubbling of carrier gas) and enhanced interfacial area (powder particles) to increase the rate of transport manifold.

In injection process, solid particles are injected into the liquid alloy with the help of a carrier gas. In contrast to top slag addition, it offers one more reaction zone, the transitory reaction zone, besides the permanent reaction zone at the top slag metal interface. In transitory contact zone the rising slag drops, forming at the moment of injection of a gas powder stream into the metal, react during their passage through melt. This additional reaction zone as well as stirring by the input carrier gas enhances the kinetics of the process. There have been several investigations [51-58] on desulphurization of hot metal by powder injection, however, the injection in ferromanganese is scarce. These studies incorporated the mechanism of enhanced kinetics of injection technique. While some author attached importance to transitory

reaction of slag drops during their ascent through melt, some added importance on permanent reaction at the top slag-metal interface. Sidorenko et. al. [50] studied the effect of ladle injection of powder mixture of lime and fluorite in hot metal on removal of non-metallic inclusions. Their calculation showed that in a 10-t arc furnace 65 % of phosphorus is removed into the slag drops (formed during injection at the bottom) while traveling through the hot metal to join top slag. Remaining 35 % of phosphorus is removed into the slag drops re-trapped from the metal surface by its volume. This study shows that transitory contact zone contributes more than permanent contact zone in the removal of phosphorus from hot metal. In similar tune to Sidorenko, Turunen[59] showed that injection lance depth had some effect on desulphurization using CaO-CaF<sub>2</sub> flux and this suggest a large contribution from transitory contact zone. Tanaka et al.[60] deduced that transitory reaction more important from a comparison of results of submerged injection and gas stirring experiments using a theoretical model. Wada et al.[61] concluded that the permanent contact reaction during flux injection was more important than the transitory reaction because desulphurization behavior was largely influenced by the properties and composition of the top slag, and the characteristic of the injection powders scarcely affected the result. Tanabe and co-workers[62-64] reported that the permanent contact reaction dominated the desulphurization process, on industrial scale plant making use of the top slag without submerged powder injection and has observed that desulphurization performance using only a top slag with gas stirring was by no means inferior than that of the CaO – CaF<sub>2</sub> – Al<sub>2</sub>O<sub>3</sub> powder injection process.

Ohguchi and Robertson [65] proposed a mathematical model to calculate the separate contribution of the transitory and permanent - contact reactions for submerged injection of CaO based powder to desulphurize molten iron. The effect of transitory and permanent contact reaction which were taken care of by two non-dimensional parameters like ‘a’ and ‘E’ respectively in the model. A infinite ‘a’

represents species equilibrium at the permanent contact interface, while 'E' equal to one represents equilibrium at the transitory contact zone. The model also enables one to make quantitative evaluation of the 'excess' desulphurization and sulfur reversion. They showed that a rapid permanent contact reaction is rather harmful at larger E values because uneconomically excess species transport beyond equilibrium value takes place to the slag phase which later on reverts back to metal phase(Fig. 2.5). However, a increase in 'a' at lower values of 'E' was found to be beneficial. They further observed that for larger values of 'a' the boundary between excess and no excess desulphurization occurs at constant 'E' values. The model was applied to simulate the data from small scale powder -injection experiments.

Seshadri et. al.[66] modified the existing injection model to takes into consideration the direct effect of variables like gas flow rate, injection depth, top slag volume, powder flow rate, particle size and solid-gas ratio. The results of the model showed that for a given powder mixture, the contribution to desulphurization in the permanent reactor can be improved by increasing the total gas flow rate, temperature, top slag volume (avoiding sulphur in the top slag), slag-metal interface area (through emulsion formation) and minimizing the quantity of carry over slag. The efficiency of the transient reactor is improved by optimizing the variables which result in an increase in the solid metal interface areas as well as residence time of the particles and bubble inside the melt, such as depth of injection, powder flow rate, particle size and solid gas ratio.

First industrial scale injection trial in India has been carried out in Rourkela Steel Plant, Orissa, India for desulphurization [55] of hot metal. The carbide based reagent is injected through the lance using air as a carrier gas (pressure  $5 \text{ kg/cm}^2$ ) dried upto a dew point --40 degree. The injection rates are kept around 35 to 60 kg / minute. At this rate the treatment is completed within 8 to 10 minutes. The sulfur level in hot metal is usually reduced from 0.08 to 0.01 at a flux rate of 6.5 kg/ thm.

The Bokaro Steel Plant is also reported to have conducted several trials using side injection of  $\text{CaC}_2$  as well as Mg based reagents in order to generate strong stirring effect [56]. Tata Steel also installed injection facility in 1994 [57] for the purpose of desulphurization. The sulfur level in hot metal is reduced to 0.015-0.02 % from the initial level of 0.07 %. Certain constraints are faced during injection such as a) heavy crust formation on top of the ladles making movement of the ladle difficult, b) temperature drop which makes the slag solid and hard thus deslagging can be difficult, c) lower lance life d) blockage in the system when lime based reagent is used because of hygroscopic nature of lime. This indicates that injection process causes lot of heat loss from the system and therefore, studies should be aimed to reduce the time of injection process such that heat loss can be restricted to a reasonable level.

## **2.4 SUMMARY OF LITERATURE REVIEW**

1. Dephosphorization of ferromanganese by oxidizing technique is difficult to achieve because the oxide of manganese is more stable than that of phosphorus at smelting temperatures [2].
2. In order to prevent the loss of manganese, attempts have been made to remove phosphorus from ferromanganese under extremely reducing conditions using metallic Calcium [21,23] but the resulting slag was found to be environmentally unfriendly. Also calcium treatment may not be applicable for high carbon ferromanganese because of its preference to form carbide instead of phosphide.
3. An alternate method for minimizing the loss of manganese could be the selective removal of phosphorus from ferromanganese under oxidizing condition by maintaining the partial pressure of oxygen under close control.[20, 21,23].

4. The partial pressure of oxygen ( $P_{O_2}$ ) corresponding to Mn-MnO equilibria is much lower ( $\sim 10^{-18}$ ) than that of Fe-FeO equilibria ( $\sim 10^{-12}$ ). Therefore, dephosphorization of ferromanganese is required to be carried out at lower oxygen potential compared to dephosphorization of iron based alloys, which necessitates the use of flux of high phosphate capacity for dephosphorization of Mn-based alloy[23].
5. From a theoretical study, BaO-MnO based flux was identified as a suitable flux for dephosphorization of ferromanganese under oxidizing conditions [3,19]. However, a major drawback of this flux is the high melting points of both the flux constituents, BaO and MnO (i.e. 2198 K and 2058 K respectively). As the conventional method of removal of phosphorus requires low temperatures, the BaO based flux may pose real difficulty. Moreover, with increase in temperature phosphate capacity of the flux decreases [3]. Fortunately, a later publication reported [27] BaO-MnO flux can be melted at lower temperature in presence of carbon.
6. As reported recently by the researchers of Tokyo University [27] the efficacy of BaO-MnO flux for dephosphorization of high carbon ferromanganese may be severely restricted for alloys with manganese content more than 70%.
7. Use of BaF<sub>2</sub> as additive has been found to reduce the melting temperature of the flux, and more importantly it was found to reduce manganese loss when added to BaO-based flux. Therefore, BaO-MnO-BaF<sub>2</sub> flux has emerged as an effective reagent for selective dephosphorization of ferromanganese. However, barium based fluxes are expensive. Therefore, some investigators [32,33] have also tried lime based flux as the master flux using barium oxide only as an additive. However, results were not encouraging for manganese-based alloy.

8. Attempts were also made to use relatively cheap  $\text{BaCO}_3$  in place of  $\text{BaO}$ . Results were encouraging, however, the tests were limited to synthetic alloy containing manganese less than 60%, whereas, actual ferromanganese contains more than 70% manganese.
  
9. In a recent study [41],  $\text{BaO-BaF}_2\text{-MnO}$  flux was used successfully for dephosphorization of ferromanganese in relatively large scale experiments (1 kg induction furnace). However, this study also suffered from certain limitations: i) the potential of  $\text{BaCO}_3$  which is economical for industrial practice, has not been investigated thoroughly, ii) the desired level of phosphorus was achieved in more than 30 minutes, which clearly indicated the necessity of the kinetics to reduce the time of reaction to a practical level.

## **2.5 AIM OF THE PRESENT WORK**

In view of the above discussion, the objectives of the present investigation are outlined as follows:

1. List out the most suitable reagents from the literature
  
2. To establish the feasibility of removal of phosphorus from high carbon liquid ferromanganese using barium carbonate as well as lime based reagents.

3. To develop a synergetic  $\text{BaCO}_3$  based flux composition, which would melt at moderate temperatures ( $<1500^\circ\text{C}$ ) in order to become effective for dephosphorization of ferromanganese.
4. To study the effect of ferromanganese alloy composition (C, Si, Mn) on the process of dephosphorization
5. To compare the dephosphorization efficiency using calcined  $\text{BaCO}_3 - \text{MnO}_2 - \text{BaF}_2$  flux pellets to that with  $\text{BaCO}_3 - \text{MnO}_2 - \text{BaF}_2$  powder.
6. To study the effect of flux injection on the kinetics of dephosphorization process.











### 3.0 MATERIAL CHARACTERIZATION

#### 3.1 CHEMICAL ANALYSIS OF RAW MATERIALS

Before designing the experiments, a list of raw materials required for conducting the experiments was prepared. Basic raw materials used in all the experiments were ferromanganese and barium carbonate. In addition to this, manganese di oxide, barium flouride and barium chloride were used as additives. Ferro-phosphorus was used to adjust the level of phosphorus in the master alloy. Commercial grade high carbon ferromanganese of following composition was used in the present investigation.

**TABLE 3.1**

**Composition of commercial grade ferromanganese as raw material**

<b>Element</b>	<b>Wt %</b>
C	6.72
Mn	67.0
Si	0.82
P	0.36

Barium carbonate of LR grade was procured and its chemical composition was analysed in the laboratory, as given in Table 3.2.

**TABLE 3.2****Chemical analysis of Barium Carbonate( $\text{BaCO}_3$ ) as raw material**

<b>Element</b>	<b>Wt %</b>
Ba	61.6
Mg	0.33
Al	0.57
Si	0.74
P	0.16
Ca	1.35
Mn	0.02
Fe	0.14
CO	0.07
Ni	0.08
Cu	0.05
Zn	0.18
Cd	0.03
Sn	0.16
Pb	0.20

Before conducting dephosphorization tests, it was decided to prepare master alloy and synthetic slags on the basis of information collected from the literature search. The high carbon ferromanganese was prepared having Mn content more than 60%. This homogenized ferromanganese was used for subsequent tests. Synthetic slags of BaO-based and lime based fluxes were prepared. The chemical analysis of these slags are given in Table 3.3 and Table 3.4.

**TABLE 3.3****Composition of BaO-based synthetically prepared slag**

<b>Slag Constituents (BaO-based)</b>	<b>Wt % Slag</b>	<b>Wt % Slag 2</b>
BaO	40	33
Al <sub>2</sub> O <sub>3</sub>	9.48	12
Ca F <sub>2</sub>	35.9	42
MnO	11	12
FeO	1.72	1.13
S	0.05	0.05
C	0.33	2.3

**TABLE 3.4****Composition of synthetically prepared lime based slag**

<b>Slag Constituents</b>	<b>Wt %</b>
CaO + CaF <sub>2</sub>	63
Al <sub>2</sub> O <sub>3</sub>	15
MnO	3
BaO	6
SiO <sub>2</sub>	0.002
C	0.16
S	0.03

### **Analysis of Desiliconized master ferromanganese alloy**

It was considered necessary to homogenize and desiliconize ferromanganese before its use as raw material for dephosphorization tests. Two heats of 6 Kg size were desiliconized by adding 250 grams mill scale in each heat. In order to compensate for the loss of phosphorus during desiliconization, about 25 g ferro phosphorus (P-22.49%, Fe-83%) was also added. A chemical analysis for the desiliconized ferromanganese was carried out in the laboratory, the result of which is given in Table 3.5.

**TABLE 3.5**  
**Composition of desiliconized ferromanganese**

<b>Element</b>	<b>Heat No 1 (Wt %)</b>	<b>Heat No. 2 (Wt %)</b>
C	6.59	6.20
Si	0.20	0.24
Mn	67.30	68.80
P	0.56	0.44

### **Instruments used for chemical analysis:**

In chemical analysis reported above, Fe and Mn were analyzed by Atomic Absorption Spectrometry (AAS). The C and S were analyzed by Leco analyzer (spark method). Silicon and phosphorus were analyzed by conventional methods[69]. Metal and slag samples were also analyzed by ICP (Inductively

Coupled Plasma spectrometry) method. From the analysis of Ba and Ca, BaO, BaF<sub>2</sub> and CaO, CaF<sub>2</sub> content were estimated.

### 3.2 XRD Analysis

In addition to the chemical analysis, barium carbonate and manganese di oxide were also characterized by X-ray Diffractometer (Make- SIEMENS D 500) to confirm their purity. In the present investigation, some experiments were carried out using BaCO<sub>3</sub>-MnO<sub>2</sub> pellets, which were precalcined in order to obtain BaO-MnO flux for treating ferromanganese alloy for better dephosphorization. Therefore, it was required to investigate the phases present in the calcined pellets and subsequently were analyzed by XRD.

The XRD was carried out using Co K<sub>α</sub> Target (Anode) with wavelength ( $\lambda_1 = 1.79026$ ) at 35 KV and 25 mA and at steps of 0.020 cs. The scan angle ( $2\theta$ ) ranged from 20° to 80°. Before the result is presented, principle of X- ray diffraction is given below in brief:

Since the wave length of X-rays is approximately equal to the distance separating the lattice planes in solids, diffraction effects are produced when a beam of X-ray strikes a crystalline substance. The diffraction of X-rays is governed by Bragg's law which is defined as:

$$n\lambda = 2d \cdot \sin\theta$$

Where, n is an integer and  $\theta$  is the angle at which X-rays are incident on the crystal plane. The angular position, ' $\theta$ ', of the diffracted X-ray beam depends on the spacing, 'd', between planes of atoms in an crystalline plane and on the X-ray

wavelength ( $\lambda$ ). As the ' $\theta$ ' increases gradually a series of positions are found corresponding to  $n = 1, 2, 3$  at which maximum reflection occurs. The diffraction maxima are called first, second, third, etc in order according to value of  $n$ . The intensity of the diffracted beam depends on the arrangement of the atoms of these planes.

### **X-ray analysis of BaCO<sub>3</sub> as received**

A typical XRD pattern of BaCO<sub>3</sub> is shown in Fig. 3.1, the 'd' (inter-planer distance) values have been compared with the 'd' values given in Powder Diffraction Files (PDF) as shown in Table 3.6. Since experimental 'd' values of almost all the peaks matched with the theoretical 'd' values of BaCO<sub>3</sub> given in PDF File No 5-378, the purity of BaCO<sub>3</sub> gets confirmed.

**TABLE 3.6**  
**XRD analysis of BaCO<sub>3</sub> as raw material**

<b>POSITION (<math>2\theta</math>)</b>	<b>'d' Value Exptl A<sup>0</sup></b>	<b>'d' Value (PDF5-378) A<sup>0</sup></b>	<b>Difference A<sup>0</sup></b>	<b>Intensity (CPS)</b>
22.562	4.5759	4.56	0.01	513
23.086	4.4733	4.45	0.02	323
27.784	3.7283	3.72	0.008	3345
28.02	3.6741	3.68	0.006	1474
32.258	3.2222	3.21	0.01	547
34.374	3.0293	3.025	0.004	269
39.358	2.6581	2.656	0.002	468
39.786	2.6307	2.628	0.003	822
40.343	2.5959	2.59	0.006	912
46.173	2.2828	2.281	0.001	333
47.349	2.2293	2.226	0.003	202

<b>POSITION (<math>2\theta</math>)</b>	<b>'d' Value Exptl <math>\text{\AA}^0</math></b>	<b>'d' Value (PDF5-378) <math>\text{\AA}^0</math></b>	<b>Difference <math>\text{\AA}^0</math></b>	<b>Intensity (CPS)</b>
49.170	2.1515	2.150	0.001	1004
50.287	2.1068	2.104	0.002	479
51.816	2.0487	2.048	0.0007	350
52.598	2.0203	2.019	0.001	670
54.923	1.9411	1.940	0.001	553
57.452	1.8624	1.859	0.001	187
58.431	1.8339	1.830	0.003	137
65.702	1.6501	1.649	0.001	304
66.418	1.6344	1.632	0.002	250
69.884	1.5629	1.563	0.001	182
72.182	1.5196	1.521	0.0004	229
81.205	1.3754	1.375	0.0004	265

### **X-ray analysis of calcined flux pellets**

XRD was also used for characterization of calcined barium carbonate based flux pellet sample. It was found that the major phase in the calcined sample at 1050<sup>0</sup>C was BaO as shown in Fig 3.2. The results are presented in Table 3.7 showing the phases present in the calcined sample.

**TABLE 3.7**

### **XRD analysis of calcined BaCO<sub>3</sub>-based flux pellet sample**

<b>Position (<math>2\theta</math>)</b>	<b>'d' Value <math>\text{\AA}^0</math></b>	<b>Intensity (CPS)</b>	<b>Phases Present</b>
24.374	4.2403	235	BaCl <sub>2</sub>
27.745	3.7334	264	BaCO <sub>3</sub>

Position ( $2\theta$ )	'd' Value $\text{\AA}$	Intensity (CPS)	Phases Present
28.204	3.6738	209	BaCO <sub>3</sub> , BaCl <sub>2</sub>
32.320	3.2162	218	BaO, BaCO <sub>3</sub>
40.349	2.5955	139	BaO, BaCO <sub>3</sub> , BaCl <sub>2</sub>
46.413	2.2716	172	BaO, BaCO <sub>3</sub>
47.386	2.2276	116	BaO, BaCO <sub>3</sub> , BaCl <sub>2</sub>
49.179	2.1512	176	BaO, BaCO <sub>3</sub> , BaCl <sub>2</sub>
52.577	2.0211	146	BaCO <sub>3</sub>
53.156	2.0007	129	BaCO <sub>3</sub>
55.674	1.9169	104	BaO
65.189	1.6617	119	BaO, BaCO <sub>3</sub> , BaCl <sub>2</sub>
67.839	1.6041	104	BaO

### X-ray analysis of slag sample

Slag sample after metal-slag dephosphorization test was also characterized by XRD as shown in Fig. 3.3. The phases which were identified with their corresponding peaks and got matched with the 'd' values given in PDF( File Nos 3-659 for BaCO<sub>4</sub>, 26-178 for BaO, 7-230 for MnO) are reported in Table 3.8. The main phase present in the sample was BaO. It was observed that BaO<sub>2</sub>.CO<sub>2</sub>(BaCO<sub>4</sub>) was also present in the unreacted flux sample. It was found that the experimental 'd' values of MnO for peaks at positions 8,9, 12 matched quite well with the theoretical 'd' values reported for MnO (PDF File No7-230). Thus MnO was present in good amount in the sample. However, peaks at the positions 8,9,11, 12 were found overlapping, therefore, it is difficult to estimate the relative amounts of the phases present.

**TABLE 3.8**  
**XRD analysis of slag sample obtained after**  
**dephosphorization of ferromanganese**

Sl. .NO.	Positions ( $2\theta$ )	'd' Values $\text{\AA}^0$	Phases present
1	24. 583	4. 2048	Barium peroxy monocarbonate ( $\text{BaCO}_4$ )
2	28. 045	3. 6943	BaO
3	30. 424	3. 4119	$\text{BaCO}_4$
4	33. 019	3.150	Barium Oxide (BaO)
5	34. 598	3.0102	$\text{BaCO}_4$
6	35. 520	2.9345	$\text{BaCO}_4$
7	40. 870	2.9031	
8	47.535	2.5638	Manganese Oxide (MnO), BaO, $\text{BaCl}_2$
9	52.588	2.2210	$\text{BaCO}_4$ , BaO, MnO, $\text{BaCl}_2$
10	60.287	2.0207	$\text{BaCO}_4$ ,
11	69. 442	1.7825	$\text{BaCO}_4$ , BaO, $\text{BaCl}_2$
12	70. 35	1.5716	$\text{BaCO}_4$ , MnO

From the above result, in a crude way it was estimated the relative amounts of  $\text{BaCO}_4$ , BaO and MnO as 40 %, 30% and 30% respectively.

### 3.3 Differential Thermal Analysis (DTA) Of Slag

After carrying out the dephosphorization tests successfully at moderate temperatures ( $<1500^{\circ}\text{C}$ ), it was considered necessary to confirm the melting temperature of slag by DTA. The equipment used was NET ZSCH DTA/TG system (Model No STA 409). The principle [69] of DTA and TG set up is given below:

Sample and reference materials kept in different crucibles, are heated at a given rate. If at a particular temperature exothermic or endothermic reaction take place either

due to chemical reaction or phase transformation, differential temperature rises or falls, which appears as a peak in the curve. DTA has been used for the determination of melting temperature of slag besides many other applications. Simultaneous measurements of DTA and TG are carried out to know the weight change along with heat effect. The plot of weight loss versus temperature is termed as thermogravimetric (TG) curve. A simultaneous depression in TG and DTA indicate to a endothermic reaction involving weight loss, while a depression in DTA but no change in TG curve, represent the phase change due to melting.

A simultaneous plots for TG and DTA was done to identify the fusion temperature of the slag. The result obtained is shown in Fig. 3.4 Sample was heated at a controlled rate of  $10^{\circ}\text{C}$  per minute and the temperature was raised up to  $1450^{\circ}\text{C}$ . The DTA line shows depression at two points A and B, which may account for chemical reaction as well as phase transformation (fusion). A superimposed TG plot confirm that the point A corresponds to a endothermic reaction producing one gas phase which causes a weight loss, while the point B corresponds to fusion reaction because there is no weight loss as shown in TG plot. Possibly,  $\text{BaCO}_3$  decomposition reaction take place corresponds to point A ( $\sim 800^{\circ}\text{C}$ ), while fusion of slag take place to the point B, i.e. around  $1050^{\circ}\text{C}$ . Further, a depression in TG at around  $100^{\circ}\text{C}$  may account for dehydration.









## 4 EXPERIMENTAL ASPECTS

The experimental work was broadly classified into three categories:

a) Use of different reagent systems in induction furnace to establish its feasibility for dephosphorization of high carbon liquid ferromanganese alloy.

b) Improvement of the reagent system and consequent enhancement in the extent of dephosphorization by following route:

- Preparation of green fluxed pellets and their calcination in the temperature range of 700-1050<sup>o</sup> C.
- Use of calcined pellets for treatment of ferromanganese alloy in the carbon resistance furnace under controlled conditions.

c) Injection of flux powders in liquid ferromanganese alloy (contained in a graphite crucible) in induction furnace in order to enhance the rate of reaction .

### 4.1 FEASIBILITY TESTS IN INDUCTION FURNACE

It was decided to try out various reagents reported in the literature in order to determine the most suitable reagents for the dephosphorization of Fe-Mn alloy. Melting temperatures of various flux systems, shown in Table 4.1, were compiled in order to select the most suitable composition which can melt near the melting temperature of ferromanganese alloy and have the adequate phosphate capacity (Fig.4.1). Amongst the reagents reported, barium oxide based fluxes were considered to be the most effective because of their high phosphate capacity. Barium carbonate ( $BaCO_3$ ) was chosen as a substitute for BaO in the present investigation because of its ready availability at low cost. Different proportions of

BaCO<sub>3</sub> and MnO<sub>2</sub> were tried in order to melt them at moderate temperature (<1500°C). External addition of MnO<sub>2</sub> was considered to restrict the manganese loss. As seen from Table 4.1, BaCO<sub>3</sub> alone can be melted at comparatively lower temperature (1300°C), but with addition of MnO<sub>2</sub>, the flux mixture could not be melted at moderate temperatures. Graphite crucible was selected for preparing synthetic slags as it was reported in the literature [27] that the small amount of carbon helps in melting BaO-MnO flux at moderate temperatures (<1500 °C). Ferromanganese was desiliconised before using BaO based flux for dephosphorization. Composition of the alloy was varied to study the effect of various constituents on the process of dephosphorization. The details of the experiments are described below:

#### **4.1.1 PREPARATION OF MOTHER ALLOY**

Two heats of 6 kg ferromanganese were made in a graphite crucible, equipped in an induction furnace. After complete homogenization, about 250 gms mixture of mill scale and lime was added to remove silicon from liquid alloy[22]. During desiliconization it is likely that some phosphorus was also removed. To compensate this loss, about 25 gms of ferro phosphorus was added. The final analysis of ferromanganese which was used for subsequent experiments, is given below:

C	-	6.70 %
Mn	-	67.30 %
P	-	0.56 %
Si	-	0.20 %
Fe	-	32.10

#### 4.1.2 DEVELOPMENT OF SUITABLE FLUX

In view of the difficulty in melting  $BaCO_3$  and  $MnO_2$  flux system, initially a low melting master lime based flux was prepared which was used for dephosphorization of Fe-Mn alloy. About 5 %  $BaCO_3$  was added for increasing the phosphate capacity of lime based flux[33]. However, due to inadequate dephosphorization with lime based fluxes, it was decided to use BaO-based flux only for subsequent trials.

Difficulty was experienced in making  $BaCO_3$  - $MnO_2$  synthetic slag as it was very viscous at moderate temperatures ( $\sim 1500^\circ C$ ). For dephosphorization of ferromanganese, it was felt necessary to develop a flux comprised of BaO and MnO and yet having a moderate temperature. A literature review indicated that even though the available information on phase equilibria for the BaO-MnO is rather limited, a low melting zone exists near 18-20 % MnO (Fig 4.2) with liquidus temperature in the range of 1300 to 1400<sup>0</sup>C [20]. Watanabe et al. [27] have reported that the BaO-MnO flux may melt at hot metal temperatures because of the presence of small amount of carbon. On the basis of this knowledge, different proportion of  $BaCO_3$  and  $MnO_2$  were tried out in order to melt them near the melting temperature of ferromanganese alloy. The objective was to find a low melting compound for this system. After several trials a method was evolved for melting the flux without any real difficulty [ 40].

#### 4.1.3 DEPHOSPHORIZATION TESTS IN INDUCTION FURNACE

A schematic of the envisaged dephosphorization is shown in Fig 4.3. The tests were carried out in a high frequency induction furnace at moderate temperatures

(<1500 ° C) under oxidizing conditions using basic fluxes. The following parameters were varied to find their effects on dephosphorization:

- a) Type of flux
- b) Quantity of flux
- c) Silicon content of the alloy
- d) Temperature

Preliminary tests were not very encouraging because the material eroded from sillimanite crucible contaminated the slag phase and there was heavy loss of manganese, though there was significant removal of phosphorus. Sillimanite crucible which contains alumina, perhaps increased the oxygen potential of the system. Therefore, subsequent experiments were conducted in graphite crucibles. Carbon saturated system ( graphite crucible) also helps in melting of flux which was difficult to melt when sillimanite crucible was used. Use of graphite crucible facilitated the melting of Fe-Mn alloy without any difficulty and virtually eliminated the loss of manganese into the slag phase. After melting the desiliconized ferromanganese alloy, a melt down sample was collected for chemical analysis.

Initially a low melting master lime based flux was used for the tests. Subsequently mixture of  $BaCO_3$ ,  $BaF_2/BaCl_2$  and  $MnO_2$  were used in a fixed proportion for adding into the melt. After several trials, other suitable compositions were evolved for melting the  $BaCO_3$  based flux at moderate temperatures (1500°C).

Metal and slag samples were taken at 15 minutes interval after addition of flux. Initially, metal samples were collected by casting liquid metal in mold and the slag samples were collected by graphite rod. For sample collection, the furnace had to be switched off which created a temperature drop. Besides samples collected were inhomogeneous. To overcome this problem silica tubes of internal diameter 4 to 5

mm fitted with a rubber bulb, were used for collecting sample from liquid melt. After sampling, the tube was quenched in cold water and samples were taken out carefully with the help of a plier for chemical analysis. Slag samples could not be collected during the experiment due to a relatively low amount of slag generated. However, final slag sample was obtained once the crucible had cooled down to room temperature. The temperature of the liquid alloy was measured with a Pt-Pt 10% Rh thermocouple. Several experiments were carried out using different proportions of  $BaCO_3$ ,  $BaF_2/BaCl_2$  and  $MnO_2$ . To increase the fluidity of slag different amount of  $BaF_2/BaCl_2/CaF_2$  were used according to the requirement. The melting temperature of the slag formed was checked by a Differential Thermal Analyzer (NET ZSCH DTA/ TG System Model NO STA409) for confirmation.

Metal samples were analyzed by Leco Combustion analyzer for analysis of carbon and sulfur. Phosphorus was analyzed by molybdenum blue colorometry method. Fe, Mn, Si and P were also analyzed by ICP (inductively coupled plasma) method. Analysis of CaO, MnO and BaO were done AAS (Atomic Absorption Spectrophotometers). These were also analyzed by ICP when bulk samples were available.

#### **4.1.4 EXPERIMENTAL DIFFICULTIES**

- a) Melting of synthetic  $BaCO_3$ -based flux
- b) Variation of raw materials composition in different supply
- c) Control of temperature in induction furnace within narrow range
- d) Control of partial pressure of oxygen
- e) Inhomogeneity in metal and slag samples
- f) Loss of flux due to evaporation

#### 4.1.5 THE PRINCIPLE OF INDUCTION FURNACE

The electromotive force of induction is given by [10]:

$$E = 4.44\Phi \max f_n \cdot 10^{-8} V$$

where n = number of inductor turns

$\Phi$  = magnetic flux density

f = alternating current frequency

V = Volts

The electromotive force induced in the metallic charge forms whirl (circular) currents in the plane of the winding turns i.e, perpendicular to the magnetic flux axis. The density of the induced current attains its maximum at the surface of the charge. The depth of the surface layer of a metal where the density of induced current is large is called penetration depth. f is inversely proportional to the mean diameter of the crucible. Thus large furnaces requires lower frequency than smaller ones. The rate of heat generation, besides other factors , directly depends upon the frequency of the power source. The modern furnaces use currents of high frequency up to the level of radio frequency (200-1000 K HZ). In laboratory, it is often required to melt metals possessing different conductivity which necessitates frequency control over a wide range. The highest temperature zone is in the bottom portion of the crucible where heat losses are lower. The charge pieces are allowed to sink and immerse into the molten metal on the bottom.

## 4.2 DEPHOSPHORIZATION TESTS USING CALCINED $BaCO_3$ - $MnO_2$ FLUX PELLETS

Once the feasibility of  $BaCO_3$  based flux powder on dephosphorization of ferromanganese was established, it was intended to make  $BaCO_3$ -based pellets as an industrial reagent for the following advantages of pellets over powder:

- i) better assimilation in the liquid Fe-Mn melt
- ii) better reactivity
- iii) pre-calcined pellet can restrict temperature drop of the Fe-Mn melt by avoiding  $BaCO_3$  decomposition in the melt
- iv)  $BaO$  (pre-calcined  $BaCO_3$ ) - $MnO$  (pre reduced  $MnO_2$ ) based flux with high phosphate capacity can be produced from in situ pre-calcined and pre-reduced  $BaCO_3$  based pellets.

It was decided to carry out some tests using  $BaO$  based flux at small scale (gm level) in graphite crucibles in a carbon resistance furnace under controlled conditions of temperature and inert atmosphere in order to improve the extent of dephosphorization and reduce the loss of manganese. Since it was difficult to store Barium oxide pellets because it is prone to form Barium Carbonate when exposed to natural atmosphere, it was decided to form  $BaO$ - $MnO$  flux in situ for subsequent treatment of liquid ferromanganese in furnace itself.

### 4.2.1 PREPARATION OF FLUX PELLETS

Green pellets of following varieties were made using conical pelletizer:

- a)  $MnO_2$  and carbon
- b)  $BaCO_3$ - $BaCl_2$  and carbon
- c)  $BaCO_3$ - $BaF_2$ ,  $MnO_2$  and carbon

Powders were weighed and mixed thoroughly in a plate. Dextrin 2-4% was added as binder. Carbon about 7% was added in the form of Pet-coke of following chemical analysis:

FC	-	90.01%	Moisture	-	0.28%
VM	-	8.21%	S	-	0.50
Ash	-	0.20%	P	-	Trace

Water was added depending upon the requirement. These pellets were dried in oven to remove moisture. After drying , pellets were stored in separate polythene covers.

#### 4.4.2 CALCINATION OF PELLETS

The flux pellets were calcined in order to remove extra oxygen atom from  $MnO_2$  and  $CO_2$  from  $BaCO_3$ . About 15 gms of these pellets were taken in a cup shaped container with a cover. A long handle was attached to each container for putting them in the hearth zone of the carbolyte furnace. Silicon carbide was used as heating elements in carbolyte furnace. The furnace contains refractory fibers in its thermal insulation. The material used may be in the form of fiber blanket or felts, vacuum formed board or shapes ,mineral wool slab or loose fill fiber. The furnace starts heating up according to programme set, power to the elements are indicated by the heater on light . This light flash on and off as the power of the furnace is controlled.

For calcination of  $MnO_2$  pellets, temperature was varied in the range of 700 to 1000 °C in order to select most suitable temperature for calcination. Soaking was done for 1 hr and samples were quenched for arresting the phases. It was reported in the

literature that the decomposition of barium carbonate without carbon takes place at about 1300 degree C whereas in the presence of carbon it decompose at lower temperature ( $\sim 1050^{\circ}\text{C}$ ). Therefore, calcination of  $\text{BaCO}_3$  was also carried out at  $1050^{\circ}\text{C}$  for 1 hour after which samples were quenched for arresting the phases. Calcined pellets samples were analyzed by X-ray Diffractometer (Make- SIEMENS D 500). From the XRD pattern, the D (inter-planer distance) values were compared with the D values given in Powder Diffraction Files (PDF) in order to find the phases present. It was found that the major phases in the samples which were calcined at  $1050^{\circ}\text{C}$  were BaO and MnO. Therefore,  $1050^{\circ}\text{C}$  for 1 hr was selected as the best combination of temperature and time for subsequent in-situ calcination.

#### **4.2.3 METAL- SLAG REACTION TESTS IN CARBON RESISTANCE FURNACE**

Desiliconised ferromanganese was used for treatment with BaO based pellets. Initially, it was decided to form BaO pellets from  $\text{BaCO}_3$  pellets by external calcination. However, it was apprehended that due to lack of proper storage facility, BaO may again form  $\text{BaCO}_3$  in contact with natural atmosphere during handling. Therefore, it was decided to calcine  $\text{BaCO}_3$  based pellets for 1hr at  $1050^{\circ}\text{C}$  in carbon resistance furnace itself before allowing metal- slag reaction to take place at 1350-1400 degree C. This will also prevent the heat loss during dephosphorization reaction due to decomposition of  $\text{BaCO}_3$  in solid state. Following parameters were varied in order to find their effect on the extent on dephosphorization:

- a) Flux Composition
- b) Flux weight
- c)  $\text{MnO}_2$  content in the flux
- d) Temperature

The carbon resistance furnace has got the facility to program the rate of temperature increment and finally control at the desired level. The temperature was raised at 25°C per minute. The crucible was made up of graphite having dimension 85 mm internal diameter and 125 mm height. Several small crucibles containing ferromanganese and the fluxes according to work plan were used for dephosphorization tests. Temperature was varied in the range of 1350-1400°C. Metal and slag were allowed to react for 30 minutes after which furnace was allowed to cool at controlled rate. Metal and slag samples were prepared for chemical and XRD analysis.

#### **4.2.4 DESCRIPTION OF CARBON RESISTANCE FURNACE**

Model - 1000-4560-FP20

Manufacturer - astro division of Thermal Technology Inc, California, USA

This is a single zone high temperature furnace which is capable of operation in dry inert, reducing and vacuum atmosphere. The basic Model 1000 system includes the graphite furnace, support column and swivel bracket, manual power supply and water cooled power leads. The hot zone consist of high density graphite resistance element and insulated by High purity Graphite Felt, retained by a solid - wall graphite tube. The furnace shell is heavy- wall, seamless extruded 606/T6 aluminium with an oxidized exterior. The bulk heads are hard anodized aluminium and the doors are nickel- plated copper. The shell and bulkheads have internal water cooling passages. Temperature up to 1800 degree C can be maintained in the vertical position and to 1000 degree C in the horizontal position.

Before starting the furnace, it is vacuum purged for removal of moisture and/ or oxidizing atmosphere. Inert atmosphere is maintained at ambient pressure during

operation. Primary power is switched on by means of the furnace on/off button on the front control panel. The switches are interlocked with a water flow switch installed in the outlet of the water cooling system. The furnace is set on “AUTO” control. The programming is done according to process requirement. The furnace is heated at the controlled rate . Water flow is maintained for cooling until furnace interior is less than 120<sup>0</sup>C. Gas flow is also maintained unless furnace interior is less than 600<sup>0</sup>C. During cooling of the furnace, the interior gas flow rate should be sufficient to prevent air being drawn back through vent port by furnace gas volume contraction.

### **4.3 KINETIC STUDY**

The experiments carried out in induction furnace and subsequently in carbon resistance furnace established the feasibility of removal of phosphorus using BaCO<sub>3</sub> based fluxes. However, the time taken to achieve the desired level of phosphorus was about 30 minutes. This long time for dephosphorization was not considered suitable for plant scale trials for effective utilization of flux and energy. It was, therefore, desired to reduce the time of dephosphorization to a practical level. In order to achieve this, attention was given to study the kinetics of the process for enhancing the reaction rate through powder injection through liquid ferromanganese. Experiments were carried out in 7 kg. carbon crucible equipped in an induction furnace to compensate for any drop in temperature during pouring and subsequent pre-injection treatment. A separate powder and lance assembly were designed and fabricated (Fig. 4.4) in our workshop to suit the requirements of the tests planned to be carried out at laboratory scale.

#### 4.3.1 SOME BASIC ASPECTS OF THE FLUX INJECTION SYSTEM

In injection metallurgy powdered solid reagents are injected in the melt through a suitable carrier gas. Injection of reagents is much superior to spraying or throwing of the same followed by mechanical stirring. This provides large slag-metal interfacial area for reaction. It also helps in homogenization of temperature, chemical composition and alloying in ladle. For dephosphorization of steel, fluxes are injected using oxygen as carrier gas but this is not desirable for dephosphorization of ferromanganese because oxide of manganese is more stable than that of phosphorus at smelting temperatures [2]. Oxygen potential affects the process of dephosphorization in a positive way only when the oxygen potential is very low. Therefore, reagents are preferred to be injected using Argon as a carrier gas.

Injection involves initial transportation followed by discharge of compressible fluid mixed particles as a submerged jet used in the treatment of liquid metal in ladle. The pneumatic injection of flux powder having good air/gas retention properties involves initial conveying followed by the subsequent discharge of gas mixed particles as submerged jet in liquid metal in a ladle. The process demands injection of powder utilizing minimum amount of carrier gas.

The injection system consists of the following essential features:

- a) The flux powder is stored in a pressurized blow tank. The powders are delivered from the blow tank at a desired rate into flowing gas stream
- b) The powders are then carried through tubing by the carrier gas stream to a suitable location of furnace/ladle where it is delivered through a graphite lance into molten metal as either a free jet or submerged jet.

The carrier gas stream mixed with powder overcome the resistance due to hydrostatic head and sudden enlargement of gas stream. Mixed gas stream upon leaving the outlet dipped in the liquid metal get a reverse motion due to buoyancy and breaks into bubbles due to hydrostatic head, surface tension and drag forces. The bubble size increases with the decrease of hydrostatic head and bubbling improves the kinetics of treatment of liquid metal. The exit pressure within injected piping around outlet may be expressed as:

$$P_{(e)} = P_{\alpha} + P_h + \frac{1}{2} \xi \rho_m U_m^2$$

where  $P_b = P_{\alpha} + P_h$ ,  $P_{\alpha}$  is ambient pressure,  $P_h$  is hydrostatic pressure and  $\xi$  is resistance factor due to sudden enlargement of flow

$U_m$  is mixed particle velocity and  $\rho_m$  is density of particles. They are defined as

$$\rho_m = \frac{M_f + M_s}{\frac{M_f}{\rho_f} + \frac{M_s}{\rho_s}}, \quad U_m = \frac{M_f \cdot U_f + M_s \cdot U_s}{M_m}$$

The average velocity of fluid/ gas depends on slippage between fluids and solids. Amount of solid particles that can be conveyed with the carrier gas depend on the loading ratio[43]. Those particles which have got poor air/ gas retention properties for them loading ratio can be maintained only up to 20:1. For  $BaCO_3$ , which was injected in the present investigation, loading ratio was kept at 15:1 considering its hygroscopic nature.

In order to achieve efficient conveying through ducting, uses of sudden enlargement, contraction, bends and joints are to be reduced to a minimum limit.

### **4.3.2 FABRICATION OF DISPENSER AND ASSEMBLY OF THE INJECTION SYSTEM**

A schematic of injector is shown in Fig 4.4. The injector was fabricated in our workshop for the experiments to be carried out at lab scale. Following materials were used:

- a. Dispenser of 5 kg capacity
- b. Audco Valve 1/2"-2Nos and 1"-1 No
- c. Stainless steel of 6 mm internal diameter, 2 mm thickness, 1.5 m length
- d. High pressure plastic tube of 10 mm diameter
- e. Mild steel sheet of 3 mm thickness
- f. O Ring seal

The dispenser body was fixed on the stand . The graphite plunging rod was fabricated for injecting the gas-flux mixture at the bottom of hot alloy melt. Another graphite plunger was kept as a standby for quick replacement. Gas pressure was controlled by means of valve. Loading ratio up to 15:1 could be maintained for BaCO<sub>3</sub> flux using this injector. The dispenser and lance assembly had the flexibility to be shifted quickly to the working place where injection is required to be carried out.

### **4.3.3 DUMMY TRIAL OF INJECTION SYSTEM**

In order to test the functioning of injection system, a dummy trial was first taken. Powder was allowed to flow in the cold water kept in a bucket. The weight difference of the water before and after injection, gave the indication of the quantity of powder injected. Pressure of carrier gas was regulated for smooth flow. The valve position was marked for subsequent tests. Powder of -60 mesh size was first

dried and then filled in the dispenser. Injection rate of carrier gas was maintained at 1Nm<sup>3</sup>/hr.

#### **4.3.4 PREPARATION DESILICONIZED FERROMANGANESE ALLOY FOR KINETIC TESTS**

It was learnt from the tests conducted in induction furnace that the flux will be effective only when the silicon content of ferromanganese is less than 0.2 percent. As the ferromanganese received from FACOR, INDIA contained about 1.5% silicon, external desiliconization was considered necessary before highly basic flux is injected for treatment of liquid ferromanganese. For this purpose the liquid ferromanganese was treated with iron ore and lime (about 5 % wt of metal ) in arc furnace in order to reduce the initial silicon level in ferromanganese to the desired mark. During desiliconization, metal sample was taken by means of a 4 mm silica tube fitted with rubber bulb after 15 minutes of addition of flux mixture. Final metal sample was also taken after pouring and solidification of liquid metal in ingot mould. The chemical composition of the ferromanganese is given below which showed that though silicon level was reduced to 0.16% and 0.18% but there was some loss of manganese and phosphorus in the slag phase.

Chemical composition of desiliconised Ferromanganese for subsequent use in kinetic study

C	-	6.09%
Si	-	0.16%
Mn	-	54.26%
P	-	0.35%
Fe	-	39.19%

#### **4.3.5 EXPERIMENTAL SET UP AND PROCEDURE FOR DEPHOSPHORIZATION TESTS USING INJECTOR**

The experimental set up for dephosphorization in induction furnace using injector is shown in Fig 4.5. A photograph for the injection system is also attached at the end of this Chapter. A graphite crucible of 9 cm internal diameter and 25 cm height was used to melt the high carbon ferromanganese. About 7kg metal weight was considered appropriate so that there is enough space for flux addition. Argon gas was used as a carrier gas. An on line rotameter in the range of 1-10 NM<sup>3</sup>/hr, was attached for regulating the flow of gas. About 1 kg flux mixture was preheated in an oven to remove moisture. This was screened on a 60 mesh sieve in order to remove bigger powder particles. The mixture was weighed again. The flux powder (-60 mesh) was fed to the dispenser and the cover was closed tightly. The functioning of injector was tested outside before putting the graphite lance into liquid metal.

About 7 kg desiliconised ferromanganese was charged in the furnace. The manganese loss occurred during desiliconization was compensated by adding 0.5 kg electrolytic manganese. Phosphorus was also added in the form of ferrophosphorus to raise its value to original level (~0.4 %). After melting a sample of ferromanganese was collected by means of 4 mm internal diameter silica tube prior to flux injection. Temperature of the melt was measured by a dipmeter having a disposable probe. The melt temperature was 1664<sup>0</sup>C. Then furnace was switched off to simulate the ladle condition for injecting the flux. The gas flux mixture was injected in deep in the hot alloy melt through a vertical graphite lance. Another graphite injector was kept as a stand by for quick replacement in case of breakage. The temperature and metal sample was collected at the beginning and end of injection.

Several experimental trials were made to make a smooth and successful injection through ferromanganese melt. Six to seven tests were discarded due to various experimental problems, like breakage of nozzle, improper functioning of injector, nozzle blocking, too much slopping and splashing etc. After repeated trials, a test condition was established for successful run.

#### **4.3.6 PRECAUTIONS**

1. The flux mixture was dried in oven to remove its moisture
2. The flux mixture was properly sieved so that bigger particle do not choke the injector pipe
3. Cold trial was carried out before using the injector for high temperature operation
4. The injector along with graphite lance was kept clean. In case of any blockage by slag particle a steel wire was used to remove the particle.
5. There may be breakage of graphite lance due to upward thrust generated by agitation during the process. For continuing the injection another graphite lance was kept as a standby for quick replacement.
6. Safety gloves was used while taking liquid metal samples
7. Blue glass was used for seeing the condition of the liquid metal
8. A superheat of more than 200<sup>0</sup> C may lead to breakage of the crucible. Therefore proper care was taken while raising the power of the furnace.
9. Some of the barium compounds are not considered environment friendly. Therefore well ventilated space was selected for carrying out the tests.
10. The flux powder is hygroscopic in nature, therefore proper care was taken for storing them in a sealed container.

11. Due to dissociation of barium carbonate at high temperature, certain splashing may occur; therefore operating personnel should be at a safe distance from the furnace.

A well coordinated effort is required to operate the furnace, gas cylinder, rotameter, temperature recorder etc. A team of 7-8 personnel are required for successfully carrying out these tests. Due to these constraints enough data could not be collected.













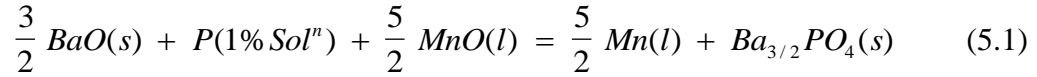


## 5.0 RESULTS AND DISCUSSIONS

### 5.1 THERMODYNAMIC ANALYSIS

Removal of phosphorus from liquid ferromanganese by oxidizing technique is usually accompanied by a significant loss of manganese. In order to prevent the loss of manganese, a thermodynamic analysis was considered necessary for identifying favorable conditions for selective removal of phosphorus from ferromanganese. The effect of chemical composition of ferromanganese on the dephosphorization of ferromanganese was also examined.

Amongst the various reagent systems reported in the literature, the BaO based reagents are considered most effective because of their high phosphate capacity [5]. The dephosphorization reaction under oxidizing conditions using BaO based fluxes may be represented as follows:



$$\Delta G^\circ = -136713 + 89.3TJ / mol \quad [4]$$

The equilibrium constant (K) and the Henrian activity of phosphorus in the melt ( $h_P$ ) for the above reaction can be expressed as:

$$K = \frac{a_{Mn(l)}^{5/2} \cdot a_{Ba_{3/2}PO_4}}{a_{BaO}^{3/2} \cdot h_P \cdot a_{MnO}^{5/2}} \quad (5.2)$$

$$h_P = \frac{a_{Mn(l)}^{5/2} \cdot a_{Ba_{3/2}PO_4}}{a_{BaO}^{3/2} \cdot K \cdot a_{MnO}^{5/2}} \quad (5.3)$$

Where  $a_i$  is the Raoultian activity of component “i” and  $h_p$  is the Henrian activity of the phosphorus dissolved in ferromanganese w.r.t. 1% standard state. From the above expressions, it is clear that for achieving a lower  $h_p$ , the desirable conditions are:

- a) Lower activity of the reaction product-  $Ba_{3/2}PO_4$  in the slag (flux) phase
- b) Lower activity of manganese in the Fe-Mn-C-P alloy
- c) High activity of BaO in the slag phase
- d) High activity of MnO in the slag phase
- e) High value of K, which is possible at lower temperature for exothermic reactions.

The calculated value of K for equation 5.2 is 0.402 at 1673 K and 0.141 at 1873 K.

### 5.1.1 PREDOMINANCE DIAGRAM

Representation of phase equilibria through predominance area diagrams is very useful for process analysis and was first developed by Kellogg and Basu [71] mainly for metal-sulfur-oxygen systems for which they adopted partial pressures of  $O_2$  and  $SO_2$  as the coordinates. For the metal-phosphorus- oxygen systems, the use of oxygen pressure and activity of phosphorus (Standard state: 1 wt pct in liquid metal) is considered appropriate.

Initially predominance area diagrams for Ca-P-O and Ba-P-O systems were constructed as shown in Fig. 3.1 in order to compare the suitability of these fluxes for dephosphorization of ferromanganese [4]. The equilibrium Mn-MnO line which corresponds to the maximum equilibrium oxygen partial pressure for dephosphorization without loss of manganese, has been superimposed on it. These figures identify the range of partial pressure of oxygen as shown by hatched area in

Fig.5.1 (a) and 5.1 (b), under which oxidative dephosphorization is possible without loss of manganese. It is also observed, minimum  $h_P$  without loss of manganese, achievable in case of Ca-P-O system is much higher (indicated by the point  $P_1$ ) compared to that in Ba-P-O system (indicated by point  $P_2$ ). A calculation shows (see Appendix-II) that dephosphorization of ferromanganese may not be feasible without loss of manganese when lime based flux is used. Even using a BaO flux rich in MnO, dephosphorization without loss of manganese is possible only at high phosphorus level in the melt. However, under non-standard conditions, which actually exist in real practice, dephosphorization without loss of manganese at moderate phosphorus levels could be possible. Therefore, the detailed analysis were done for BaO-based flux under standard as well as non standard conditions.

The predominance area diagrams for the ternary system Ba-P-O were constructed at temperatures from 1573 to 1873 K (Fig 5.2 to 5.4 ) at standard states. The Mn-MnO equilibrium has been superimposed in these diagrams. It indicates the equilibrium partial pressure of oxygen at each temperature from 1573 K to 1873 K below which it is possible to carry out dephosphorization without manganese loss. The data for the Gibbs energies of formation of the condensed phases were taken from Turkdogan[72], Kubaschewski and Alcock[73] and more recent studies [3,21,74] which are listed in Table 5.1. The pertinent chemical equilibria are expressed by reactions 1a, 2a, 3a, 6a (Table 5.1) for the ternary Ba-P-O system. These diagrams showed that it is thermodynamically feasible to remove phosphorus selectively under oxidizing conditions (without oxidizing manganese) by reacting the alloy with a BaO saturated slag rich in MnO. However, the range of oxygen potential becomes narrower on increasing temperatures from 1573 to 1873 K. Therefore, the preferred temperature was 1573 K. Initially, as a first approximation, the activities of the condensed reactants/ products were taken as unity. However, in view of the fact that most condensed species are present as dissolved constituents in metal or slag solutions, more realistic values were also considered for the calculation of Henrian activity ( $h_P$ ) of phosphorus. The calculated values are shown in Fig 5.5

which shows that for the activities of Mn, MnO and  $Ba_3(PO_4)_2$  chosen at 0.3, 0.5 and 0.1 respectively, effective dephosphorization  $[P] \leq 0.2\%$  can be achieved at 1573 K by maintaining  $h_P$  below 2.18 (calculation shown in Appendix III) which requires the oxygen partial pressure ( $p_{O_2}$ ) to be below  $3.0 \times 10^{-17}$  atm as indicated by the hatched area in Fig. 5.5.

The basis of chosen activities of various constituents under non-standard state (mentioned above) are discussed below.

#### Activity of manganese in Mn-Fe-C-P solution

The activities of manganese in Mn-Fe-C melt as calculated by Healy [76] are shown in Fig 5.6 which indicates  $a_{Mn} = 0.3$  for an alloy containing 70% Mn and 6-7 % carbon at 1573 K. Liu et al [41] had also calculated  $a_{Mn}$  as 0.23 and 0.28 at 1573 K and 1623 K respectively for an alloy containing 70% Mn, 7% C and balance Fe. It appears from these data that a carbon saturated system is helpful in reducing the activity of manganese. Therefore graphite crucible was selected for carrying out dephosphorization of high carbon ferromanganese. This will ensure low activity of Mn which is a desirable condition for dephosphorization of FeMn. Carbon reportedly [4] cuts down the activity of manganese drastically. However, with increase in temperature the effect of carbon on the activity of manganese decreases gradually [41]

#### b) Activity of manganese oxide

Ma et. al. [21] assumed an activity of MnO in slag from 0.5 to 1 depending upon the amount of MnO dissolved in the slag. It was also reported [27] that the solubility of MnO in BaO-MnO system at 1573 K is about 32%. Thus it is quite likely that the activity of manganese oxide will be more than 0.5 when the MnO

content of slag is in the range of 20-30. This was confirmed from the study of Liu et.al.[41]who calculated the activity of MnO at different partial pressure of oxygen. According to them even at low  $p_{O_2} = 1 \times 10^{-17}$  atm, the MnO activity relative to pure solid substance in slag can go up to 0.6 for treating ferromanganese. Therefore, the composition of the flux should be selected in such a way which increases the activity coefficient of MnO. Studies [79] have shown that calcium fluoride in slag can significantly increase the activity coefficient of MnO. The BaF<sub>2</sub> is expected to perform similar role as observed by Shim et al.[28] who recently investigated the thermodynamic properties of BaO-MnO flux system. BaF<sub>2</sub> as additive to BaO-MnO flux is selected because it also increases the phosphate capacity of flux [27].

#### c) Activity of reaction product

Lower activity of reaction product (phosphate) is achievable when a flux of high phosphate capacity is used. Phosphate capacities of various flux systems are shown in Fig 5.7. The phosphate capacities of BaO- BaF<sub>2</sub> system are higher by 3 orders of magnitude in comparison with CaO- CaF<sub>2</sub> systems [27]. The phosphate capacity of a given flux increases with a decrease in reaction temperature. Thus it may be possible to attain the value of  $a_{Ba_3(PO_4)_2}$  near 0.1 (as per the calculations shown in Appendix IV) when BaO- BaF<sub>2</sub> flux is used at 1573 K. The activity of Ca<sub>3</sub>(PO<sub>4</sub>)<sub>2</sub> in 3Ca<sub>3</sub>(PO<sub>4</sub>)<sub>2</sub>.CaF<sub>2</sub> coexisting with that of CaF<sub>2</sub> has been found less than 0.1 at 1300°C thus contributing to dephosphorization by stabilizing Ca<sub>3</sub>(PO<sub>4</sub>)<sub>2</sub> [41]. Similar activity of Ba<sub>3</sub>(PO<sub>4</sub>)<sub>2</sub> is expected in Ba<sub>3</sub>(PO<sub>4</sub>)<sub>2</sub>.BaF<sub>2</sub> slag also, when slag is saturated with BaO.

Besides the above factors, the chemical composition of ferromanganese is known to have significant influence on the removal of phosphorus which is discussed below:

### 5.1.2 EFFECT OF INITIAL C, Mn, Si CONTENTS ON DEPHOSPHORIZATION

Iwase et. al.[78] observed that there is a definite lack of thermodynamic information on the activities of P<sub>2</sub>O<sub>5</sub> in BaO based molten fluxes. Experimental data on the activities of phosphorus in manganese based multicomponent alloys are not available in the literature [21], so the activity coefficient of phosphorus in Mn base alloys could not be calculated. However, the same can be calculated from the thermodynamic data available for liquid iron alloys as iron and manganese exhibit similar behavior in liquid solution.

$$\log f_p = e_p^C[\%C] + e_p^P[\%P] + e_p^{Si}[\%Si] + e_p^{Fe}[\%Fe] + e_p^S[\%S]$$

(5.4)

Typical compositions of ferromanganese alloys considered for calculation are given in appendix II The values of interaction parameters were taken from the compilation of Sigworth and Elliott[75]. The calculated phosphorus activity  $h_p$  is plotted against the phosphorus content of the liquid alloy (Fig 5.8). These results indicate that phosphorus removal should be easier from high carbon ferromanganese alloy because of a strong repulsive interaction between carbon and phosphorus. Carbon is also known to reduce the activity of Mn [76] which has been already discussed.

Dephosphorization efficiency decreases with higher initial silicon content of the ferromanganese alloy. Ferromanganese produced in India contains more than 0.6% silicon [81]. Fig. 5.9 shows the effect of initial silicon content in HC Fe-Mn alloy on the degree of dephosphorization. It shows that the silicon content of the ferromanganese alloy should be less than 0.2% for carrying out dephosphorization under oxidizing conditions [5,20,22,]. If the silicon content of the alloy is more than

0.2 %, the silica content of the slag will increase which may consume highly basic flux BaO, thereby adversely affecting the dephosphorization.

Fujita et. al.[20] found that dephosphorization efficiency decreases with increasing content of manganese. Fig 5.10 shows that, at a fixed temperature, the equilibrium partition ratio for phosphorus between slag and metal phase decreases with an increase in the manganese content of the ferromanganese alloy [27]. This indicates that the dephosphorization of the high carbon ferromanganese with manganese in the range of 65-75 % is difficult, hence necessitating the use of a stronger base.

### 5.1.3 EFFECT OF FLUX COMPOSITION ON DEPHOSPHORIZATION

The composition of flux affects its phosphate capacity. The presence of BaF<sub>2</sub> is reported to increase the phosphate capacity of BaO based flux[3,23]. Fig 5.7 shows the phosphate capacities of different reagent systems. It varies with temperature and composition of flux. The presence of MnO has strong effect on the phosphate capacity of BaO-MnO- BaF<sub>2</sub> flux. According to thermodynamic analysis [4], high activity of MnO in the slag favors dephosphorization whereas Lee [23] pointed out that the activity of P<sub>2</sub>O<sub>5</sub> is raised by the addition of MnO in the slag. Therefore, the MnO content of the slag needs to be optimized in order to achieve best possible experimental conditions for dephosphorization. The minimum phosphate capacity of a slag which should be used for effective dephosphorization depends on the activity of phosphorus in ferromanganese and on the oxygen partial pressure used. Therefore, the effect of partial pressure of oxygen ( $p_{O_2}$ ) on dephosphorization should also be examined.

#### 5.1.4 EFFECT OF OXYGEN PARTIAL PRESSURE

Fig 5.11 gives the relation between phosphorus distribution ratio and oxygen partial pressure at different phosphate capacities at 1300<sup>0</sup>C[41]. The dashed line in the figure denotes  $L_p=30$  required for making dephosphorization economically viable. If a slag of low phosphate capacity (say  $10^{26}$ ) is used than the oxygen partial pressure should be more than  $10^{-16}$  atm in order to achieve a partition ratio of more than 30 but this will lead to oxidation of manganese whereas if slags of high phosphate capacity  $10^{29}$  are used then dephosphorization is possible even at low oxygen partial pressure ( $10^{-17}$  atm). This will eliminate the loss of manganese into the slag.

The manganese activity in ferromanganese determines the maximum partial pressure possible to be used in dephosphorization. Considering the non equilibrium state and a lower oxygen partial pressure than  $31 \times 10^{-18}$  atm, a slag with phosphate capacity higher than  $10^{27}$  should be selected. The maximum phosphate capacity of BaO based slag is reported to be  $10^{29}$  compared to  $10^{26}$  for CaO based slag at 1300<sup>0</sup>C [3,4,27]. However, CaO based slag is considered to be cheaper than BaO based slag and is easily available [33]. Therefore, it was decided to carry out dephosphorization of ferromanganese using barium oxide as well as lime based slag in order to compare their merits and demerits.

#### 5.1.5 CALCULATION OF FLUX WEIGHT

Different investigators have used different quantity of flux for their experiments [21-23]. Ma et al [21] varied the slag weight from 100 gm per kg to 400 gm per kg of ferromanganese alloy. The degree of dephosphorization increased with increase in quantity of flux. Lee et. al [22] recommended that the barium oxide content by weight in the barium containing agent should be a minimum of about 50 times of the

weight of phosphorus to be removed from the alloy. Fujita et al.[20] used a flux-metal ratio of 0.04 for dephosphorization of Mn-Fe-C-P alloy while Lee[23] varied the flux quantity from 1.4 to 8.6 %. In view of these variation it was considered necessary to calculate the flux weight which is shown in Appendix V . As per this calculation 10 pct flux of metal weight was considered adequate for achieving 75 pct phosphorus removal, if the equilibrium partition ratio is 30. If the partition ratio is less then 30 than more quantity of flux will be required to achieve same level of dephosphorization. as shown in Appendix V.

### **5.1.6 SUMMARY OF THERMODYNAMIC ANALYSIS**

The results of the thermodynamic analysis of removal of phosphorus dissolved in liquid ferromanganese are summarized below:

1. It is possible to remove phosphorus selectively from ferromanganese using BaO based fluxes under oxidizing conditions without extensive oxidation of manganese, even though the oxide of manganese is more stable than that of phosphorus at smelting temperatures[2].
2. For this purpose, predominance area diagrams for the system Ba-P-O and Mn-O were constructed initially assuming unit activity of all the condensed phases at temperatures 1573-1873 K and subsequently for realistic activities of all the condensed phases at 1573 K as a lower temperature is considered more favorable. The predominance area diagram shows the stability of various phases such as barium phosphate, barium phosphide, manganese oxide with respect to partial pressure of oxygen at a given temperature.

3. The results indicate that it is possible to achieve effective dephosphorization  $[P] \leq 0.2\%$  at 1573 K by maintaining  $h_p$  below 2.18 as shown by the hatched area in Fig. 5.6 under non standard conditions as mentioned below:

- a)  $a_{Mn} = 0.3$
- b)  $a_{MnO} = 0.5$
- c)  $a_{Ba_3(PO_4)_2} = 0.1$
- d) Temperature 1573 K
- e) Oxygen potential about  $3.0 \times 10^{-17}$  atm

The justification for assuming the above values have already been discussed.

5. The high manganese content of the Fe-Mn alloy decreases the equilibrium phosphorus partition ratio at a fixed temperature [27] making the dephosphorization of high carbon ferromanganese (Mn>70%) difficult. However, it was recognized that if the flux is molten near the melting temperature of the ferromanganese alloy (1250-1300°C), it would be possible to achieve partition ratio of phosphorus in the desirable range of 20-40.
6. High carbon ferromanganese is helpful in dephosphorization because it not only increases the activity of phosphorus but also reduces the activity of manganese to about 0.3 at 1300°C. Therefore, graphite crucible was considered suitable for dephosphorization of high carbon ferromanganese.
7. Thermodynamic calculation showed that about 76 g BaO-based flux is required to treat 1 kg of ferromanganese for removal of 3g phosphorus in the form of phosphate. However 100 g flux per kg ferromanganese was considered adequate. The flux quantity also depends on the equilibrium partition ratio of

phosphorus for a given flux. If the partition ratio is less, the required flux quantity will be more for achieving same level of phosphorus removal.

The above thermodynamic analysis helped in identifying the favorable conditions for dephosphorization of ferromanganese. The BaO-MnO flux was considered the most suitable reagent for dephosphorization. However, in view of the high melting temperatures of BaO and MnO (1925 and 1785<sup>0</sup>C respectively), it was considered desirable to synthesize fluxes which have moderate melting temperatures (<1500<sup>0</sup>C). In order to confirm the predictions of thermodynamic analysis, experiments were carried out in a graphite crucible (1kg scale) in a high frequency induction furnace using *BaCO*<sub>3</sub> based flux (Fig 5.12). The results are discussed in the sections that follow

























## 5.2 RESULTS OF FEASIBILITY TESTS CONDUCTED IN AN INDUCTION FURNACE USING $BaCO_3$ BASED FLUXES

The aim of this study was to develop a suitable flux for dephosphorization of ferromanganese under oxidizing conditions. From the thermodynamic consideration discussed in Section 5.1, it was felt necessary to develop and use a flux comprised of BaO and MnO and yet having a moderate melting temperature ( $<1500^{\circ}C$ ). A literature review indicated that even though the available information on phase equilibria for the BaO-MnO binary is rather limited, a low melting region does exist near 18-20 % MnO with liquidus temperature in the range of 1300 to  $1350^{\circ}C$  as shown in Fig. 5.13 [20]

Melting the BaO-MnO flux at moderate temperatures ( $<1500^{\circ}C$ ) was a first step in using such  $BaCO_3$ -based fluxes for dephosphorization of ferromanganese. During the experiments, it was observed that melting of  $BaCO_3$  was easier without external addition of  $MnO_2$ . The MnO content in the slag was maintained in the range of 15-25% which was just sufficient to bring down the melting temperature of the flux to about  $1300^{\circ}C$  (Fig 5.13) and to provide the desired oxygen potential for selective removal of phosphorus. The viscosity of slag was further reduced by the addition of halides ( $BaF_2$ ,  $BaCl_2$ ). The additive ( $BaF_2$ ) also helped in increasing the phosphate capacity and reducing the manganese capacity of the slag. This was confirmed when the samples of ferromanganese treated with these fluxes were analyzed. The result showed that with the use of a  $BaCO_3$ -  $BaF_2$  it was possible to remove approximately two-third phosphorus at a moderate temperatures of about  $1350^{\circ}C$ . The manganese loss varied in the range of 2-5%.

Several tests were carried out using lime as well as barium oxide based fluxes. The results are shown in Table 5.2. In view of the difficulties experienced in melting  $BaCO_3$  and  $MnO_2$  flux mixture separately, initially lime based flux was used to treat

ferromanganese for removal of phosphorus. A study [83] showed that at 1200<sup>0</sup>C the phosphate capacity of CaO-based slag was 10<sup>26.5</sup> which was considered worth trying for the treatment of ferromanganese also. About 5 % *BaCO*<sub>3</sub> was added to increase the phosphate capacity of lime based flux. The details of these two tests (F1 and F2) are given in Table 5.3. It was found that only 25 % phosphorus could be removed. The reason for inadequate dephosphorization is possibly the lower phosphate capacity of the lime based flux.. Since it was difficult to prepare a synthetic slag of flux mixture of *BaCO*<sub>3</sub> and *MnO*<sub>2</sub>, some trials were made by directly adding this flux powder mixture from the top. After several tests, a few tests were partially successful (Test Nos F7, F8 and F11). Test Nos F3-F6, F9-F10 do not appear in Table 5.2 because trial experiments with *BaCO*<sub>3</sub> and *MnO*<sub>2</sub> fluxes were not successful due to difficulty in melting such slags and the breakage of crucibles at abnormally high temperatures. The results of the test No F7, F8 and F11 of Table 5.2 show inadequate dephosphorization, varying in the range of 4-25%. The reason for low degree of dephosphorization was attributed to the difficulty encountered in melting *BaCO*<sub>3</sub> and *MnO*<sub>2</sub> flux. The slag got solidified at frequent intervals which probably hampered the slag- metal reaction leading to a low degree of phosphorus removal in spite of the high phosphate capacity of the flux. According to the thermodynamic analysis of Goel and Srikanth [4], addition of *MnO*<sub>2</sub> should have helped the phosphorus removal but melting of flux with *MnO*<sub>2</sub> appeared to be a hard task. Therefore, it was decided to carry out subsequent experiments without external addition of *MnO*<sub>2</sub>, while stressing on the in-situ formation of *MnO*. It appears that the *MnO* formed is sufficient to provide the required quantity of oxygen for oxidation of phosphorus to phosphorus penta oxide in presence of a stronger base (*BaO*).

The results of the Test Nos F7, F8 and F11 also show the effect of initial silicon content on dephosphorization, as depicted in Fig. 5.14. The degree of dephosphorization improved from 7% for Test no F8 to about 25% for Test no F11

when the initial silicon content was reduced from 0.72% to 0.16%. The damaging influence of initial high silicon content on dephosphorization has also been reported elsewhere [21-23]. A high silica content in the slag decreases the basicity and consequently the phosphate capacity of the slag. In view of this result it was decided to prepare a master ferromanganese alloy having a silicon content less than 0.2% for use in subsequent tests.

When experiments were conducted using  $BaCO_3$  (Composition given in chapter 3) as flux without addition of  $MnO_2$ , the flux was found molten even at  $1300^{\circ}C$ . Addition of  $BaF_2$ /  $BaCl_2$  helped in improving the fluidity of slag. Test No F12 shows the effect of  $BaCl_2$  addition which is discussed later. In Test No F13 (Table 5.2), the phosphorus level was brought down to 0.18% from an initial level of 0.56% (Fig 5.15) after allowing the reaction to continue for 30 minutes. However, the manganese content in the ferromanganese got reduced from 67.3 % to 63.8 % indicating a loss of about 5% during the dephosphorization test. These results are in good agreement with a recent publication of Liu et. al [41] who reported a 61% removal of phosphorus in 30 minutes at a 5% manganese loss when  $BaCO_3$  was used as flux at 130g/ Kg ferromanganese in an induction furnace. However, in the present study the maximum phosphorus removal was 68 %. This may be due to the addition of  $BaF_2$  which perhaps increased the phosphate capacity of the flux [23].

Liu [84] carried out only one test using  $BaCO_3$ , and the potential of the  $BaCO_3$  as flux which is readily available at low cost has not been investigated thoroughly. Therefore, the present study focused on the development of  $BaCO_3$  based fluxes and addressed the drawbacks encountered in the previous studies. The effects of following parameters were examined which are discussed below:

- a) Type of flux
- b) Quantity of flux
- c) Silicon content of the ferromanganese alloy

- d) Temperature
- e) Reaction Time

### 5.2.1 EFFECT OF FLUX TYPE ON DEPHOSPHORIZATION

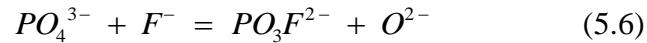
Fig 5.16 compares the extent of dephosphorization obtained using different  $BaCO_3$  based fluxes. Amongst the reagents investigated,  $BaCO_3$ - $BaF_2$  was found to be most effective. Substitution of  $BaF_2$  by  $BaCl_2$  lowered the extent of dephosphorization. The degree of dephosphorization was further reduced when  $MnO_2$  was added along with  $BaCO_3$ . The effect of these additives on the  $BaCO_3$ -based flux is discussed below:

#### a) Effect of addition of $BaF_2$

The effect of  $BaF_2$  addition on the degree of dephosphorization ( $\eta$ ) is shown separately in Table No 5.4. It also shows the quantum of manganese loss during treatment. Fig 5.16 shows that about 70 % phosphorus was removed for Test No F13 when about 30 %  $BaF_2$  was added along with  $BaCO_3$  in the liquid ferromanganese. The addition of barium fluoride helped the melting of flux at 1300-1350<sup>0</sup>C which facilitated good slag metal reaction. In Test No F14 about 60 % phosphorus removal was obtained at relatively higher temperature (1380<sup>0</sup>C) but it required only 15 minutes as compared to 30 minutes for test No 13. In this test only 15%  $BaF_2$  was used which was adequate to provide the required fluidity of slag at 1380<sup>0</sup>C. The degree of dephosphorization was comparable to that obtained at lower temperature (1300<sup>0</sup>C) for Test No F13. The reason may be the high BaO content (47%) in slag compared to 37% for Test No F13 as shown in the Table 5.4 which is known to increase the phosphate capacity of slag[23]. Slag analysis (Table5.4) also showed that  $P_2O_5$  content in the slag was higher (3.27 %) compared to 2.68% for Test No F13. The MnO content was almost identical at about 25 % in both the slag. However, metal analysis showed that manganese loss was less than 2% for test No

F14 compared to about 5 % in test No F13. This is expected because the oxidation of manganese is a highly exothermic reaction with an enthalpy change of -415 KJ/mole [41].

The above findings are in close agreement with those of Lee [23] who reported that the degree of dephosphorization increased from 40 % to about 65 % when  $BaCO_3$  is partially replaced by  $BaF_2$ . The presence of  $BaF_2$  in slag helped increase the fluidity of slag and is also known to increase the activity coefficient of MnO [23]. Due to increase in the activity coefficient of MnO, it is possible to carry out dephosphorization of ferromanganese at a relatively higher oxygen partial pressure without excessive oxidation of manganese. It has been also reported [84] that fluoride ions in slag can replace oxygen in phosphate ions and enhance dephosphorization by stabilizing it as per the reaction given below:



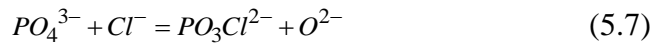
The release of oxygen ions promotes the formation of phosphates thus increasing the degree of dephosphorization. Shim et. al [28] also studied the role of  $BaF_2$  on the thermodynamic properties of the BaO-MnO flux system. As shown in Fig. 5.17 the solubility of MnO in slag decreases from a maximum of 32%  $BaF_2$  to around 23% at 30%  $BaF_2$  indicating a strong repulsive interaction between  $BaF_2$  and MnO. They observed that the manganese oxidation loss may be decreased by adding  $BaF_2$  during dephosphorization of Fe-Mn alloys with  $BaCO_3$ . However, the quantity of addition should be optimized. This supports the conclusion of present investigation which clearly established this fact that dephosphorization of ferromanganese can be carried out to a significant extent (around 70% under near equilibrium study) and at the same time restricting the manganese loss to a very low level (around 2%).

Thus the addition of  $BaF_2$  not only increases the phosphate capacity of flux but also minimizes the manganese loss from ferromanganese while using  $BaCO_3$  instead of  $BaO$  as flux. It has been reported [23] that the manganese loss can go up to 7 % when the  $BaCO_3$ -based flux is used. Therefore, the addition of  $BaF_2$  is helpful in cutting down the manganese loss. Recently  $BaO$ - $BaF_2$  slag has been also used successfully for simultaneous desulphurization and dephosphorization of hot metal [85].

#### **b) Effect of addition of $BaCl_2$**

Compared to  $BaF_2$ , addition of  $BaCl_2$  is less effective in promoting dephosphorization. It was possible to remove about 40 % phosphorus for Test No. F12 (Table 5.5) when  $BaCO_3$  was partly replaced by  $BaCl_2$  (Fig 5.18). In Test No F19, lower quantity of flux (13%) was used compared to about 18% for Test No F12. The results of the slag analysis for test No F19 showed that the  $P_2O_5$  Content in slag was higher ( 3.41%) which is comparable with the result obtained with  $BaF_2$  as additive for Test No F14. Thus shows that it is possible to achieve good partition ratio (about 5) even when  $BaCl_2$  was used as additive. However, it is less effective compared to  $BaF_2$  which was expected because substitution of  $BaCl_2$  for  $BaO$  has the effect of lowering the phosphate capacity. Iwase et. al. [77] has pointed out that substitution of  $BaCl_2$  for  $BaO$  increases the activity of  $P_2O_5$ . They observed that chloride ion lowers the basicity of slag. From thermodynamic point of view, better dephosphorization can be achieved by using fluxes of greater  $BaO/ BaCl_2$  molar ratio. For deciding this ratio, slag fluidity as well as slag basicity should be taken into consideration because chloride is helpful in improving the fluidity of slag. From this point of view  $BaCl_2$  has advantage over  $BaF_2$  because its melting point ( $980^{\circ}C$ ) is lower than that of  $BaF_2$  ( $1250^{\circ}C$  approx.).

The addition of BaCl<sub>2</sub> helped in reducing the melting temperature of BaCO<sub>3</sub> flux near the melting temperature of the ferromanganese alloy. This is likely to promote dephosphorization due to good slag metal reaction. The phosphate capacity of BaO-BaCl<sub>2</sub>-MnO have been reported to be slightly higher than 10<sup>27</sup> at 1300<sup>0</sup>C[84] which is considered adequate for dephosphorization of Fe-Mn alloy if other conditions are favorable. Inoue et. al [80] pointed out that the phosphate capacity of CaO-CaCl<sub>2</sub> flux was far larger than those of conventional slags for treatment of iron based alloys. The addition of only 10% CaCl<sub>2</sub> to CaO can greatly improve the coefficient of utilization of flux. Similar behavior of chloride is expected with BaCO<sub>3</sub> based flux. Chloride ions in slag can also replace oxygen in phosphate ions and enhance dephosphorization by stabilizing it as per the reaction given below [84]:



The release of oxygen ions promotes the formation of phosphates thus increasing the degree of dephosphorization. However, MnO content in the slag increased from 23% to 31% when BaF<sub>2</sub> was replaced by BaCl<sub>2</sub> [41].

Since barium chloride is less expensive than the barium fluoride, it can be considered as a potential additive to be used with barium carbonate for dephosphorization of high carbon liquid ferromanganese for commercial application.

### c) **Effect of addition of MnO<sub>2</sub>**

The removal of phosphorus hardly took place when MnO<sub>2</sub> was externally added along with BaCO<sub>3</sub> for Test Nos F7, F8 as shown in Table 5.2. MnO<sub>2</sub> was added along with BaCO<sub>3</sub> in order to increase the activity of manganese in the slag but the experience showed that this was not effective from the point of view of difficulty in melting BaCO<sub>3</sub>- MnO<sub>2</sub> flux externally. When MnO<sub>2</sub> was not added, it was possible

to form a BaO-MnO slag in a molten condition at about 1573 K. It was realized that the role of MnO as oxygen supplier and eutectic forming compound can be met by CO<sub>2</sub> released by dissociation of BaCO<sub>3</sub> added in liquid ferromanganese; hence there is no need to add MnO<sub>2</sub> externally for oxidation of phosphorus. It was observed that in situ oxidation of Mn helps in the reduction of melting temperature of BaO-based flux. A slag analysis, in the present investigation using BaCO<sub>3</sub>/ BaF<sub>2</sub> flux showed that in-situ formed MnO content was in the range of 20-25 % which could remove about two-third phosphorus[40]. The values were quite close to the values of MnO in slag reported by Liu et. al.[41]. According to this study, a suitable slag composition for dephosphorization of ferromanganese using BaCO<sub>3</sub>+ BaF<sub>2</sub> should be as shown in Table 5.4:

( BaO)	=	35-50 %
(BaF <sub>2</sub> )	=	10-25 %
(MnO)	=	20-25 %

However, the MnO content shown above did not match with the value reported by Lee[23] which was in the range of 55-80 % in the slag calculated on the basis of material balance indicating a manganese loss of 7% when BaCO<sub>3</sub> was used for dephosphorization of Fe-Mn alloy. The reason for this difference may be the composition of flux and the process control. We used barium carbonate with additives whereas their results show the use of only barium carbonate. The MnO content in the slag was about 75% when they used only 1.4 % BaCO<sub>3</sub> of metal weight. It appears that high MnO content was responsible for the lower degree of dephosphorization (< 50 %). The high content of MnO reduced the phosphate capacity of flux. It has been reported[27] that manganese oxide in BaO-BaF<sub>2</sub>-MnO slag behaves as an acidic oxide which may consume highly basic slag reducing its capability for dephosphorization.

Dephosphorization of ferromanganese alloy is carried out at an oxygen potential just below that for the Mn- MnO reaction, however certain oxidation of Mn is unavoidable. The MnO content should be restricted to 20 % in order to minimize the loss of manganese. According to Ma et. al. [21], an MnO content of 18-20 % in a BaO -MnO slag can help it fuse at about 1300<sup>0</sup>C. This is a desirable condition for dephosphorization of Fe-Mn alloy. It appears that the melting point of BaO-MnO slag is less than 1500<sup>0</sup>C when the MnO content in the slag is below 30 % . Above this there may be the formation of intermediate compound which can hamper dephosphorization.. Therefore MnO content should be maintained at desired level by using proper additives and process control [40].

It has also been reported [82] that the suitable MnO content in BaO- MnO slags for dephosphorization of ferromanganese should be in the range of 20-40 % in order to provide the necessary oxygen potential at the slag/ metal interface without deteriorating the dephosphorization ability of the slags. In a recent publication [27], it has been reported that BaO-MnO flux may be useful for iron base alloy containing high manganese but this may not be suitable for dephosphorization of high carbon ferromanganese. This is because the partition ratio of phosphorus decreases sharply with increase in manganese content of the alloy. For example, the equilibrium phosphorus partition ratio between a BaO-MnO slag and an Fe-14%Mn-C<sub>satd</sub> alloy at 1300<sup>0</sup>C is reported to be 840 and decreases to 50 when the manganese content in the alloy is increased to 50 %. This ratio is likely to go down further at higher temperatures (>1500<sup>0</sup>C) making dephosphorization difficult, as shown in Fig 5.10.

According to Lee[23] the activity of P<sub>2</sub>O<sub>5</sub> is raised by the addition of MnO in the slag which is contrary to our results ( Table 5.6) calculated on the basis of thermodynamic analysis as per which activity of MnO should be high (closer to 1) for better dephosphorization. Thus the role of MnO needs further investigations for

both  $BaCO_3$  and  $BaO$  based fluxes. This has been discussed in the next part of this study.

### **5.2.2 EFFECT OF SILICON CONTENT OF THE ALLOY**

Fig 5.14 shows the effect of initial silicon content on the degree of dephosphorization. Dephosphorization efficiency decreased from 23 % to 7 % when silicon content increased from 0.16 % to 0.72 %. Even though the degree of dephosphorization may have dropped to a minor extent because of the other factors also yet the effect of silicon on the dephosphorization is quite clear. The degree of dephosphorization improved to 68 % when the silicon content of the alloy was kept at less than 0.2% and other factors were favorable (Test No F13, Fig 5.16). These results match with the findings of Lee et. al. [22] who carried out dephosphorization of two ferromanganese alloys, one having a silicon content of 0.66% and the other only 0.27% with a barium oxide containing agent under oxidizing conditions. The phosphorus content got reduced from initial level of 0.31% to 0.19% for the lower silicon melt whereas no phosphorus removal was observed in the melt containing 0.66% silicon. The silica content of the slag increases due to oxidation of high amounts of silicon which consumes highly basic  $BaO$  based slag thereby affecting dephosphorization. Therefore, desiliconization is considered necessary if the silicon content is higher than 0.2% prior to dephosphorization under oxidizing condition.

### **5.2.3 EFFECT OF FLUX WEIGHT ON DEPHOSPHORIZATION**

Fig 5.16 shows the improvement in degree of dephosphorization with increase in the quantity of flux added.  $BaCO_3$  along with  $BaF_2$  was considered a most suitable reagent system as consistently high phosphorus removal ( at 68% and 60%) were achieved for Test Nos F13 and F14 using about 16 % of these fluxes. Attempts

were made to reduce the flux quantity to half and one fourth (Test Nos F16,F18 and F17 as shown in Table 5.4) for economical use of the flux. This was also done because different quantities of flux has been used by different investigators [20,21,23]for dephosphorization of Fe-Mn alloys. Fujita et. al.[20] used a flux-metal ratio of 0.04 while Lee[23] varied the flux quantity from 1.4% to 8.6% of. Ma et al[21] varied the flux quantity from 10% to 40% of metal weight. The results in the present study showed that the degree of dephosphorization ( $\eta$ ) decreased from 68%at 16 wt % flux for Test No F13 to about 30% when the flux content was reduced to 8% for Test No F16 and F18 and to about 10 % at 4 wt % flux for Test No F17 as shown in Table 5.4. The maximum removal of phosphorus (68%) was obtained when 160 gm  $BaCO_3$  flux was added in a kg of liquid ferromanganese alloy. Thus a flux dosage of 16% by metal weight was considered an optimum quantity and agrees with the value reported by Ma et al [21] who considered 15 wt %  $BaCO_3$ as an optimum quantity for dephosphorization of ferromanganese alloy.

#### **5.2.4 EFFECT OF TEMPERATURE ON DEPHOSPHORIZATION**

As per our thermodynamic analysis lower temperature favors the dephosphorization under oxidizing conditions. This was conclusively proved when the metal slag reaction took place at low temperatures (1300-1350<sup>0</sup>C) which reduced the phosphorus content to desired level (0.18% )from an initial content of 0.56% in Test No F13 (Fig 5.15). The low melting temperature of the slag of Test No F13 was confirmed by DTA (Differential Thermal Analysis) as shown in Fig 5.19.

Earlier, on the basis of their equilibrium study Liu et al [38] have reported that the phosphorus distribution ratio decreases with increasing temperature, at a given slag composition. Though, a lower temperature favors the dephosphorization under oxidizing conditions from thermodynamic point of view as discussed in section 5.1,

the time taken to reach near equilibrium value may be relatively long whereas higher temperature will tend to improve the reaction kinetics point of view and the time taken to reach the equilibrium value may be short. As shown in Table 5.2 the phosphorus removal obtained at relatively higher temperature (1380<sup>0</sup>C Test no F14) was comparable to that obtained at a lower temperature (1300-1350<sup>0</sup>C, Test No F13) but it required only 15 minutes as compared with 30 minutes for the later. This may be due to the fact that at high temperature, oxygen partial pressure is more at slag/ metal interface for a fixed slag composition which appears to have compensated the lower phosphate capacity of flux due to higher temperature. The test conducted at 1380<sup>0</sup>C also showed that manganese loss was less than 2%. This is expected because the oxidation of manganese is a highly exothermic reaction with an enthalpy of change of -415 KJ/ mole[41].

It is to be noted that the desired phosphorus levels (<0.2%) obtained within 30 minutes at moderate temperatures of 1573-1673 K in the induction furnace tests may not be easily reproduced in a ladle (stagnant bath) conditions unless the bath is adequately agitated. This calls for the thorough investigation of the reaction kinetics of the process by injecting flux for treatment of ferromanganese. It is suggested that the temperature of the liquid ferromanganese must be maintained 100-150<sup>0</sup>C higher than the liquidus temperature in order to compensate for the heat loss during treatment. Since the decomposition of BaCO<sub>3</sub> is endothermic reaction, a heating arrangement may be required to preheat the ladle.

### **5.2.5 EFFECT OF REACTION TIME**

Fig 5.18 shows the degree of dephosphorization against the reaction time after the addition of flux for Test No F12. The degree of dephosphorization reaches a maximum value at about 30 minutes of flux addition. The samples were collected

after 15, 30 and 45 minutes of addition of flux. It was observed that the lowest value of phosphorus in alloy is reached in less than 30 minutes. This was in good agreement with the time indicated by Liu et. al [41] but differed with Ma et al [21] who indicated that near equilibrium is reached in about 7 minutes time in test carried out at a small scale .

### 5.2.6 SUMMARY OF RESULTS OF FEASIBILITY TESTS

1. The present investigation clearly established the fact that dephosphorization of ferromanganese can be carried out to a significant extent (68%) using BaCO<sub>3</sub>-BaF<sub>2</sub> flux mixture. The phosphorus contents were reduced to desired levels (<0.25%) from the initial levels (>0.40%) present in the ferromanganese alloy.
2. Barium carbonate(BaCO<sub>3</sub>) was used as a substitute for BaO in the present investigation because of its ready availability at low cost. It was difficult to melt the BaCO<sub>3</sub> and MnO<sub>2</sub> flux mixture initially but after several trials suitable compositions (BaCO<sub>3</sub>-BaF<sub>2</sub>/BaCl<sub>2</sub>) were identified to melt the flux at moderate temperatures (<1500<sup>0</sup>C). It was observed that BaCO<sub>3</sub> could not be melted in the presence of MnO<sub>2</sub>.
3. The manganese loss was restricted within 2-5 % compared to more than 5 % reported by other investigators. Probably, the addition of BaF<sub>2</sub> with BaCO<sub>3</sub> increased the activity of manganese oxide, thereby cutting the manganese loss.
4. Compared to BaF<sub>2</sub>, the addition of BaCl<sub>2</sub> with BaCO<sub>3</sub> was less effective. The maximum removal of phosphorus achieved was 40 % compared to 68 % when BaF<sub>2</sub> is added.

5. It was observed that a moderate 20-25 % MnO content in slag was helpful in achieving high levels (>60%) of phosphorus removal without significant loss (<5%) of manganese
  
6. Dephosphorization was found to be very sensitive to the initial silicon content of ferromanganese. It was found that under oxidizing conditions, the degree of dephosphorization decreased significantly with increase in the initial silicon content of the ferromanganese alloy. An initial silicon content of less than 0.2% is recommended from this investigation.
  
7. The degree of dephosphorization increased with increase in the quantity of flux (powder) added but showed no improvement in dephosphorization beyond 16 % addition.
  
8. Lower temperatures favor the dephosphorization under oxidizing conditions. The Efficiency of BaO- based fluxes increased due to melting near hot metal temperatures.
  
9. Maximum level of phosphorus was removed within 30 minutes of flux addition.



























### **5.3 RESULTS OF THE DEPHOSPHORIZATION TESTS USING CALCINED BaCO<sub>3</sub>(BaO) BASED FLUX PELLETS**

The experimental results from the present study have established the feasibility of using BaCO<sub>3</sub>-based flux powder for dephosphorization of high carbon liquid ferromanganese in the induction furnace. However, in plant operation the addition of powder in the ladle containing liquid ferromanganese would be difficult. The low density of powder would not allow uniform mixing and assimilation of the flux powder with liquid ferromanganese when powder is fed from the top. There may be some loss of powder as dust which can be hazardous. Besides some of the flux powders will be burnt away due to the intense heat of liquid metal. These difficulties can be overcome if flux is charged in the form of pellets instead of powders. These pellets will go to the bottom of ladle immediately and get melted and mixed with liquid alloy quickly. Thus the dephosphorization will also take place during the rise of the powder particles to the metal slag interface. In this way, the reactivity of pellets is expected to be much faster than that of powders. Another advantage of using pellets is that it utilizes manganese ore fines which is a waste material in the ferromanganese industry. Also pellets are easier to handle and eliminate the loss of flux as dust which occurs when powder is added.

Another disadvantage of BaCO<sub>3</sub>-based flux powder addition is that its decomposition reaction is highly endothermic i.e. it takes away lots of heat from liquid ferromanganese which is not desirable. Therefore, it was decided to carry out calcination beforehand. The carbon in the form of coke, tar or carbon block, is added to the carbonate based pellets to lower reaction temperature from about 1300<sup>0</sup>C to 1050<sup>0</sup>C. Thus the heat loss from liquid metal can be minimized, if the pre-calcination of barium carbonate pellet is carried out in presence of carbon at 1050<sup>0</sup>C. This will ensure that the BaO is available for reacting with P<sub>2</sub>O<sub>5</sub> when the temperature is raised from 1050<sup>0</sup>C to 1350<sup>0</sup>C for melting of ferromanganese alloy

and the flux. The pre- reduction of pellets with carbon also improves its porosity. It was found [42] that the porosity of manganese oxide pellets in presence of carbon was in the range of 24-27 % when it was calcined at 1173 K. Thus the reactivity of calcined pellets will be much better than those of powders. The addition of calcined pellets will also save energy, if pre-reduction of BaCO<sub>3</sub>-based pellets are carried out in the solid state before charging them into liquid ferromanganese. Thus no heat will be removed from liquid ferromanganese for removal of extra atom of oxygen from MnO<sub>2</sub> and CO<sub>2</sub> from BaCO<sub>3</sub>.

In view of the advantages of precalcined BaCO<sub>3</sub>-based pellets, it was decided to prepare them for subsequent tests. However, it was apprehended that BaO pellets formed after calcination may revert to BaCO<sub>3</sub> if not stored properly and the advantage of precalcination will be lost. Therefore, it was also decided to carry out the calcination as well as dephosphorization in the same furnace (carbon resistance furnace) under controlled atmosphere and temperature within  $\pm 2^{\circ}\text{C}$ . It was planned to make green pellets from the powder mixture (of BaCO<sub>3</sub>-MnO<sub>2</sub>-BaF<sub>2</sub> ) in the presence of carbon in a specific proportion with the help of a binder and moisture. These pellets were dried for 24 hours before calcining them at about 1000-1100<sup>0</sup>C in order to impart strength and porosity. Partial in-situ precalcining of BaCO<sub>3</sub> at solid state was aimed to avoid temperature drop in the reaction furnace due to endothermic decomposition of BaCO<sub>3</sub>. Besides, total in situ decomposition of BaCO<sub>3</sub> may lead to excess manganese loss due to existing CO<sub>2</sub> bubbles in the system. The idea behind this approach was to develop BaO -based pellets so that once it is developed it can be added into the ladle for the removal of phosphorus from liquid ferromanganese. Thus the BaO will be in situ available to react with P<sub>2</sub>O<sub>5</sub> which may improve the dephosphorization efficiency and reduce the loss of manganese.

The work was divided into three broad steps:

1. Preparation of green fluxed pellets
2. Calcination of pellets to form BaO from BaCO<sub>3</sub> and MnO from MnO<sub>2</sub>
3. Metal-slag reaction tests

MnO<sub>2</sub> was pre-reduced to MnO by heating the pellets in the carbolyte furnace. The temperature was varied from 700 to 1000<sup>0</sup>C. The results indicated that the MnO<sub>2</sub> content decreases with increase in temperature (Fig 5.20). After soaking at 1000<sup>0</sup>C for 1 hr, it was found that all the MnO<sub>2</sub> has been converted. This formed the basis of fixing pre-reduction temperature of MnO<sub>2</sub> for formation of MnO.

Regarding calcination of BaCO<sub>3</sub>, it is known to be stable up to the temperature of 1300<sup>0</sup>C. However, in the presence of carbon it decomposes at 1050<sup>0</sup>C. This was confirmed by carrying out the calcination tests at 1050<sup>0</sup>C for 1 hr in a carbolyte furnace. Samples were quenched for arresting the phases. These samples were analyzed by X-ray diffraction (XRD). The XRD pattern (Fig 5.21) indicated that the major phase present was barium oxide. This formed the basis of fixing calcination temperature (1050<sup>0</sup>C) for the formation of BaO+MnO from BaCO<sub>3</sub> and MnO<sub>2</sub>.

Since barium oxide is highly reactive towards CO<sub>2</sub> in presence of water vapor and is converted to the hydroxide and carbonate when exposed to air and therefore needs proper storage under inert atmosphere which was not possible in present case, therefore, it was decided to form BaO+MnO in the carbon resistance furnace itself by heating the BaCO<sub>3</sub> and MnO<sub>2</sub> based green pellets at 1050<sup>0</sup>C for 1 hr before carrying out dephosphorization tests at 1350-1400<sup>0</sup>C.

From the feasibility tests carried out in induction furnace, it was observed that the silicon content in ferromanganese is detrimental for dephosphorization by BaO based flux under oxidizing conditions, therefore it was planned to use synthetic Mn-

Fe-C-P alloy free from silicon for this part of the tests but it could not be possible due to high cost and non availability of pure materials. Therefore, commercial grade of ferromanganese was desiliconized in induction furnace for use in subsequent tests. The composition of the desiliconized ferromanganese is given below:

C	-	6.5%
Mn	-	60%
Si	-	0.1%
P	-	0.39%

The results of tests carried out in the carbon resistance furnace are shown in Table No.5.7. Several small graphite crucibles with cover were used for the treatment of ferromanganese with BaO-based pellets formed in situ from the calcination of BaCO<sub>3</sub>-based pellets. These crucibles were kept in a bigger graphite crucible in a carbon resistance furnace having dimensions of 85 mm internal diameter and 125 mm height. The first series of experiments P1-P6 were done using pellets of different compositions to identify the most suitable composition. From these tests BaO-BaF<sub>2</sub>-MnO was identified as the most suitable flux for dephosphorization of ferromanganese. The lowest phosphorus removal took place for Test No P5 when only BaO (calcined BaCO<sub>3</sub>) was used as a flux. This indicates the importance of the presence of MnO in a BaO-based flux. Using this identified flux, second series of experiments P7-P9 were carried out to examine the effect of flux dosage on dephosphorization. It was observed that the external addition of MnO was possible in the pellets. Therefore, third series of experiments P10-P17 were carried out to study the effect of MnO content of the flux on dephosphorization. The results of these tests are discussed in the next section

### 5.3.1 EFFECT OF DIFFERENT TYPES OF FLUX ON DEPHOSPHORIZATION

Various types of flux pellets such as  $\text{BaCO}_3\text{-MnO}_2\text{-BaF}_2$ ,  $\text{BaCO}_3$ ,  $\text{BaCO}_3\text{-MnO}_2\text{-BaCl}_2$ ,  $\text{BaCO}_3\text{-BaCl}_2$  were used. The proportion was varied for other two compositions. The temperature of the furnace was raised at the rate of  $25^\circ\text{C}$  per minute. Soaking was done at  $1050^\circ\text{C}$  for 1 hr for the formation of  $\text{BaO-MnO}$  from  $\text{BaCO}_3\text{-MnO}_2$  fluxed pellets. After this the temperature was raised to  $1400^\circ\text{C}$  to allow metal - slag reaction to take place for 30 minutes. Amongst the fluxes used,  $\text{BaO-MnO-BaF}_2$  was found to be the most suitable flux for dephosphorization of ferromanganese. About 80% phosphorus was removed compared to 66% when  $\text{BaO-MnO-BaCl}_2$  flux was used (Table 5.8). The flux quantity (15%) was identical in both the cases. It was also observed that the dephosphorization efficiency achieved was better than the maximum of 68% when carbonate based flux  $\text{BaCO}_3\text{-BaF}_2$  was used. The result was also found to be in good agreement with the findings of Liu et. al [41] who achieved about 80% phosphorus removal when  $\text{BaO-BaF}_2\text{-MnO}$  flux was used. This is expected because addition of  $\text{BaF}_2$  is known to reduce the activity of  $\text{P}_2\text{O}_5$  [23] besides increasing the fluidity of slag. Shim et. al. [28] reported that the addition of  $\text{BaF}_2$  reduce the solubility of  $\text{MnO}$  in slag (Fig.5.17) thus increasing the activity of  $\text{MnO}$  in the slag which is another desirable condition for dephosphorization of Fe-Mn as discussed earlier in Section 5.1.

### 5.3.2 EFFECT OF FLUX WEIGHT

In the second series of experiments the flux dosage was varied from 5 to 20 % of the metal weight using the identified composition of the flux. Metal analysis did not show any significant variation in the final phosphorus content with the flux weight when  $\text{BaO-MnO-BaF}_2$  flux was used (Fig5.22). However, recovery of the phosphorus in slag increased from 34 to 66 % with increase in flux weight to

20% (as shown in Table 5.8). On the basis of this observation it was concluded that phosphorus removal increases with increase in the quantity of flux used. This was also confirmed by the Fig 5.23 which shows that the %  $P_2O_5$  in slag increases from 0.8% to 2.1% when the flux metal ratio increased from 0.05 to 0.2 at 1350°C. However, the extent of dephosphorization was higher with increase in flux metal ratio up to 0.1 than it was in the range of 0.1 to 0.2. The reason for this trend could be the decrease in the phosphorus gradient compared to initial gradient. Similar trend was also observed when BaO-MnO-BaCl<sub>2</sub> flux was used. Fig. 5.24 shows that the final [P] content in the metal decreases with increase in the quantity of flux used. However, there was no significant change in the removal of phosphorus from the metal when the flux quantity increased beyond 10 %. Thus 10 % flux of metal weight was considered to be economical for dephosphorization of Fe-Mn. This matches with the findings of Liu et al [41] who considered 10 % flux weight as the optimum quantity to be used for dephosphorization of ferromanganese.

### 5.2.3 EFFECT OF TEMPERATURE

Fig 5.25 shows that the partition ratio of phosphorus between the slag and metal increases with a decrease in the reaction temperature from 1400 to 1350°C for a given flux composition. This was expected as per the thermodynamic considerations, the value of K increases with decrease in temperature for the exothermic reaction 5.5 which reduces the activity of phosphorus ( $a_P$ ). From a thermodynamic point of view, the melting of the flux near the melting temperature of the ferromanganese alloy was a most desirable condition for dephosphorization under oxidizing conditions using BaO-based fluxes. The results of the present investigation match with the findings of other investigators. Ma et.al.[21] varied the temperature between 1300 to 1400°C using BaCO<sub>3</sub> flux and found that the dephosphorization is favored with a decrease in temperature. Liu et. al. [41] observed that the degree of

dephosphorization is low at higher temperatures due to decrease in the phosphate capacity of flux but the time to reach equilibrium is short.

Predominance diagrams (Fig 5.2 to 5.4) show that with increase in temperature from 1573 K to 1873 K, dephosphorization becomes difficult but the partial pressure of oxygen corresponding to Mn-MnO equilibria becomes higher that means the manganese loss will be less at higher temperatures. The oxidation of manganese is highly exothermic with an enthalpy change of -415 KJ/ mole [39] and is thus favored at lower temperatures.

#### **5.3.4 EFFECT OF MnO CONTENT IN THE REAGENT**

The third series of experiments were carried out by varying the MnO<sub>2</sub> contents in two identified flux systems BaCO<sub>3</sub>-BaCl<sub>2</sub>-MnO<sub>2</sub> and BaCO<sub>3</sub>-BaF<sub>2</sub>-MnO<sub>2</sub>. Fig 5.26 shows that the partition ratio of phosphorus increases up to 20 with increase in MnO<sub>2</sub> content from 10% to 40% in the flux BaCO<sub>3</sub>-BaCl<sub>2</sub>-MnO<sub>2</sub> (Test No P10 to P13 of Table 5.7) beyond which it starts decreasing. The % P<sub>2</sub>O<sub>5</sub> content of the slag was also found to increase with MnO content in the reagent up to 30 % beyond which it shows decreasing trend (Fig. 5.27). The result was found in good agreements with the observations made by Xioaya Liu [84]. On the basis of their equilibrium study[38], the phosphate capacity of 10<sup>27.5</sup> was achieved for BaO-BaCl<sub>2</sub>-MnO slag which led them to conclude that the slag system can meet the requirements of ferromanganese dephosphorization. The phosphate capacity of such high order was obtained when mole fraction of MnO in slag was about 0.25. Later they used the BaO-BaCl<sub>2</sub>-MnO flux for dephosphorization of high carbon ferromanganese in an induction furnace. The value of phosphorus distribution was not as good as obtained in the equilibrium experiments. The reason was probably the high MnO content in the final slag and a non-equilibrium state. So the MnO content

beyond a certain value is definitely detrimental to the dephosphorizing capability of the BaO-BaCl<sub>2</sub>-MnO slag.

Experiments were also carried out by varying the MnO<sub>2</sub> content in the flux BaCO<sub>3</sub>-BaF<sub>2</sub>-MnO<sub>2</sub> (Test Nos P14 to P17 of table 5.7) in the range of 10 to 40 % to see its effect on dephosphorization of ferromanganese. Fig 5.28 shows that the partition ratio of phosphorus increases to 10 when the MnO<sub>2</sub> content in the BaCO<sub>3</sub>-BaF<sub>2</sub>-MnO<sub>2</sub> flux increased from 12 to 30 % beyond which it decreases. Similar trend was also observed in the variation of % P<sub>2</sub>O<sub>5</sub> content in the slag (Fig. 5.29). The reason for this change in trend was obviously the MnO content in the slag beyond a desired value. Therefore MnO content in the slag was analyzed with the variation of MnO<sub>2</sub> content in the reagent. Table 5.9 shows the variation of MnO and P<sub>2</sub>O<sub>5</sub> content in the slag with variation of MnO<sub>2</sub> content in the reagent. The MnO content in the slag was more than 40% when the MnO<sub>2</sub> content in the reagent was increased beyond 30% in BaCO<sub>3</sub>-BaF<sub>2</sub>-MnO<sub>2</sub> flux (Fig. 5.30). A similar trend was also observed when MnO content in the slag was analyzed with a variation of MnO<sub>2</sub> content in BaCO<sub>3</sub>-BaCl<sub>2</sub>-MnO<sub>2</sub> flux (Fig. 5.31). The high content of MnO in slag beyond 35-40% decreased the % P<sub>2</sub>O<sub>5</sub> content in both the slag (Fig. 5.32 and 5.33). When the MnO<sub>2</sub> content is increased from 30% to 40% in the BaCO<sub>3</sub>-BaCl<sub>2</sub>-MnO<sub>2</sub> reagent, the % P<sub>2</sub>O<sub>5</sub> content in the slag decreases from 1.28% to 1.19% as shown in Table 5.9, affecting the dephosphorization. The reason for the decrease in the % P<sub>2</sub>O<sub>5</sub> content in the slag could be the adverse effect of MnO on the phosphate capacity of slag. According to Watanabe et. al. [28], since BaO is an extremely basic oxide, MnO behaves in the system as an acidic component which reduces the basicity of slag and hence the change in the trend of dephosphorization. Therefore, MnO content in the reagent should be just sufficient to provide the oxygen when BaO-based flux is used and the MnO content in the slag should not exceed 35% for dephosphorization of manganese. This will also ensure manganese loss within tolerable limits. On the basis

of above results, a 30% MnO<sub>2</sub> content in the reagent appears to be the optimum amount.

A theoretical quantitative analysis on the effect of MnO content in slag on various thermodynamic parameters is shown in Table 5.10. It is observed that with increase in MnO content in slag (in BaO-BaF<sub>2</sub>-MnO slag, keeping BaF<sub>2</sub> constant at 30%) the equilibrium partial pressure of oxygen for Mn-MnO system (calculated using  $a_{\text{Mn}}=0.3$  [76] and  $\gamma_{\text{MnO}}=1$  [28]) increases, which indicates that dephosphorization can be carried out at higher oxygen potential without loss of manganese and consequently higher dephosphorization can be obtained (lower  $h_p$ ), as obvious from predominance area diagram, shown in Fig.5.5. A calculation in the present investigation as shown in Appendix III showed that effective dephosphorization ( $[\%P] \leq 0.2$ ) can be achieved at 30% MnO content in the slag as shown in Table 5.10. It is also observed from the above Table 5.10 that the phosphate capacity decreases significantly, as also the phosphorus partition ratio ( $L_p$ ) [84], but a  $L_p$  of 63 at MnO=30% could be considered enough because higher degree of dephosphorization can be achieved with reasonable amount of slag. But the more serious problem lies with the melting of the slag. As observed from this table the melting temperature decreases with increase in MnO content of the slag up to around 30% [20]. Melting temperatures beyond 30% MnO content in slag is not available in literature which may probably be due to the fact that the solubility of MnO in slag ceases at 32% in BaO-MnO slag and it further decreases with addition of BaF<sub>2</sub> content in the slag (see Fig. 5.17). Therefore, above discussion indicates that 30% MnO content in slag could be considered as optimum which is in agreement with the experimental results.

A comparison of dephosphorization efficiency using calcined BaCO<sub>3</sub>-MnO<sub>2</sub>-BaF<sub>2</sub> pellets with that using BaCO<sub>3</sub>-BaF<sub>2</sub> powders shows an improvement using pellets (phosphorus removal achieved 80%) over powders (68% only). The result was also

found to be in good agreement with the findings of Liu et al.[18] who achieved about 80% phosphorus removal when BaO-MnO-BaF<sub>2</sub> flux was used. But due to experimental limitations, the Mn-loss increased in case of pellets which may be attributed to the arrested carbon dioxide in the system as shown by the XRD plot (Fig. No. 5.34) which appears to have increased the oxygen potential in the system.

However, it may be possible to modify the set up for the escape of carbon dioxide during calcination of barium carbonate pellets for subsequent treatment of liquid ferromanganese in order to minimize the manganese loss.







































## **5.4 INJECTION OF FLUX POWDERS THROUGH FERROMANGANESE MELT TO IMPROVE THE KINETICS OF THE PROCESS**

The results of tests conducted in 1 kg induction furnace, as discussed in previous section, was found to be encouraging for removal of phosphorus. It was possible to remove about two third phosphorus using barium carbonate flux but the time taken was about 30 minutes. This prolonged time for dephosphorization was not considered practical because large amount of external energy will be required to keep the bath in molten condition during this extended oxidizing operation. Therefore, attention was paid to enhance the kinetics of the process by flux powder injection and to reduce the time of the process to reasonably low levels.

### **5.4.1 RESULTS OF THE KINETIC TESTS**

Several experimental trials were made to make a smooth and successful injection through ferromanganese melt. Six to seven tests were discarded due to various experimental problems, like breakage of nozzle, improper functioning of injector, nozzle blocking, too much slopping and splashing etc. After repeated trials, a test condition was established for successful run, details of which are given in Table 5.11. Carrier gas flow rate at  $1\text{Nm}^3/\text{hr}$  was found to produce a smooth run. The injection was carried out in a 7 kg crucible placed in an induction furnace. 10 wt% flux (700 g) was injected in 5 minutes time, which corresponds to powder injection rate of  $7.77 \times 10^{-7} \text{ m}^3/\text{s}$ . Two alloy sample were taken to determine the degree of dephosphorization. One sample was taken before injection and another after the injection. Hot metal samples were collected using silica tube attached with a rubber suction bulb at the other end. It was observed that phosphorus level is reduced to 0.08 wt% at the end of injection from a original 0.43 wt% phosphorus in the melt, registering 81% removal of phosphorus in 5 minutes.



## 5.4.2 MATHEMATICAL MODEL FOR INJECTION PROCESS

A injection model [65,68] was studied to understand the fundamentals of injection process, which is described below:

A typical injection process may be represented schematically as shown in Fig. 5.35 [47]. Refractory lance is immersed into the melt from top, and as shown in the diagram, the injected gas and powder rise up through the melt and the slag accumulates on the top surface of liquid bath.

In injection process, the interaction between the injected gas, flux powder and metal (please note “liquid ferromanganese alloy” has been mentioned as “metal” everywhere in this section) is complex because of variety of reaction interfaces. The overall reactions can be conceived broadly as two reactions occurring parallelly, namely the transitory reaction, taking place between the ascending powder particles and the metal, and the permanent reaction, taking place between the metal and the top slag interface. Therefore, drawing an electrical analogy (Fig. 5.36), the overall dephosphorization rate ( $R_{OV}$ ) during powder injection can be expressed as the sum of the rate of transitory reaction ( $R_t$ ) and permanent reaction ( $R_p$ ) as given below:

$$R_{OV} = -V_m \frac{d[\%P]}{dt} = R_p + R_t \quad (5.8)$$

Where  $V_m$  is the volume of metal ( $m^3$ ),  $[\%P]$  is the phosphorus concentration in the metal.

### Permanent Reaction

Assuming mass transfer in the metal side boundary layer as the rate controlling step and the bulk alloy is thoroughly mixed (see Fig. 5.37, for corresponding concentration profile),  $R_p$  can be represented as:

$$R_p = A_p \cdot K_p ([\%P] - [\%P]_i) \quad (5.9)$$

Where  $A_p$  is the nominal surface area at the permanent contact zone (i.e., top slag-metal interface) and  $[\%P]_i$  is the phosphorus concentration in the metal at the top slag-metal interface.

By introducing equilibrium partition coefficient,  $L_p$ , defined as:

$$L_p = \frac{(\%P)_i}{[\%P]_i} = \frac{(\%P)}{[\%P]_i}, \text{ equation (5.9) can be expressed as:}$$

$$R_p = A_p \cdot K_p ([\%P] - (\%P) / L_p) \quad (5.10)$$

Here,  $(\%P)_i$  and  $(\%P)$  represent the weight percent of phosphorus in the slag at the top-slag metal interface and bulk slag respectively.

### **Transitory Reaction:**

The reaction on a powder particle, which is probably liquid phase trapped on a gas bubble during flotation (see Fig. 5.37) in the metal bath can be expressed as:

$$\frac{d[\%P]}{dt} = \frac{A_{Pow}}{V_{Pow}} K_{t.ov} ([\%P] - \frac{(\%P)_{pow}}{L_p}) \quad (5.11)$$

and

$$R_t = v_{in} (\%P)_{pow,e} \quad (5.12)$$

Where  $v_{in}$  is the rate of powder injection,  $(\%P)_{pow,e}$  is the concentration of phosphorus in the molten powder particle at the end of flotation through melt, which can be obtained by solution of the equation 5.11, with the assumptions that i) fresh powder particles do not any phosphorus and the  $[\%P]$  remain constant and uniform during the flotation. It may be noted that as the time required for a powder particle (attached to a spherical cap bubble) to rise to the metal surface is short compared with the total powder injection period, the phosphorus concentration in the metal phase  $[\%P]$  can be regarded as constant during the flotation of any powder particle.

A overall phosphorus balance can also be written as:

$$([\%P]_O - [\%P])V_m = (\%P)t'v_{in} \quad (5.13)$$

where,

$$\begin{aligned} t' &= t & 0 \leq t \leq t_{in} \\ t' &= t_{in} & t \geq t_{in} \end{aligned}$$

Here, [%P]<sub>o</sub> is the initial phosphorus concentration in the metal, and t<sub>in</sub> is the injection period. The above condition indicate that beyond injection period addition to slag volume (t'<sub>v<sub>in</sub></sub>) ceases. Combining equations 5.10 to 5.13 and after non-dimensionalization the final equation of dephosphorization becomes [65]:

$$-\frac{dy}{d\xi} = a\left(y - \frac{1-y}{\xi'}\right) + Ey \quad (5.14)$$

where,  $\xi$  represent the non-dimensional time, defined as:  $\xi = \frac{L_{vol}v_{in}}{V_m} t$

y, non-dimensional concentration in metal phase , defined as  $y = [\%P] / [\%P]_o$

x, non-dimensional concentration in top slag , defined as  $x = (\%P)_{ts} / L_P [\%P]_o$

a, dimensionless rate constant for permanent reaction , defined as:  $a = (K_{P,ov} A_p / L_p v_{in})$

A parameter E, defined below, is produced to indicate the measure of the efficiency of transitory reaction.

$$E = 1 - \exp(-A_t K_t / L_P v_{in}) \quad (5.15)$$

A large value for “a” represents the equilibrium between metal-top slag interface and similarly, E=1 corresponds to the condition of equilibrium between the powder particles and the surrounding metal during flotation

### **Determination of mass transfer Coefficients:**

Volumetric mass transfer coefficients at the metal -top slag boundary layer, is defined as:

$$k' = (K_P A_p / V_m)$$

K<sub>P</sub>, the mass transfer coefficient at the permanent contact zone, has been calculated as follows [66,68]

$$K_p = \beta \left( D_p \frac{Q}{A_p} \right)^{1/2} \text{ where, } Q = \frac{Q' T \cdot P_a}{273P} \quad (5.16)$$

$D_p$  is coefficient of diffusion of phosphorus in the metal ( $m^2/s$ )

$Q', Q$  are the inlet gas flow-rate and gas flow-rate at the metal-slag interface respectively ( $Nm^3/s$ ),  $P$  and  $T$  are the pressure and temperature at the metal-slag interface and  $P_a$  is the atmospheric pressure.

$\beta$  is an empirical parameter which take care of improved mass transfer due to agitation in the melt caused by gas injection [66,68]. A value of  $\beta$  equal to  $50m^{-0.5}$  was observed to yield a mass transfer coefficient of the order of  $10^{-3}$ , a value that matched with the experimentally observed value in a laboratory scale desulphurization study by powder injection at 3.5 kg scale by Robertson et al.[65].

Mass Transfer Coefficient at Transitory reaction zone ( $K_t$ ), and the total surface area for reaction ( $A_t$ ) was calculated using the model as proposed by Engh et al. [67] which consider mass transfer from liquid slag encircling a spherical cap gas bubble during its ascend through melt.

In this model the total interfacial area available for the transitory reaction is proposed as:

$$A_t = 3v_g \Omega H / rv_b \quad (5.17)$$

The reaction area mentioned is slightly over estimated because the liquid slag particles are more likely to attach at the bottom of a spherical cap bubble rather than fully encircling it (see Fig. 5.35). Therefore, effective reaction area has been taken as 1/3 of the value indicated by equation (5.17), as suggested by Robertson et al. [65]. The bubble radius  $r$  and its upward velocity  $v_b$ , were expressed as:

$$r = \frac{12\sigma}{\rho_m f v_b^2} \quad \text{and} \quad v_b = \left( \frac{4\sigma g}{f\rho_m} \right)^{1/4}$$

Here,  $v_g$  is the injection gas flow rate,  $\Omega$  is the shape factor of the gas bubble = 1.5 [67],  $H$  is the lance immersion depth = 20 cm(in the present investigation),  $\sigma$  is the surface tension of the metal,  $f$  is the friction factor for the rise of the gas bubble =0.5 [67],  $\rho_m$  is the density of the metal

The mass transfer coefficient in the transitory reaction zone may be estimated as:

$$K_t = \left( \frac{8Dv_b}{\pi r} \right)^{1/2} \quad (5.18)$$

Where,  $D$  is the diffusivity of the phosphorus in metal.

From these equations (5.17 and 5.18) the product of surface area and transitory mass transfer coefficient in terms of independent variables can be represented as:

$$A_t K_t = 0.27 D^{1/2} \left( \frac{f \rho_m}{\sigma} \right)^{7/8} g^{3/8} v_g \Omega H \quad (5.19)$$

**TABLE:5.12**

**Various constants used in the present model [67,46,65,68]**

$\sigma$ (J/m <sup>2</sup> )	$\rho_m$ (kg/m <sup>3</sup> )	$\rho_{sl}$ (kg/m <sup>3</sup> )	$\Omega$	$f$	$H(m)$	$D$ (m <sup>2</sup> /s)	$Q'$ (Nm <sup>3</sup> /hr)	$\beta$ (m <sup>-0.5</sup> )
1.564	7300	3000	1.5	0.5	0.20	1.0x10 <sup>-9</sup>	1.0	50

#### 5.4.3 DISCUSSION OF RESULT USING THE KINETIC MODEL:

In Fig. 5.38, the concentration of phosphorus in the metal phase has been plotted against time. It shows that phosphorus concentration in the metal phase can be lowered from 0.43 to 0.05 wt% after 5 minutes of injection which is in agreement

with the experimental data, shown in the figure by black circle symbol. The theoretical equilibrium line for metal phase concentration which is superimposed on this plot and shown by dotted line, has been calculated by assuming a very large value for non-dimensional rate constant at the top metal-slag interface (i.e.,  $a = 100$ ). It is observed that phosphorus concentration line goes below the equilibrium concentration line at about 180 secs and consequently a reversion reaction (transfer of phosphorus from slag to metal) is expected in the permanent contact zone thereafter. But the overall reversion by upward trend of concentration is not observed before injection stops, because fresh powder continues to add from the bottom and metal concentration goes down further through transitory reaction before injection ceases. And as soon as the injection stops, the gradual rise in concentration with time till it reaches equilibrium value shows the clear indication of phosphorus reversion from slag to metal. This phenomenon of phosphorus reversion is more clear from Fig.5.39 which compares the relative contribution of the transitory reaction to the permanent reaction. It shows that permanent reaction goes negative after 180 seconds when the phosphorus concentration in metal goes below the equilibrium value (from Fig. 5.38). But transitory reaction remain dominating and positive which accounts for further lowering of metal concentration during injection even though the top slag has attained equilibrium.

Most importantly, the Fig. 5.39 can be used to quantify the relative contribution of transitory to permanent reaction. It is also observed from Fig.5.39 that contribution of transitory reaction (62%) to overall reaction dominates over the effective contribution of permanent reaction(38%). The effective contribution of permanent reaction is composed of two components, i) positive contribution of permanent reaction, which accounts for the contribution of the permanent reaction before the top slag-metal interface attains equilibrium, ii) negative contribution of permanent reaction, which accounts for the contribution of the permanent reaction after the top slag metal reaction attains equilibrium and phosphorus reversion takes place.











## 6.0 SUMMARY AND CONCLUSIONS

### 6.1 SUMMARY

The high carbon ferromanganese produced in India usually have more than 0.4 % phosphorus which is not considered suitable for producing high quality steels such as ball bearing steels and high manganese / chromium steels. These high levels of phosphorus in high carbon ferromanganese originate from manganese ores, majority of which contain more than 0.2 % phosphorus. At present, there is no suitable method for economical removal of phosphorus from these ores. High grade ores containing low phosphorus are depleting fast and the ferromanganese manufacturers in India will have no choice but to use these high phosphorus inferior grade ores in near future either fully or in the blended form with relatively low phosphorus ores. Thus the ferromanganese produced in India using these high phosphorus ores and coke containing more than 0.25% P will continue to have more than 0.4% phosphorus whereas desirable level of phosphorus in ferromanganese is less than 0.2% for producing quality steels. In view of this scenario, the present study was taken up to develop a viable process for reducing the phosphorus content from >0.4 0 % to <0.25 % in high carbon ferromanganese.

A literature search showed that the conventional method of phosphorus removal from liquid ferromanganese under oxidizing conditions is usually accompanied by a significant loss of manganese because the oxide of manganese is more stable than that of phosphorus at smelting temperatures. The alternative way of removing phosphorus as phosphides under highly reducing conditions at high temperatures is considered environmentally unfriendly since the reaction product (  $\text{Ca}_3\text{P}_2$  or  $\text{Ba}_3\text{P}_2$ ) in slag is likely to release phosphene when it comes in contact with moisture. Gaseous dephosphorization is also not suitable because the partial pressure of manganese is higher than that of phosphorus at smelting temperatures. However, a

theoretical analysis showed that preferential removal of phosphorus is possible if dephosphorization is carried out in a narrow range of oxygen partial pressure ( $p_{O_2}$ ) using BaO-based fluxes rich in MnO. But the melting of BaO -MnO fluxes at moderate temperatures ( $<1500^{\circ}\text{C}$ ) was a problem possibly because of the high melting points of pure components ( $1925$  and  $1785^{\circ}\text{C}$  respectively) whereas oxidative dephosphorization is favored at low temperatures. Besides, high manganese content ( $>60\%$ ) in ferromanganese is known to reduce the equilibrium partition ratio of phosphorus between the liquid flux and the alloy sharply to a very low level ( $<10$ ) when the process is carried out with the BaO-MnO flux at a fixed temperature ( $1400^{\circ}\text{C}$ ).

The problems associated with oxidative dephosphorization have been addressed in the present work and the following studies have been undertaken to develop a viable process for dephosphorization of ferromanganese:

1. Thermodynamic analysis to identify the most suitable experimental conditions for dephosphorization of ferromanganese.
2. Feasibility tests at 1 kg scale in a graphite crucible fitted in an induction furnace using  $\text{BaCO}_3$  based flux powders to find out the most suitable composition of flux/slag suitable for dephosphorization of ferromanganese.
3. Dephosphorization tests in a carbon resistance furnace under controlled conditions using calcined  $\text{BaCO}_3$  based fluxes (major phase BaO) in order to improve the dephosphorization efficiency and reduce the manganese loss.
4. Kinetic study to reduce the reaction time from 30 minutes for a stagnant bath to less than 10 minutes when the flux is added through injection.

The summaries of these studies are given below:

### 6.1.1 THERMODYNAMIC ANALYSIS

A thermodynamic analysis was conducted in order to identify the most suitable conditions for removal of phosphorus under oxidizing conditions without loss of manganese. For this purpose various flux systems available in the literature were analyzed and BaO-based fluxes were selected because of their higher phosphate capacity than lime based fluxes. Predominance area diagrams for the Ba-P-O ternary superimposed by Mn-MnO line were drawn first assuming unit activities of all the phases at temperature's varying from 1573-1873K and later assuming more realistic values of activities of all the condensed phases at a selected temperature (1573 K). The predominance area diagram shows the stability of various phases such as barium phosphate, barium phosphide, manganese oxide with respect to partial pressure of oxygen at a given temperatures which makes it possible to identify the suitable conditions of dephosphorization without the loss of manganese. It was found that there is a narrow range of oxygen partial pressure in which it is possible to remove phosphorus selectively from ferromanganese using BaO based fluxes under oxidizing conditions without extensive oxidation of manganese, even though the oxide of manganese is more stable than that of phosphorus at smelting temperatures. The range becomes narrower with increase in temperature from 1573 to 1873 K making the dephosphorization difficult. The results of thermodynamic analysis indicated that it is possible to achieve effective removal of phosphorus less than 0.2% at relatively lower temperature by maintaining  $p_P$  below 2.18 as per the calculation shown in Appendix 1 under the following conditions:

a)  $a_{Mn} = 0.3$

b)  $a_{MnO} = 0.5$

c)  $a_{Ba_3(PO_4)_2} = 0.1$

- d) Temperature 1300<sup>0</sup>C
- e) Oxygen potential about 3.0X 10<sup>-17</sup>atm

The above thermodynamic analysis has helped in identifying the favorable conditions of dephosphorization of ferromanganese. In order to confirm the predictions of thermodynamic analysis, feasibility tests were carried out, summary of which are given below. A graphite crucible was chosen to get  $a_{Mn} = 0.3$  as reported in the literature. The BaCO<sub>3</sub>-based flux having high phosphate capacity of the order 10<sup>29</sup> was selected to achieve  $a_{Ba_3(PO_4)_2} = 0.1$ . The composition of slag was selected in such a way to obtain  $a_{MnO} = 0.5$ . However, in view of the high melting temperatures of BaO and MnO (1925 and 1785<sup>0</sup>C respectively) several trials were made in order to melt the flux at 1300<sup>0</sup>C, details of which are given below:

### 6.1.2 THE FEASIBILITY TESTS

Dephosphorization tests were carried out in a graphite crucible in a high frequency induction furnace at moderate temperature (<1500<sup>0</sup>C) under oxidizing conditions using lime as well as barium carbonate based fluxes. Melting temperatures of various flux systems were compiled in order to select the most suitable composition which can melt near the melting temperature of ferromanganese alloy and have the adequate phosphate capacity. Different proportions of BaCO<sub>3</sub> and MnO<sub>2</sub> were tried in order to melt them at moderate temperature (<1500<sup>0</sup>C). It was found that BaCO<sub>3</sub> alone can be melted at comparatively lower temperature (1300<sup>0</sup>C) but with addition of MnO<sub>2</sub> which was intended to restrict the Mn loss, could not be possible. After several trials, other suitable compositions were evolved for melting the BaCO<sub>3</sub> based flux without any real difficulty. It was observed that in situ oxidation of manganese forms a eutectic with BaO in presence of carbon. Once it was possible to melt the flux at 1300<sup>0</sup>C, the effect of various parameters such as (i) type of flux, (ii) quantity

of flux, (iii) silicon content of the alloy, (iv) temperature (v) time were studied on the degree of dephosphorization. Results showed that it was possible to remove about 68% phosphorus from desiliconized melt. Phosphorus contents were reduced to desired levels ( $<0.25\%$ ) from the initial levels ( $>0.40\%$ ) present in the ferromanganese alloy. It was observed that the efficiency of BaO based flux increased due to melting near hot metal temperatures. The manganese loss was restricted to 2-5 % compared to more than 7% reported earlier by Lee. The degree of dephosphorization increased with increase in quantity of flux added. The maximum level of phosphorus (68%) was removed when the flux added was 16 wt % of the metal weight. Amongst the reagents investigated,  $\text{BaCO}_3\text{-BaF}_2$  was found to be most effective. The addition of  $\text{BaF}_2$  not only increases the phosphate capacity of flux but also minimizes the manganese loss by increasing the activity of MnO in slag. Maximum level of phosphorus was removed at about 30 minutes of flux addition which was not considered suitable for trials at the industrial scale. Hence there is a need for thorough investigation of the kinetics of the process (Summary is given in Section 6.4). It was also decided to improve the efficiency of process by using BaO-based (Calcined  $\text{BaCO}_3$ ) flux pellets instead of  $\text{BaCO}_3$  powders, summary of which are given below:

### **6.1.3 DEPHOSPHORIZATION TESTS USING CALCINED FLUX PELLETS**

Once the feasibility of  $\text{BaCO}_3$  based flux powder on dephosphorization of ferromanganese was established, it was decided to make  $\text{BaCO}_3$ -based pellets as an industrial reagent for the following advantages of pellets over powder:

- i) better assimilation in the liquid Fe-Mn melt
- ii) better reactivity

- iii) pre-calcined pellet can restrict temperature drop of the Fe-Mn melt by avoiding  $\text{BaCO}_3$  decomposition in the melt
- iv)  $\text{BaO}$  (pre-calcined  $\text{BaCO}_3$ ) - $\text{MnO}$  (pre reduced  $\text{MnO}_2$ ) based flux with high phosphate capacity can be produced from in situ pre-calcined and pre-reduced  $\text{BaCO}_3$  based pellets.

Green pellets were prepared using powders of flux mixture of  $\text{BaCO}_3$ ,  $\text{MnO}_2$ ,  $\text{BaCl}_2/\text{BaF}_2$  and Carbon in a disc pelletizer. The pellets were dried for 24 hours and stored in a separate polythene cover. External calcination of pellets were carried out in carbolyte furnace where automatic control of temperature was possible. Temperature was varied in the range of 700-1050<sup>0</sup>C and soaking was done for 1 hr. Samples were quenched for arresting the phases and were analyzed by XRD. It was found that major phases present were  $\text{BaO}$  and  $\text{MnO}$  when calcination was carried out at 1050<sup>0</sup>C. However, it was apprehended that  $\text{BaO}$  formed by calcination of  $\text{BaCO}_3$  may revert back to  $\text{BaCO}_3$ , if it is not stored properly and the advantage of external pre-calcination will be lost. Therefore, it was decided to carry out in-situ calcination of  $\text{BaCO}_3$ -based pellets as well as dephosphorization in carbon resistance furnace itself under controlled atmosphere and temperature within  $\pm 2^0\text{C}$  which was not possible to maintain for the tests carried out in induction furnace. Several small graphite crucibles having flux of different composition and weight, were used to see their effect on dephosphorization. Soaking was done at 1050<sup>0</sup>C for 1 hr for calcination and to form  $\text{BaO}$ -  $\text{MnO}$  flux pellets from  $\text{BaCO}_3$ -  $\text{MnO}_2$  pellets. Subsequently the temperature was raised to 1350-1400<sup>0</sup>C at the controlled rate for reaction to take place in the liquid state for 30 minutes. Furnace was cooled at the controlled rate under inert atmosphere. The effect of type of flux and its dosage, temperature and  $\text{MnO}$  content of the flux on dephosphorization were studied.

First series of experiments were conducted varying the composition of flux pellets. The results showed that maximum removal of phosphorus (~80%) occurred with  $\text{BaO}$ - $\text{MnO}$ - $\text{BaF}_2$  flux pellets compared to 66% in case of  $\text{BaO}$ - $\text{MnO}$ - $\text{BaCl}_2$  under

identical quantity of flux used. The lowest phosphorus removal took place when only BaO (calcined BaCO<sub>3</sub>) was used as a flux. This indicates the importance of presence of MnO in a BaO-based flux.

In second series of experiments, flux weight was varied from 5 to 20 % of metal weight using the most suitable BaO-MnO-BaF<sub>2</sub> flux pellets. It was observed that the removal of phosphorus increases with increase in the quantity of flux used. However, there was no significant change in the removal of phosphorus beyond 10 %, therefore, 10% flux of metal weight was considered as suitable quantity for economical dephosphorization.

The third series of experiments were carried out to study the effect of varying the MnO<sub>2</sub> contents in two identified reagents, BaCO<sub>3</sub>-BaCl<sub>2</sub>-MnO<sub>2</sub> and BaCO<sub>3</sub>-BaF<sub>2</sub>-MnO<sub>2</sub> on the phosphorus removal. Based on alloy and slag analysis after 30 minutes, i.e at the attainment of near equilibrium, phosphorus partition ratios were calculated. It was found that the phosphorus partition ratio increases up to 20 with increase in MnO<sub>2</sub> content in the reagent (BaCO<sub>3</sub>-BaCl<sub>2</sub>-MnO<sub>2</sub>) from 10% to 30% beyond which it starts decreasing. The % P<sub>2</sub>O<sub>5</sub> content of the slag was also found to increase with increase in MnO<sub>2</sub> content in the reagent up to 30% beyond which it starts decreasing. A similar trend was also observed for BaO-BaF<sub>2</sub>-MnO slag system. The effect of MnO<sub>2</sub> content in the reagent on the MnO content of the slag was also analyzed which showed that MnO content in the slag initially increases with increase in MnO<sub>2</sub> content in the reagent (BaCO<sub>3</sub>-MnO<sub>2</sub>-BaF<sub>2</sub>) and beyond 30%, it do not increase significantly. Interestingly it was also observed that a high content of MnO in slag beyond 30-35% decreased the % P<sub>2</sub>O<sub>5</sub> content in slag. On the basis of above results, it was concluded that 30% MnO<sub>2</sub> content in the reagent which generates about 30% MnO in slag appears to be the optimum amount.

A theoretical quantitative analysis showed that phosphate capacity and partition ratio (L<sub>p</sub>) decreases with increase in MnO content in the slag. Calculation showed

that ( $L_p$ ) of about 63 is achievable at 30% MnO in slag which is adequate for obtaining high degree of dephosphorization with reasonable amount of slag but the more serious problem lies with the melting of slag when MnO content is increased beyond 30%, possibly because of formation of intermediate compounds. Therefore, MnO content in slag around 30% could be considered as optimum which is in agreement with experimental results discussed above.

A comparison of dephosphorization efficiency using calcined  $\text{BaCO}_3\text{-MnO}_2\text{-BaF}_2$  pellets with that using  $\text{BaCO}_3\text{-BaF}_2$  powders (Feasibility Tests) shows an improvement using pellets (phosphorus removal achieved 80%) over powders (68% only) but due to experimental limitations, the Mn-loss increased in case of pellets which may be attributed to the arrested carbon dioxide in the system released during in-situ calcination of  $\text{BaCO}_3$ , which appears to have increased the oxygen potential in the system. However, it may be possible to modify the set up for the escape of carbon dioxide during calcination of barium carbonate pellets for subsequent treatment of liquid ferromanganese in order to minimize the manganese loss.

#### **6.1.4 KINETIC STUDY**

The results of the feasibility tests (as discussed in Section 6.2) using  $\text{BaCO}_3\text{-BaF}_2$  fluxes were found encouraging which indicated that more than 60 % phosphorus could be removed but the time taken was about 30 minutes. This prolonged duration of dephosphorization was not considered suitable for plant scale trials. Therefore, this study was taken up to reduce the reaction time to less than 10 minutes so that flux and energy could be utilized economically. For this purpose an injection system was designed for purging powder particles from the bottom using a submerged lance. The pneumatic injection of flux powder involves initial conveying followed by subsequent discharge of gas mixed particles as submerged jet in liquid metal in a

ladle The dispenser body of 5 kg capacity was fixed on the stand. A graphite injector was fabricated (keeping in view of the depth of liquid metal) so that it can be fitted with stainless steel tube, carrying the gas powder mixture from the injector. Pressure was controlled by means of Audco valve. Loading ratio up to 15:1 for barium carbonate based fluxes could be maintained using this injector.

About 7 kg desiliconized ferromanganese was melted in a graphite crucible fitted in induction furnace. After melting, a sample was collected. The melt temperature was raised to about 1600<sup>0</sup>C. The furnace was switched off at the onset of injection to simulate the ladle condition and the flux was injected in the liquid ferromanganese. The injection time varied from 2 to 5 minutes. About 6-7 tests were discarded due to various experimental problems, like breakage of nozzle, improper functioning of injector, nozzle blocking, too much slopping and splashing etc. After repeated trials a test condition was established for successful run. It was possible to carry out a smooth run by injecting 10 wt% flux in 5 minutes keeping the carrier gas flow rate maintained at 1Nm<sup>3</sup>/hr. The results showed that about 80% removal of phosphorus was possible in around 5 minutes.

A mathematical model has been developed to understand the kinetics of the process. The model considers two parallel reactions taking place simultaneously in the injection process; one during the ascent of the powder particles through melt, called the transitory reaction, second at the top slag-metal interface, called the permanent reaction. The model shows that the contribution of transitory reaction (62%) to overall reaction, dominates over the effective contribution of permanent reaction(38%). The effective contribution of permanent zone combines its positive contribution (42%) with its negative contribution (-4%), that counts for the reversion of phosphorus from slag to metal which takes place due to excess dephosphorization near the end of injection.

## 6.2 CONCLUSIONS

The major conclusions drawn from above studies on dephosphorization of ferromanganese are as follows:

1. On the basis of a thermodynamic analysis and relevant predominance area diagrams, a BaO-based flux rich in MnO was identified as the most suitable flux for selective removal of phosphorus from ferromanganese
2. Barium carbonate ( $\text{BaCO}_3$ ) was used as a substitute for BaO in the present investigation because of its ready availability at low cost. It was difficult to melt the  $\text{BaCO}_3$  and  $\text{MnO}_2$  flux mixture initially but after several trials suitable compositions ( $\text{BaCO}_3\text{-BaF}_2/\text{BaCl}_2$ ) were identified to melt the flux at moderate temperatures ( $<1500^\circ\text{C}$ ). It was observed that  $\text{BaCO}_3$  could not be melted in the presence of  $\text{MnO}_2$ .
3. The present investigation clearly established the fact that dephosphorization of ferromanganese can be carried out to a significant extent 68% using  $\text{BaCO}_3\text{-BaF}_2$  flux mixture and at the same time restricting the manganese loss to a very low level 2-5 %.
4. Dephosphorization was found to be very sensitive to the initial silicon content of ferromanganese. It was found that under oxidizing conditions, the degree of dephosphorization decreased significantly with increase in the initial silicon content of the ferromanganese alloy. An initial silicon content of less than 0.2% is recommended from this investigation.

5. The degree of dephosphorization increased with increase in quantity of flux (powder) added and beyond 16 wt% hardly any improvement in dephosphorization could be observed.
6. The results of the tests carried out in carbon resistance furnace using calcined (in-situ)  $\text{BaCO}_3$  based flux pellets showed that the degree of dephosphorization was higher (more than 80% )compared to a maximum of 68% only when a carbonate based flux powder was used. However, because of experimental limitations the manganese loss was higher (3-15%), the reason of which was attributed to the arrested carbon dioxide in the system generated during in situ calcination of barium carbonate.
7. A study on the effect of  $\text{MnO}_2$  content in the flux pellets showed that 30%  $\text{MnO}_2$  should be the optimum quantity for effective dephosphorization (more than 80%) of ferromanganese.
8. The results of the kinetic study showed that it is possible to remove about 80% phosphorus in around five minutes by injecting 10wt% flux in liquid ferromanganese alloy using submerged lance from top.
9. A mathematical model for the injection process investigated showed that the transitory reaction contributes 62% to overall reaction.

## REFERENCES

1. "Technology and Norms study in Ferro Alloy Industry", Dept. of Science and Technology , New Delhi, April 1991.
2. J. F. Elliott, M. Gleiser and V. Ramakrishna , " Thermochemistry for steel making" , Vol 1 Addison-Wesley , 1961,p214
3. S. Tabuchi and N. Sano , Met. Trans. Vol 15 B, 1984, p351-356
4. R.P. Goel and S. Srikanth " A thermodynamic analysis of ferromanganese" paper presented at the 46 th ATM of IIM, Nov, 1992
5. P. N. Chaudhary and R.P. Goel "Dephosphorization of liquid ferromanganese" paper presented during 4 th refresher course on Ferro Alloy, held at Jamshedpur during 12 -14 January, 1994
6. P. N. Chaudhary, R.P.Goel, R. K. Minj, K. Chandrasekhar and K.G.Sengupta" Dephosphorization of ferromanganese using basic fluxes". Internal Report (Project No 14493245) of NML, Jamshedpur December ,1994, "
7. P. N. Chaudhary, R.P.Goel, M.C. Goswami, Ajoy Roy, S.Srikanth, K.G.Sengupta and K. Chandrasekhar " Dephosphorization of Fe-Mn-C-P alloys " Internal Report (Project No OLP-007331) of NML, Jamshedpur , December 1997.
8. R. K. Minj, P.N. Chaudhary, R. P. Goel, D.K. Biswas, Sukomal Ghosh, R. K. Sharma and K. G. Sengupta," Study of dephosphorization of high carbon liquid ferromanganese through flux injection" Internal Report of NML, Jamshedpur , August 1998.
9. S. M. Joshi , " Bright future for Ferro Alloy Industry" Minerals & Metals Review, April 1993 , p 51-62
10. F. P. Edneral , " Electrometallurgy of steel and ferro-alloys" Vol 2 Mir Publishers 1979 p154
11. K. Raghbendran and N. Mitra , " An introduction to Indian Standards on Ferro Alloys" paper presented in the national workshop on Ferro Alloy Industries in the Liberalised Economy.held at NML Jamshedpur during August 20-21, 1996.

12. M. Subramanian , O. Seetharamaayya and C. N. Harman , “ A strategy for utilization of low grade high phosphorus manganese ores in the production of high carbon ferromanganese” paper presented at national seminar on problems and prospects of Ferro Alloy Industry in India organised by NML and IIM, Jamshedpur , October 24-26 1983.
13. V. Raghavan “ Physical Metallurgy Principles and Practices” Prentice- Hall of India Pvt Ltd, New Delhi-1, 1993
14. S.M. Rao , “ Ferro Alloy raw materials of India-mineral resources, characterization and beneficiation” paper presented during 4 th refresher course on Ferro Alloys held at NML Jamshedpur during 12-14 January 1994
15. S. K.S Pashine et. al. “Ferro alloy industry in India , changing scenario” paper published in Metal News Vol. 12, No2, April 1990 pp1-7.
16. B. C. Acharya et. al.“Phosphorus in the silicious manganese ores of Nishikhal Orissa” Indian Journal of Geology Vol 66 No 1, 1994 pp15-23.
17. B. V. K. Raju et. al. “ Processing of high phosphorus manganese ores -a new method adopted at Andhra University , Visakhapatnam” paper presented during National Seminar on Energy , Environment and Resource Development for Mineral Industry during 18-19 January 1995.
18. R. H. Tupkari, “Introduction to Modern Steelmaking” Khanna publishers, Delhi,1983
19. R. P. Goel , “ Thermodynamic consideration of bulk ferro alloys” paper presented during 4 th refresher course on Ferro Alloy, held at Jamshedpur during 12 -14 January, 1994
20. M. Fujita, H. Katayama, A Yamamoto and N. Matso, Tetsu-to-Hagane 74 (1984) p286.
21. Z. Ma, R. Ni ,C. Zheng and J. wang Steel Research 63 (1992) No 3, pp112-119
22. Y.E. Lee and R.H. Kauser, U. S. Patent No 4752327, 1988
23. Y. E. Lee “ Characterization of dephosphorization for Mn alloys” , Proceedings of the 6<sup>th</sup> International Iron and Steel Congress, 1990 Nagoya , ISIJ. pp327-333

24. N. Sano, " Physical chemistry of melts: slags Thermodynamics of phosphorus and sulfur in basic slags" , Proceedings of the Elliott Symposium , ISS-AIME ,1990 pp173-190.
25. S. Simenov, C. Ivenchew and Drakalysky , 3<sup>rd</sup> International Conference on Molten Slags and Fluxes , June 1988 University of Strathclde , Glasgow , pp283-284
26. A. P. Prasad ,S.B. Sarkar and A. K. Chakraborty , Cast Metals , Vol 5 , No 4 ,1993
27. Y.Watanabe ,K. Kitamura , F. Rache , T. Sukihaski , and N. Sano, Met Trans. ,Vol 20B April 1993 ,pp339-347.
28. Sang Chul Shim, Fumitaka Tsukihashi and Nobuo Sano, " Thermodynamic properties of BaO-MnO flux system" Metallurgical Transactions B Vol. 24B, April 1993, pp333-37
29. N. Masumitsu , K. Ito and R. J. Fruehan , " Thermodynamics of Ca-  $CaF_2$  and Ca-CaCl<sub>2</sub> systems for dephosphorization of steel" , Met. Trans. , Vol. 193, 1988 , pp643-648.
30. N. Sano , " Thermodynamic aspects of dephosphorization of Fe-Cr and Fe-Mn alloy 1994 Turkdogan Symposium Proceedings pp 95-108.
31. O. Wijk, " The phosphorus in Iron and steel making" Scandanavian Journal of metallurgy 22 , 1993 pp 130-138.
32. C. Nassaralla , R. J. Fruehan and D. J. Min , Met. Trans. Vol 22B February 1991 pp33-38
33. C. Nassaralla and R.J. Fruehan " Phosphate capacity of CaO-  $Al_2O_3$  slags containing  $CaF_2$  , BaO ,  $Li_2O$  or  $Na_2O$  . Metallurgical Transaction 23 B, April 1992 p 117.
34. D. Wang , X. Shao : iron Steel in China , April 1983, 18 (4) , pp14-21.
35. N. Sano ,Tsukishi and A. Tagaya ISIJ International , (1991) Vol 16, pp1345-1347
36. P. K. Sen, P. Basu and S.S. Gupta , " Dephosphorization of high carbon ferromanganese" SEAIISI Quaterly April 1996, P 96-104.

37. S. Singh et. al. “ Investigation on dephosphorization of high carbon ferromanganese” paper presented at the 49 th ATM of IIM , November 1995.
38. X. liu, O. Wijk, R. Salin and J. O. Edstrom, “ Phosphorus equilibrium between BaO-BaF<sub>2</sub>-MnO fluxes and ferromanganese melts” Steel Research 66(1995) No3 pp90-102.
39. X. liu, O. Wijk, R. Salin and J. O. Edstrom, “ Manganese equilibrium between BaO-BaF<sub>2</sub>-MnO fluxes and Ferro-manganese melts” ISIJ International, Vol. 35(1995) pp250-257.
40. P. N. Chaudhary , R. P. Goel and R. K. Minj , CSIR Patent application No 2459 / DEL / 95 dated 29 / 12 / 95
41. X. Liu, O. Wijk, R. Selin and J. O. Edstrom “Oxidizing dephosphorization of ferromanganese” Scandinavian Journal of metallurgy 1998:25 pp 204-215
42. R. C. Nascimento Jr and J. D. T. Capocchi, “ Recycling of manganese ore fines” EPD Congress, 1995 edited by C. W. Warren, The Minerals, Metals & Minerals Society, 1995 .
43. D. K. Biswas , “ An approach to design consideration of Powder Dispenser-cun - Injector” Powder handling processing Vol 6 No 2 April/june 1994
44. D. K. Biswas et al. “ Some aspects of pneumatic injection with particular reference to the design of dischargers and lock feeders” Powder handling processing Vol 16 . No 1 January/March 1996.
45. Julian Szekely and Nickolas J Themelis : Rate phenomena in process Metallurgy
46. H. S. Ray and A. Ghosh , “ Principles of Extractive Metallurgy , New Age International (P) Limited , Publishers , August 1995 , pp227-228.
47. Ahindra Ghosh, “Principles of secondary processing and casting of liquid steel”, Oxford & IBH Publishing Co Pvt Ltd New Delhi, 1990
48. S. Kitamura, “ Development of analysis and control method for hot metal dephosphorization process by computer simulation” , ISIJ International , Vol 35 (1995), No 11 , pp1374-1380

49. O. Haida , K. Nakanishi and T. Emi , “ Recent progress in Japan in ladle metallurgy with emphasis on the application on the injection technology” SCANINJECT II 2<sup>nd</sup> International conference on injection metallurgy , Lulea , Sweden , June 12-13 , 1980 pp 2.01to 2.25.
50. M. F. Sidorenko , “ Powder injection intensifies the process and raises metal quality” SCANINJECT II 2<sup>nd</sup> International conference on injection metallurgy , Lulea , Sweden , June 12-13 , 1980 pp3.01-3.18.
51. Sustumu Mukawa and Yoshimasa Mizukami , “ Effect of stirring energy and rate of oxygen supply on the rate of hot metal dephosphorization” ISIJ International, Vol 35 (1995) , NO 11 , pp1374-1380.
52. Nakajima et. al. , “ Process of dephosphorization of hot metal” Steelmaking conference proceedings , Vol 72, Chicago, Illinois USA, 2-5 April 1989
53. Ishizaka et. al. , “ Kinetic study on dephosphorization of hot metal by lime based flux injection in different vessels” 1989 Ironmaking Conference proceedings pp 257-261.
54. J. J. Pak et. al. , “ Hot metal dephosphorization and improved BOF operation at POHANG Works” 1994 Ironmaking Conference Proceedings pp 291-306
55. Kumar et. al. , “ Pretreatment of hot metal at Rourkela Steel Plant” Proceedings of the 27<sup>th</sup> Steelmaking Operating Committee April 1995, RDCIS (SAIL) Ranchi, India
56. S.Verma et. al. , “ Experience of hot metal desulfurization by side injection at Bokaro Steel Plant” Proceedings of the 27<sup>th</sup> Steelmaking Operating Committee April 1995, RDCIS (SAIL) Ranchi, India
57. Venkatraghvan et. al. , “ Hot metal desulfurization at Tata Steel" Proceedings of the 27<sup>th</sup> Steelmaking Operating Committee April 1995, RDCIS (SAIL) Ranchi, India
58. C. Liu et. al. , Hugong Yejin (Engineering Chemistry and Metallurgy) 13, (2), 95-102 May, 1992.
59. M.Turunen: Jernkontorets Ann.,1975,159 p7.

60. S. Tanaka et al: Tetsu-to-Hagane (J. Iron Steel Inst. Japan)1980,66, S262
61. K. wada, S. Ogibayashi, K. Shimomura, S. Ariga, H. Nakashima and S. Tsuruoka,  
“ Investigation of desulphurization and deoxidation in injection metallurgy”  
SCANINJECT II 2<sup>nd</sup> International conference on injection metallurgy , Lulea ,  
Sweden , June 12-13 , 1980 pp21.01-21.15
62. H.Tanabe et. al.: Tetsu-to-Hagane(J. Iron Steel Inst. Japan) 1980, 66, S258
63. T. Usui.et. al.: .: Tetsu-to-Hagane(J. Iron Steel Inst. Japan)1980,66, S259
64. Fukuyama works, Nippan Kokan Kk: proc 75<sup>th</sup> Symp. Steelmaking Committee,  
Japan society for promotion of science, March 1980.
65. S. Ohguchi and D. G. C. Robertson, “ Kinetic model for refining by submerged  
powder injection: part 1 Transitory and permanent contact reaction” Ironmaking  
and Steelmaking 1984 . Vol. 11 No 6 pp262-273
66. Varadrajn Seshadri, Carlos Antonio da Silva, Itavahn Alves da Silva and Paulo  
Von Kruger , “ A kinetic model applied to the molten pig iron desulfurization by  
injection of lime based powders” ISIJ International Vol 37 (1997) No1 PP 21-30.
67. T. A. ENGH et. al. : Scand. J. Metall., 1972, 1, 103
68. B. Deo and R. Boom: Fundamentals of steelmaking Metallurgy, Prentice Hall,  
New York, (1993)
69. Arthur I. Vogel, “A Text Book of Micro and Semi-micro Qualitative Inorganic  
Analysis” Orient Longman Limited, New Delhi, 1971
70. Hem Shanker Ray, “Kinetics of Metallurgical Reactions” Oxford & IBH  
Publishing Co. Pvt. Ltd, New Delhi 1993
71. H. H. Kellogg and S. K. Basu, TMS-AIME, Vol.218,1960,pp70-81
72. E. T. Turkdogan, “Physical Chemistry of High Temperature Technology”,  
Academic Press,1980 pp5-24
73. O. Kubaschewski and C. B. Alcock, “Metallurgical Thermochemistry”,5<sup>th</sup> edition,  
Pergomon Press 1979
74. Y.E.Lee “Thermodynamics of the Mn-P system” Met. Trans. Vol. 17B, 1986,  
pp777-783

75. G. K. Sigworth and J.F. Elliott, Metal Science, Vol.8,1974 pp298-310
76. G. W. Healy , “ Proceedings of the International Symposium on Ferrous and Non Ferrous Alloy process , Hamilton Ontario, August 1990 edited by R. A. Bergman , Pergaman Press, pp97-108
- .
77. H. Fujiwara , E Ichise , K. Ashida and M. Iwase , Trans. of Iron and Steelmaker 17 (1990) No 2 p51
78. M. Iwase, H. Fujiwara , E. Ichise, K.Ashida and Akizaki, “ A themodynamic study of BaO + BaCl<sub>2</sub> + P<sub>2</sub>O<sub>5</sub> liquid slags firmid at the later stages of dephosphorization of chromium hot metal, Transaction of the ISS Iron and Steelmaker May 1988 pp69-80
79. P. N. Smith and M. W. Davis, Trans. Inst. Mining Met., Sec C, 80(1971),pp87
80. H.Inoue , Y. Shigeno, M. Tokuda and M. Outani, “Simultaneous desulphurization and dephosphorization of hot metal by CaCl<sub>2</sub>-CaO slags SCANINJECT II 2<sup>nd</sup> International conference on injection metallurgy , Lulea , Sweden , June 12-13 , 1980 pp19..01-19.04.
81. P. N. chaudhary, R. P .Goel, R. K. Minj and S.B.Sarkar, “ A flux based dephosphorization process for high carbon liquid ferromanganese” paper presented during national seminar on “Ferro Alloys present and future” held at Jamshedpur on 5-6<sup>th</sup> May, 1995 organized by Tata Steel and IIM chapter Jamshedpur, India.
82. M. Fujita et. al., Tetsu-to-Hagane, 74 (1988), pp816

83. Yindong Yang, Alex McLean , Iain D. Sommerville and Alan R. McKague, Steel Research 66 (1995) No3, pp103-109.
  
84. Xioya Liu, “ Dephosphorization of ferromanganese under oxidizing conditions”  
Dissertation , Department of Production Technology , Mining and steel Industry ,  
The Royal Institute of Technology , Stockholm ,1993.
  
85. Edmundo Burgos Cruz, Eduardo Camargo de Oliveira Pinto and Jose Deodoro  
Trani Capocchi, Steel Research 70 (1999) No3 , pp96-103.